NASA TECHNICAL MEMORANDUM

NASA TM-78298

MATED VERTICAL GROUND VIBRATION TEST

By Edward W. Ivey
Systems Dynamics Laboratory

(NASA-TM-78298) MATED VERTICAL GROUND VIBRATION TEST (NASA) 96 p HC A05/MF A01 CSCL 22B

N80-32425

Unclas

G3/16 28757

July 1980

NASA

George C. Marshall Space Flight Center
Marshall Space Flight Center, Alabama

TABLE OF CONTENTS

PRECEDING PAGE BLANK NOT FILMED

LIST OF TABLES

LIST OF TABLES (Continued)

LIST OF ILLUSTRATIONS

LIST OF ILLUSTRATIONS (Continued)

TECHNICAL MEMORANDUM

MATED VERTICAL GROUND VIBRATION TEST

I. SUMMARY

The Mated Vertical Ground Vibration Test (MVGVT) was conducted to provide an experimental data base in the form of structural dynamic characteristics for the Shuttle vehicle. This data base was used in developing high confidence analytical models for the prediction and design of loads, pogo controls and flutter criteria for the Space Shuttle under various payloads and operational missions.

The MVGVT program consisted of two basic configurations. The two configurations tested were simulated launch and boost. The launch configuration was composed of two Solid Rocket Boosters (SRB's), an External Tank (ET), and an Orbiter (OV 101).

For the launch configuration, the liftoff and endburn (Pre-SRB Separation) flight conditions were tested. The liftoff testing began on October 20, 1978, and ended December 2, 1978. The end burn testing started on January 30, 1979, and ended February 28, 1979.

The boost configuration was composed of the ET and the OV-101. For the boost configuration, three flight conditions (start boost, mid boost, and end boost) were tested. The boost test started on May 30, 1978, and ended July 14, 1978.

The Shuttle test program was conducted under Johnson Space Center's (JSC) direction and implemented by Rockwell International Corporation. Marshall Space Flight Center (MSFC) was heavily involved in all phases of the test. They were responsible for the ET, the SRB, and the Space Shuttle Main Engine (SSME) dynamic math models. MSFC was also involved in the LOX modal survey test. For MGVGT, MSFC was responsible for the suspension system design for launch and boost and was also involved in establishing the test plans and requirements. Additional responsibilities included data evaluation and analytical correlation.

II. INTRODUCTION

The purpose of this report is to present the MVGVT boost and launch program evolution, the test configurations, their suspensions, and the test results compared with predicted analytical results.

III. BACKGROUND

The dynamic behavior of space vehicles during different mission phases is a key consideration in their design, development, and verification. The complexity of a space vehicle like the Space Shuttle increases the difficulty required to accurately calculate this dynamic behavior especially to the accuracy requirements required by the Shuttle vehicle. The accuracy requirements are shown in Table 1 and were established by the various disciplines of pogo, loads, controls, and flutter. To meet this accuracy a full scale Mated Vertical Ground Vibration Test (MVGVT) program was required. The complexity of the Shuttle vehicle is unique. The Shuttle complexity is created by the coupled interaction of a four body system with many joints and local load paths. In addition, the Shuttle includes the viscoelastic effects of the SRB's with the unsymmetrical stiffness and mass effects of the Orbiter.

In the early phases of the test program there were a number of test configuration options available that would have possibly met configuration requirements. However, the problem was to arrive at a configuration that would be acceptable for the prediction and verification of an analytical structural dynamic model to a prescribed accuracy for use in controls, loads, pogo, and flutter while maintaining a program of low cost and minimum schedule impact. This led to the inevitable evolution of the test, test article, and test requirements.

The following at one time were considerations in the MVGVT program and deleted:

1) Use of water to simulate the LH_2 in the ET — The water would have introduced hydroelastic effects. Also, an 8 psid internal tank pressure would have had to be maintained in the tank during loading and testing or the aft dome would have sustained structural failure.

2) Use of polystyrene granules to simulate the LH_2 in the ET — The granules would have caused friction which could have affected damping and the granules themselves would have been costly.

3) Testing the maximum Q time condition — This time point was eliminated primarily due to cost; however, it was felt that testing of the two end conditions (liftoff and end burn) would be adequate.

4) Reduction of the orbiter payload from 65,000 to 32,000 lb — The payload weight was reduced because 32,000 lb was the heaviest payload flown on the first six flights. It was believed that the rigid 32,000 lb payload would adequately "work" the longerons in the payload bay without unduly influencing orbiter modes. Since it was not feasible to simulate various payload configurations, the scheme of adding ballast to the existing approach and landing test pallets was the least expensive method of providing for a dummy payload.

TABLE 1. TECHNICAL PROBLEM AREAS AND REQUIREMENTS

Items/Users	Control	Pogo	Flutter	Loads
Structure Model	Motion Sensor / Gimbal Force	Propellant Pressure / Thrust Force	Surface Motion / Aero Forces	High Stress Points / All Forces
Frequency Range	0 - 10 Hz	0 - 40 Hz	0 - 40 Hz	0 - 40 Hz
Frequency Accuracy	5% < 4 Hz, 10% > 4 Hz	5% < 3 Hz, 15% > 3 Hz	5%	10%
Damping Range	> 0.005	∿ 0.01	∿ 0.01	∿ 0.01
Damping Accuracy	10% < 4 Hz, 20% > 4 Hz	20%	20%	20%
Slope Accuracy	10% < 4 Hz, 20% > 4 Hz	N/A	15%	20%
Deflection Accuracy	10% < 4 Hz, 20% > 4 Hz	20%	15%	20%
Pressure Accuracy	N/A	30%	Not Tested	Not Tested

5) Use of water or drillers mud instead of inert propellant in the SRB for maximum Q — The use of these materials would have introduced adverse hydroelastic effects.

6) Have the SRB motors loaded with inert propellant to maximum Q then ballast the SRB for liftoff with sleeves either internal or external — This would have degraded the viscoelastic effect and in addition the stiffness of the SRBs would have been different from flight.

7) Considered a flexible payload, rather than one that was rigid — This would have overly complicated the analysis and math model correlation and subsequent modification of the math model benefit, although a rigid simulation on flexible supports was advantageous to check out payload/Orbiter interaction.

In the early phase of MVGVT there was a concern in the boost test that the test article would couple dynamically with Building 4550 through the overhead support truss and air bag assembly to the extent that the test data would be invalidated. To resolve this question, structural dynamic math modes of Building 4550, the overhead truss and air bag assembly, and the test article were generated. Modal characteristics of the coupled system were calculated and compared. The results showed that the spring supported test article provided isolation from Building 4550 and that the elastic modes of the test article were not affected by the modes of the building and the overhead truss.

IV. TEST REQUIREMENTS

The test article was subjected to sinusoidal excitation by driving shakers selected and located so as to excite and isolate all significant modes of vibration both symmetrical and antisymmetrical. The frequency range of interest that was surveyed is as follows:

1) For transverse excitation 1.5 to 30.0 Hz.

2) For longitudinal excitation 1.5 to 50.0 Hz.

The test objectives of the Shuttle vehicle MVGVT were:

1) To verify the coupled dynamic math models of the mated Shuttle configurations through correlation of analytical predictions to measured test data. These data shall consist of mated structural resonant frequencies, mode shapes and damping characteristics for selected simulated flight conditions.

2) To obtain experimentally the modal translation and rotations at the Orbiter and SRB guidance sensor and effector locations for the mated Orbiter/ET and Orbiter/ET/SRB configurations.

3) To obtain experimentally the test transfer functions from the excitation sources to the guidance and control sensor locations for the mated configurations.

4) To measure ET umbilical feedline modal data to verify the feedline math model.

A listing of the accuracy requirements for the Shuttle dynamic modal data as specified by the users, namely controls, pogo, flutter and loads are listed by disciplines in Table 1.

V. INSTRUMENTATION

The accelerometer locations selected were based on the Shuttle System pretest vibration analysis. The interfaces, ET/SRB (launch) and the ET/Orbiter (launch and boost), were of prime importance and were heavily instrumented. Instrumentation on the ET LOX tank, side walls, bulkhead, and sump areas were also emphasized such that the instrumentation correlated as much as possible with the LOX tank modal survey test. The instrumentation used was as follows:

1) Accelerometers - 320 Channels

2) Strain Gauges - 30 Channels

3) Force Transducers - 40 Channels

4) Pressure Transducers - 10 Channels

5) Rate Gyros - 9 Channels

VI. SHAKERS

The shakers used in the MVGVT were either rigid or suspended 150 lbf and 1000 lbf electrodynamic shakers. The rigid shakers were such that the combined shaker and support had no natural frequencies less than 100 Hz. The suspended shakers were free pendulum with a maximum frequency of 0.5 Hz.

For the launch liftoff and end burn tests, the pendulum frequencies of the cable mounted shaker assemblies prevented adequate shaker force from being transmitted to the test vehicle at low frequencies (Up to 2.5 Hz). This problem was solved by rigid mounting 20 selected 1000 lbf shakers which, once the low frequency data were obtained, were derigidized and cable mounted again.

VII. TEST EQUIPMENT

The data acquisition system used was SMTAS. The system has the capability to monitor, record, and process excitation input parameters up to 24 channels and display selected input parameters to the console operators. It has the capability to monitor, record, and process signals from 320 accelerometers and rate gyros, 45 force, and 50 pressure and strain gauge measurements. SMTAS provided control for a maximum of 24 shaker channels capable of driving a maximum of 38 shakers.

VIII. DATA REDUCTION

The modal frequencies determined to be of interest during the sweeps were individually tuned and purified. This isolation was accomplished by utilizing the following techniques.

1) Observation of input force/velocity Lissajous patterns.

2) Vector resolutions of force and acceleration in coquad plots.

3) Strip chart recordings of selected channels and decay traces.

4) Orthogonality charts.

SMTAS provided data printout for test evaluation by furnishing the following data formats:

1) Normalized orthogonality matrix showing mode numbers.

2) Shaker force distribution and polarity listing.

3) Transfer function plots — transducer response (Engineering units) versus frequency.

4) Modal vector plots.

5) Coincident — quadrature plots versus frequency.

6) Kinetic energy distribution tables.

7) Modal dwell data.

8) Plots of digitized decay traces.

9) Calculated force distribution listings.

10) Linear regression plots (launch).

11) Cross orthogonality plots (launch).

IX LAUNCH

A. Liftoff

1. Configuration. The liftoff (T + 0 sec) configuration tested consisted of the OV-101 Orbiter mated with an ET and two full solid SRB (Fig. 1).

a. External Tank. The ET was a flight weight tank assembly of production design configuration including the nose fairing, LOX tank assembly, intertank assembly, LH_2 tank assembly, orbiter to tank attach fitting, SRB to tank attach fittings, feedline and external tank to orbiter feedline disconnects. There was no simulated LH_2. The LOX tank fuel was simulated with de-ionized sodium-chromate-inhibited water.

b. Orbiter. The Orbiter OV-101 was a flight type production with modifications required for MVGVT. The OMS Pc ' were mass simulators with elastic link actuator simulators with gimbal blocks. The payload installed on the orbiter consisted of two 16,000 lb rigid ballasted pallets.

c. SRB. The SRB's were flight type production assemblies. A pressure ring on each of the SRB's for liftoff only was installed at the aft SRB/ET attachment. These rings were installed to simulate the effects of internal pressure of the ignited SRB's by adding stiffness. The pressure rings were removed later during the test to examine the dynamic effects between the "rings on" and "rings off" condition. The SRB nozzles were omitted.

2. Suspension. The liftoff test configuration utilized a soft suspension system that was provided by the four existing Saturn V Hydrodynamic Support (HDS) Units. The HDS's provided the vertical support as shown in Figure 2 and six degrees of freedom for the supported vehicle. Each SRB aft skirt was attached to an adapter truss which rested on the HDS system. The lateral stability and soft spring rate in pitch and yaw were provided by Firestone air bags #323 and #319, respectively. The lower bags were attached to the SRB aft skirt and the upper bags were attached to the SRB frustrum. The suspension system is presented in Figure 3.

3. Test Results and Analysis.

a. Suspension System Modes. Six rigid body suspension system modes were obtained and are summarized in Table 2. The suspension system modes assure that an adequate separation exists between the elastic modes and the rigid body modes. Phasing of the instrumentation was also accomplished at this time. All six modes showed excellent agreement.

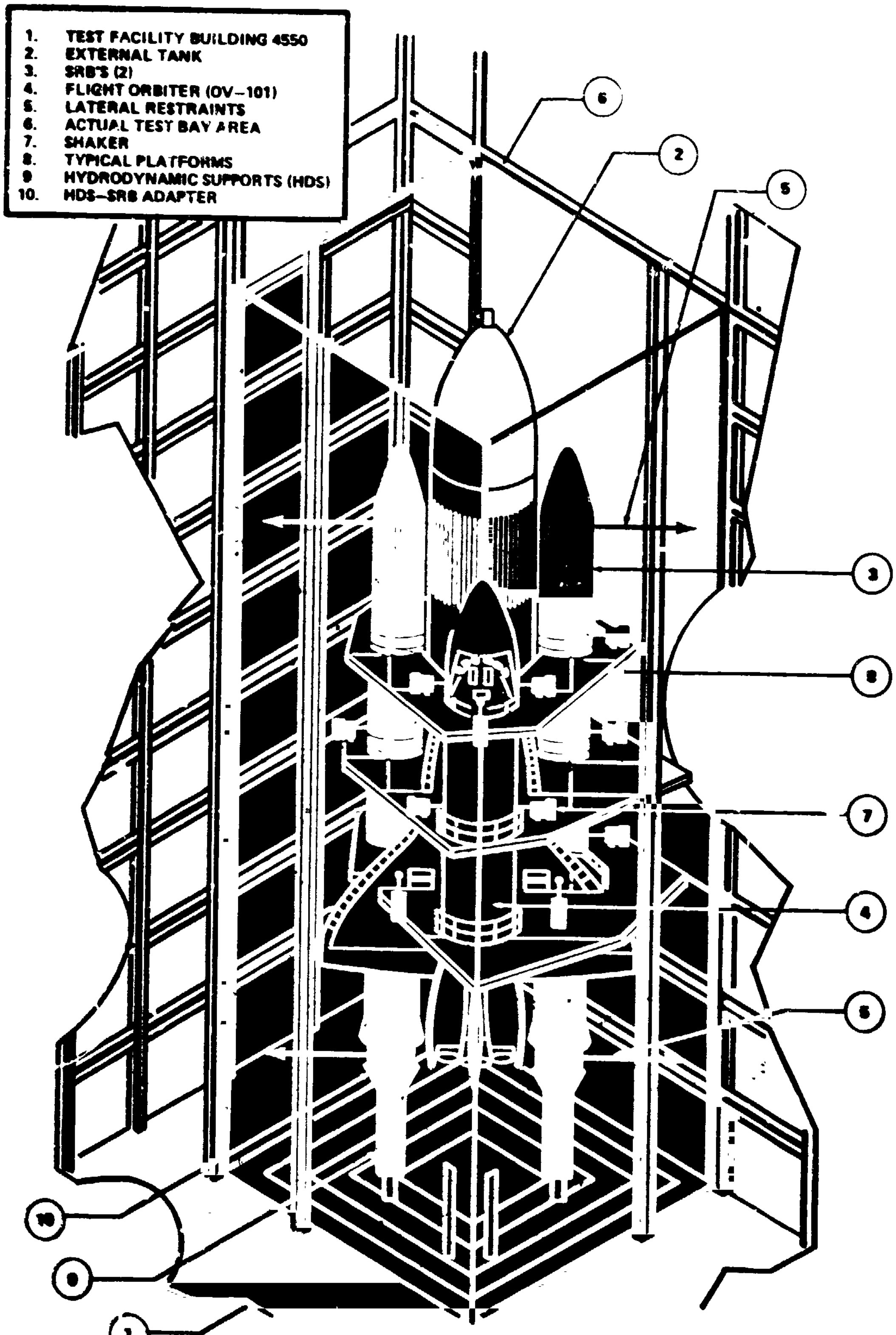

Figure 1. Launch configuration.

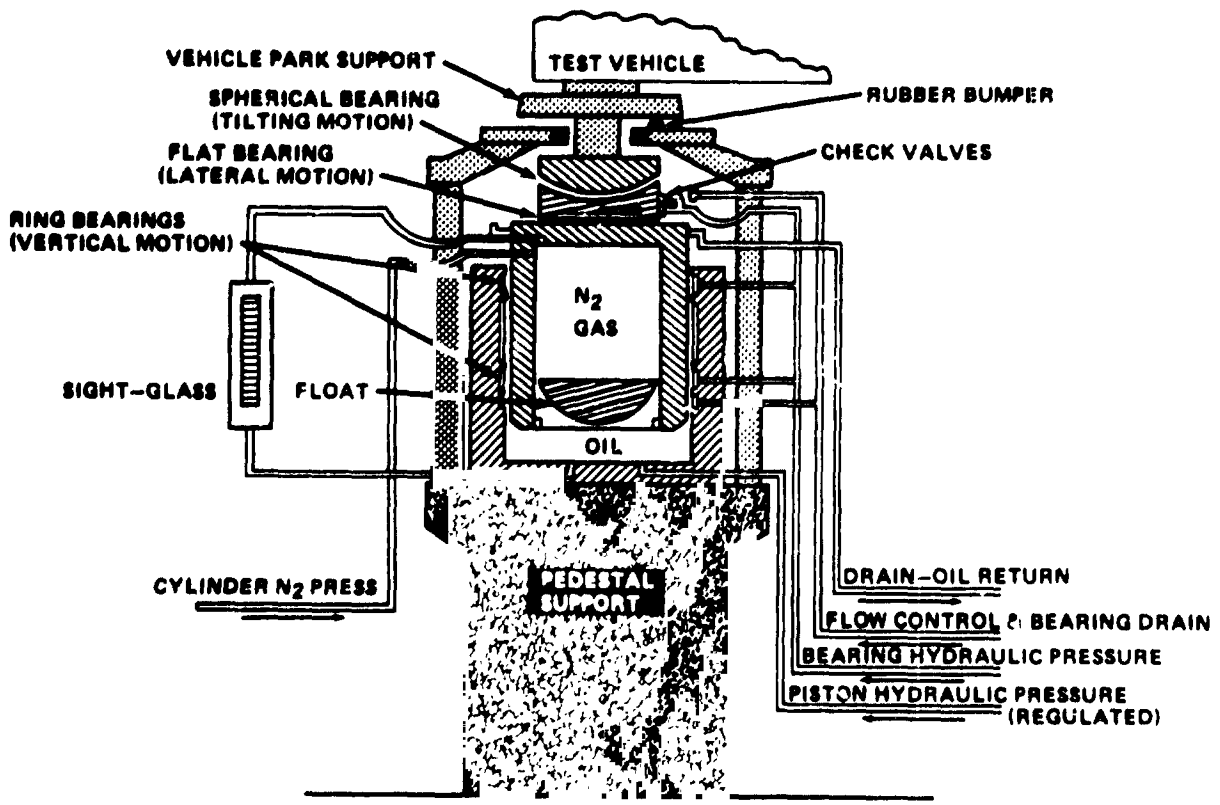

Figure 2. Typical hydraulic dynamic support.

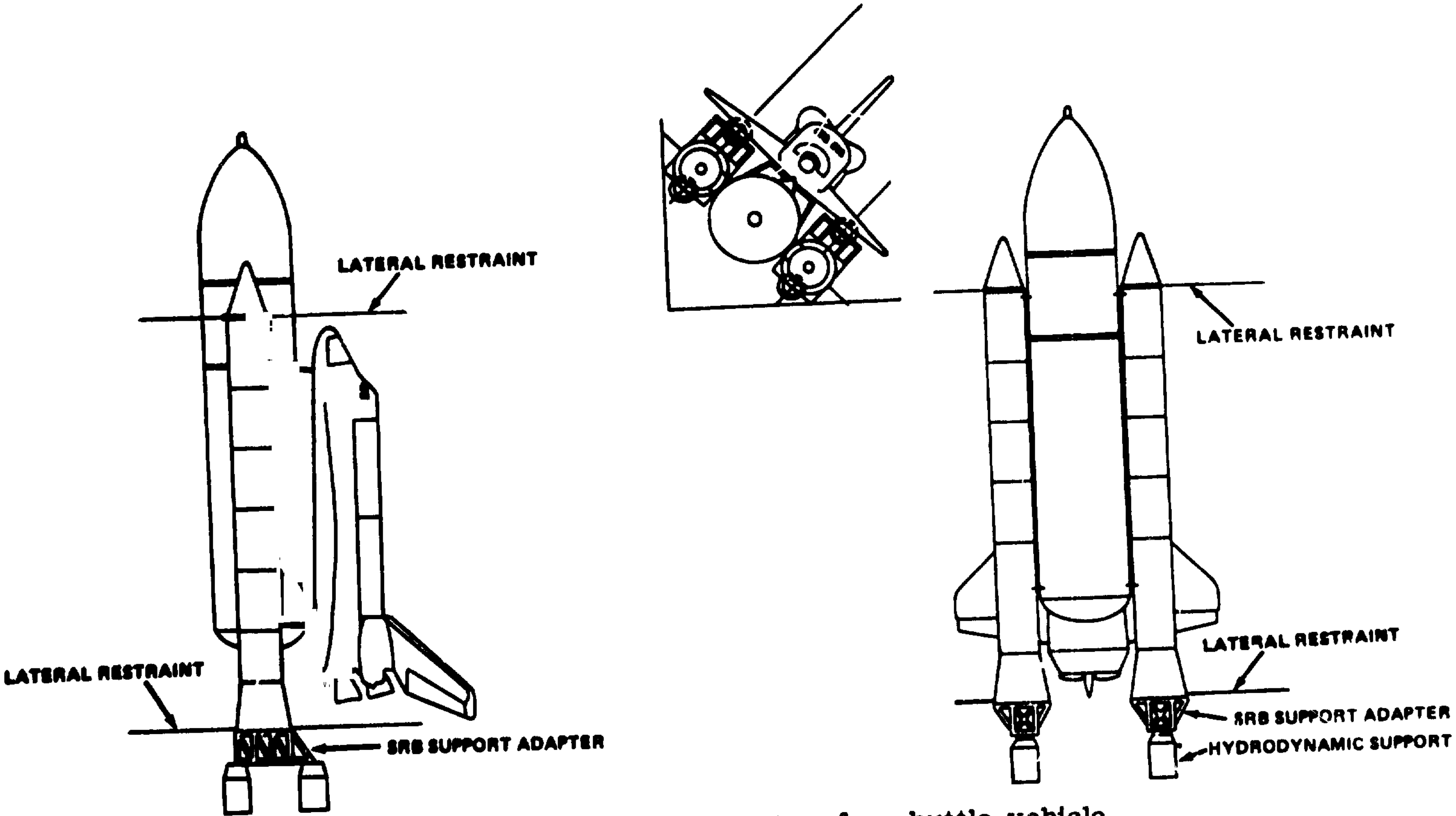

Figure 3. Suspension system for shuttle vehicle.

TABLE 2. LIFTOFF SUSPENSION SYSTEM MODES

Mode No.	Test Frequency (Hz)	Predicted Frequency (Hz)	Description of Motion
3	0.196	0.193	Z-Translation
6	0.24	0.23	Y-Translation
35	0.27	0.27	θX (Roll)
4	0.314	0.338	θY (Pitch)
4	0.510	0.50	θZ (Yaw)
1	0.67	0.68	X-Translation

b. Flight Control Transfer Functions. Flight control transfer functions for seven sweeps are enumerated in Table 3. Three additional sweeps were taken using shakers on the Orbiter and SRB to excite the modes and are shown in Table 3A.

During one of the sweeps an abnormally high transfer function value was observed on both SRB's at the forward SRB mounting rings where the rate gyros are mounted. This was due to a local resonance of the rate gyros caused by a large (Approximately 200 lb) avionic box mounted on the ring frame. The left SRB local resonance occurred at 23 Hz and the right SRB resonance occurred at 25 Hz. These local resonances were subsequently verified in a separate modal survey test of the left and right SRB forward skirt and nose cone assembly. To alleviate this problem, the ring frames of both SRB's were structurally stiffened which increased the local resonant frequency and decreased the amplitude gain.

The flight control group identified a number of significant structural modes that appeared on the transfer function sweeps. These modes were assigned priority numbers based on importance to flight controls and are listed in Tables 4 and 5.

c. Pogo Wide Band Sweeps. Wide band frequency sweeps were run independently on all three orbiter main engines. The excitation force in each case was along the engine longitudinal axis. Table 6 lists the sweep number and frequency range for each engine sweep. The six engine axial modes above 16 Hz were identified and dwells were taken.

d. Modal Test Results versus Pretest Analysis. All acceptable modes tuned during liftoff symmetric tests are shown in Table 7. The antisymmetrical modes are shown in Table 8. The correlating pretest analytical frequency and the computed modal damping from the decay traces are also shown in those tables. The last column gives the percent error between the test and analytical mode.

For each modal dwell, at a resonant frequency, a set of data was generated by SMTAS for that mode. A typical data set is shown in Figures 4 through 19. This particular mode is a symmetric mode that occurs at a frequency of 2.059 Hz and is a coupled pitch/roll mode of the SRB's. Figures 4 through 10 show the overall view of the test article with displacement vectors (quad amplitude) which is an aid in defining the mode.

Figure 11 presents a tabulation of the acceleration broken down into coincident (CO) and quadrature (quad) with phase angle for each accelerometer recorded. Figure 12 shows the force levels used to tune that particular mode to its resonance. There are 32 shakers available; however, only a few selected ones are used in the tuning of a particular mode. The orthogonality between the test modes is shown in a matrix in Figure 13 and Figure 15 lists the modal generalized mass.

TABLE 3. LIFTOFF FCS SWEEPS

Sweep No.	Shakers	Phase (deg)	Type Motion		SMTAS Sweep No. 1-7 Hz	SMTAS Sweep No. 7-17 Hz	SMTAS Sweep No. 17-30 Hz
1	RT/RB14Y LT/LB14Y	180/0 0/180	SRB Yaw		1	6	7
2	FL10Y FL11Y	0 0	ORB Yaw		5	8	9
3	RR06Z/RL07Z LL06Z/LR07Z	0/180 0/180	SRB Pitch	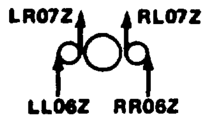	17	19	20
4	FB10Z/FB11Z	0/0	ORB Pitch		4	10	11
5	RR06Z/RL07Z LL06Z/LR07Z	180/0 0/180	SRB Roll	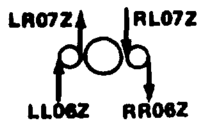	18	21	22
6	FB10Z/FB11Z	0/180	ORB Roll		3	12	13
7	MT01X	0	ENG No. 1 Axial		2-30 Hz 14		

TABLE 3A. (Concluded)

Sweep No.	Shakers	Phase (deg)	Type Motion	SMTAS Sweep No. 2-15 Hz
8	RR/LL06Z RL/LR07Z FB10Z/FB11Z	0/180 180/0 0/180	Pitch 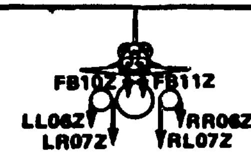	24
9	RB/RT14Y LB/LT14Y FL10Y FL11Y	0/180 180/0 0 0	Yaw 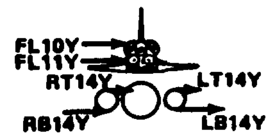	23
10	RR/LL06Z RL/LR07Z FB10Z/FB11Z	0/180 180/0 0/180	Roll 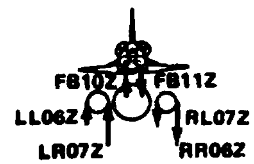	25

TABLE 4. FLIGHT CONTROL FREQUENCY PRIORITIES
(SYMMETRIC MVGVT LIFTOFF MODES)

Test		Approximate Transfer Function Resp. Freq. (Hz)	Test Mode Description Dominant Motion (Kinetic Energy)	Response Channel Priority*			
Mode No.	Frequency (Hz)			SRB Pitch RGA's	ORB Pitch RGA's	ORB Norm. Flt. Cont. Accel.	Nav. Base Pitch RGA
5	2.05	2.1	SRB Pitch (0.25) and Roll (0.34), ORB-ET Z Trans (0.24)	1	1	1	3
9	3.02	3.0	SRB Pitch (0.38) and Roll (0.27). ET Pitch (0.10). ORB Z Trans (0.10)	1	1	1	3
11	3.23	3.3	ORB Pitch (0.33), X (0.36), SRB Z Bend (0.25)	2	1	1	3
23	4.39	4.4	FDLN-X (0.17). ORB Z (0.17), SRB X (0.17). Z (0.22)		2		3
14	5.25	5.2	ORB Z Bend (0.17), ET Z Bend (0.27), SRB 1st Z Bend (0.46)	1	2	2	3
18	5.65	5.6	ORB X (0.18), Z (0.55), SRB Z (0.09)		2	2	3
13	9.0	9.0	ORB Z Bend (0.76), Out of ℄ with SRB Z Bend (0.06)			4	4
2 A/S?	10.1 A/S?	10.0		4	4		4
26	11.94	12.2	SRB 2nd Y (0.7), I.T. (0.08)				4
22	12.41	12.5	LWR Ogive (0.19), Dome Bulge, Feedline (0.15)				4
19	14.52	14.5	F/A Payload X (0.05) Out of ℄, ORB Z Bend (0.08) LWR ENG P (0.07)				4
--	--	23	Local LSRB RGA Ring Resonance/SRB 4th Z Bend	1			
--	--	25	Local RSRB RGA Ring Resonance/SRB 3rd Y Bend	1			

*Code: 1 = Most Significant
4 = Least Significant

TABLE 5. FLIGHT CONTROL FREQUENCY PRIORITIES (ANTISYMMETRIC MVGVT LIFTOFF MODES)

Test: Mode No.	Test: Frequency (Hz)	Approximate Transfer Function Response Freq. (Hz)	Test Mode Description Dominant Motion (Kinetic Energy)	Response Channel Priority*: SRB Yaw RGA	ORB RGA's: Yaw	ORB RGA's: Roll	ORB FC Accel.: Norm	ORB FC Accel.: Lat	Nav. Base RGA's: Yaw	Nav. Base RGA's: Roll
10	2.08	2.1	SRB Y Bend (0.63) ET out : with SRB (0.21). SRB X (0.12)	1	1			1	2	
8	2.23	2.2	SRB Pitch (0.48) and Roll (0.13). ORB Y (0.21)			1	1	1	2	1
11	2.47	2.5	SRB Pitch (0.59) and Roll (0.13). ORB Roll and Yaw (0.12). ET Roll			1	1	1		1
13	3.57	3.5	SRB Pitch (0.12). Rell (0.07) and Yaw (0.08). V.T. Side Bend (0.26)		2			2		
27	3.53	3.5	Gear Train. ORB Y (0.42). SRB Z (0.28)		2			2		
5	4.12	4.2	SRB Z Bend (0.62) with Roll (0.08). ORB Yaw (0.18)	1	3			1	3	
205	5.13	5.2	SRB 1st Y Bending	1	1			3		
1	5.45	5.5	SRB 1st Z Bend (0.43). Y Bend (0.12). Wing Bend (0.07)		3			3		
10 sym?	6.43 sym?	6.2			3					
18	9.3	9.5	Upper E.T. Torsion						4	
19	10.65	10.8	SRB 2nd Y Bend (0.61). Z Bend (0.29)	4	4				4	
31	13.89	13.8	V.T. Torsion (0.68). Elevon Z (0.09)						4	
7	23.84	23	Local LSRB RGA Ring Resonance/SRB 4th Z Bend (0.65)	1						
30	24.81	25	Local RSRB RGA Ring Resonance/SRB 3rd Y Bend	1						

*Code: 1 = Most Significant
4 = Least Significant

TABLE 6. LIFTOFF POGO SWEEPS

Excitation	Frequency Range Segments, Hz Sweep No. ( )		
Upper SSME Axial	2-12 (1)	12-30 (2)	30-50 (3)
Lower Left SSME Axial	2-12 (4)	12-30 (5)	30-50 (6)
Lower Right SSME Axial	2-12 (7)	12-30 (8)	30-50 (9)

TABLE 7. MVGVT MODAL CORRELATION [CONFIGURATION – LIFTOFF (SYMMETRIC)]

Test Mode				Analysis Mode			
Mode No.	Freq.	Damp	Description	Mode No.	Freq.	Description	Percent Error
5	2.05	0.013	SRB Roll (0.34), Pitch (0.25), Yaw (0.16), Orbiter Pitch (0.08), ET-Z (0.13)	4	2.11	SRB Roll (0.38), Pitch (0.45), Yaw (0.04), Orbiter Pitch (0.04), ET-Z (0.07)	3
7	2.64	0.014	SRB Yaw (0.95), ET Pitch (0.02)	6 5	2.93 2.45	SRB Yaw (0.84), ET Pitch (0.02) SRB Yaw (0.83), ET X (0.07)	11 8
9	3.02	0.017	SRB Pitch (0.38), Roll (0.27), ET-Z, Bending (0.10), Orbiter-Z (0.07)	8	3.18	SRB Pitch (0.38), Roll (0.34), ET-Z, Bending (0.06), Orbiter-Z (0.08)	5
11	3.24	0.010	ORB Bending (0.32), X (0.36), SRB Z-Bending (0.25)	7	3.14	Orbiter Bending (0.44), X (0.43), SRB Z-Bending (0.06)	-3
12	3.88	0.015	SRB-X (0.60), Yaw (0.13), FWD ET Shell (0.24)	9	3.87	SRB-X (0.47), Yaw (0.38), FWD ET Shell (0.14)	< 1
23	4.39	0.0013	SRB Z-Bending (0.22), Roll (0.08), F/L Fluid (0.17), Orbiter Bend (0.17)	11	5.16	SRB Z-Bending (0.26), Roll (0.06), Orbiter Bending (0.54)	* 18
14	5.26	0.016	SRB Z-Bending (0.47), ET Bending (0.27), Orbiter Bending (0.17)	12	5.39	SRB Z-Bending (0.15), Y-Bending (0.13), ET Bending, Axial (0.33), ORB Bend (0.15)	2
13	5.65	0.005	Orbiter Pitch, Bending, In-Phase Wing Bending (0.55), Orbiter X (0.18)	11	5.16	Orbiter Z, Bending, In-Phase Wing Bending (0.54), Orbiter X (0.03)	-9
10	6.43	0.037	1st Wing Bending (0.68), Out-of-Phase Upper SSME (0.13)	15	6.60	1st Wing Bending (0.64)	3
21	6.78	0.011	SRB Sym Yaw and Y-Bending (0.85)	18	7.62	SRB Sym Yaw and Y-Bending (0.67), Propellant (0.12)	12
15	7.02	0.011	VERT Tail FWD/AFT Rocking (0.21), Out-of-Phase Wing Bending (0.18)	16	6.88	Vert Tail FWD/AFT Rocking (0.07), Out-of-Phase Wing Bending (0.22)	-2

*Correlation not reliable
% error–error not applicable

TABLE 7. (Continued)

Test Mode				Analysis Mode			
Mode No.	Freq.	Damp	Description	Mode No.	Freq.	Description	Percent Error
32	7.45	0.031	SSME No. 3 Pitch (0.20), Out-of-Phase V.T. FWD/AFT Rocking (0.11)	20	8.08	LWR SSME Pitch (0.50), Out-of-Phase V.T. FWD/AFT Rocking (0.41)	8
27	7.77	0.009	1st LOX Tank Bulge. UPR LH_2 (0.34). LOX Ogive (0.14)	18	7.62	Bulge Mode Overwhelmed by SRB Energy	-2
16	8.42	0.016	SRB 2nd Z-Bending (0.62). Roll (0.05)	22	8.36	SRB 2nd Z-Bending (0.67), Roll (0.08)	-1
13	9.00	0.008	Orbiter Pitch and Bending (0.76). Out-of-Phase SRB Pitch (0.06)	26	9.40	Orbiter Pitch and Bending (0.76). Out-of-Phase SRB (0.02)	4
26	11.94	0.025	SRB 2nd Y-Bending (0.71). Motor Case No. 3 Prop (0.00)	32	10.91	SRB 2nd Y-Bend (0.37). No. 3 Prop (0.48)	10
				50	14.20	SRB 2nd Y-Bend (0.47). ET Y-Bend (0.40)	19
22	12.41	0.002	LOX Dome Bulge (0.0016). F/L (0.15). LOX Tank (0.29)	44	12.99	LOX Dome Bulge (0.0064). F/L (0.0001). LOX Tank (0.55)	5
19	14.52	0.010	FWD/AFT P/L X Out-of-Phase (0.14). LWR SSME Pitch (0.16)	72	17.89	FWD/AFT P/L X Out-of-Phase (0.31)	23
30	14.87	0.022	SRB Torsion (0.58). ET (0.14)	54	14.73	SRB Torsion (0.37), ET (0.12)	1
31	14.87	0.030	Outb'd Elev ROT Out-of-Phase With Inb'd Elev (0.22)	53	14.61	Outb'd Elev ROT Out-of-Phase With Inb'd Elev (0.11), SRB Torsion (0.30)	2
33	15.97	0.008	LOX Dome Bulge (0.0066). LOX Tank (0.30). SRB Axial (0.12)	57	15.15	LOX Dome Bulge (0.0025), LOX Tank (0.17), SRB Propellant (0.42)	5
17	15.97	0.027	Payload Pitch (0.12), OMS POD X (0.18). ET (0.25)				

TABLE 7. (Concluded)

Test Mode				Analysis Mode			
Mode No.	Freq.	Damp	Description	Mode No.	Freq.	Description	Percent Error
25	16.15	0.012	OMS POS X (0.16), Out-of-Phase P/L X (0.07), Crew Mod X (0.03) and Z (0.05), ET (0.28)				
35	18.96	0.041	SRB Axial (0.43), LOX Dome (0.0092), ET (0.48)	6[illegible]	15.90	SRB Axial Out-of-Phase with Propellant (0.12), LOX Dome (0.0054), ET (0.85)	19
36	27.48		SSME Axial, UPR Out-of-Phase with LWR (0.22) OMS POD (0.33), ET (0.20)				
39	30.53	0.014	SSME Axial, LWR Out-of-Phase with UPR (0.28), OMS POD (0.06), ET (0.35)				
34	31.23	0.044	UPR SSME Axial (0.31), OMS POD (0.19), ET (0.24)	169	32.97	UPR SSME Axial (0.44), OMS POD (0.07), ET (0.16)	6
37	34.74	0.018	UPR SSME (0.48) Axial In-Phase with LWR (0.01), OMS POD (0.14), ET (0.07)	184	36.69	UPR SSME Axial (0.56), OMS POD (0.05), ET (0.01)	6

TABLE 8. MVGVT MODAL CORRELATION [CONFIGURATION - LIFTOFF (ANTISYMMETRIC)]

Test Mode				Analysis Mode			Percent Error
Mode No.	Freq.	Damp	Description	Mode No.	Freq.	Description	
10	2.08	0.010	SRB Yaw and Y-Bending (0.63), ET YB (0.20)	4	2.20	SRB Yaw and Y-Bending (0.74)	6
8	2.24	0.010	SRB Pitch (0.33), Roll (0.18), Orbiter Y-Bend (0.29), Roll (0.03)	5	2.31	SRB Pitch (0.82), Roll (0.07), Orbiter Y-Bend (0.03)	3
11	2.47	0.014	SRB Pitch (0.60), Roll (0.12), Orbiter Roll and Yaw (0.12)	6	2.73	SRB Pitch (0.13), Roll (0.31), Orbiter Roll and Yaw (0.41)	10
15	3.37	0.016 0.022	SRB X(0.35), Y-Bend (0.16), Vert Tail Y-Bend (0.16)	7	3.61	SRB X (0.58), Y-Bend (0.13), Vert Tail Y-Bend (0.06)	7
27	3.53	0.005 0.007	Gear Train, SRB Roll (0.08), ET (0.09), Vert Tail Y-Bend (0.40)	8	3.76	Gear Train, SRB Roll (0.11), ET (0.01), Vert Tail Y-Bend (0.57)	7
5	4.12	0.014	SRB Roll (0.20), Z-Bend (0.0[illegible]), ORB Yaw (0.44), Incld C/M Y (0.10)	9	3.86	SRB Roll (0.25), Z-Bend (0.16), ORB Yaw (0.27), Incld C/M Y (0.07)	7
21	4.71	0.010	SRB Roll (0.27), Pitch (0.12), ORB Yaw and Roll (0.39)	11	4.88	SRB Yaw (0.25), Pitch (0.05), Roll (0.02), ORB Yaw and Roll (0.58)	4
28	4.98	0.016	Wing 1st Bend (0.38), SRB Y (0.14), SRB Z (0.19), FUS Y (0.08)	15	6.0	Wing 1st Bending (0.27), F P/L Y 0.20), SRB Y (0.09), SRB Z (0.06), Fuse Y (0.05)	
20	5.14	0.014 0.017	SRB Y-Bend (0.59), Z (0.13), Roll (0.03), ET Y Bend (0.13)	12	5.42	SRB Y-Bend (0.41), ET Y-Bend (0.23)	5
1	5.45	0.013	SRB Z-Bend (0.43), Y-Bend (0.12), OMS POD Y (0.05)	14	5.55	SRB Z-Bend (0.64), Y-Bend (0.03), Roll (0.03)	2
25	5.57	0.016	Orbiter Yaw and Y-Bend (0.31), SRB Y-Bend (0.18), Z-Bend (0.15), Roll (0.04)	15	6.01	Orbiter Yaw and Y-Bend (0.47), SRB Y-Bend (0.09), Z-Bend (0.07)	8

TABLE 8. (Continued)

Test Mode				Analysis Mode			
Mode No.	Freq.	Damp	Description	Mode No.	Freq.	Description	Percent Error
16	7.41	0.22 0.28	ET Y-Bend (0.72), SRB Y-Bend (0.11)	18	6.99	ET Y-Bend (0.46), SRB Y-Bend (0.28)	6
24	8.30	0.010	Payload Y Out-of-Phase (0.21), FUS Torsion (0.21), Out-of-Phase Wing Bend (0.10)	23	8.90	AFT Payload (0.03), FUS Torsion (0.20), Out-of-Phase Wing Bend (0.14)	7
18	9.28	0.011	ET LOX Tank Torsion	28	10.21	ET LOX Tank Torsion	10
2	10.10	0.028	SRB 2nd Z-Bend (0.60), Yaw (0.10), Axial (0.04)	32	10.63	SRB 2nd Z-Bend (0.56), Yaw (0.15), Axial (0.04)	5
19	10.65	0.022	SRB 2nd Y-Bend (0.61), Z-Bend (0.29)	35	11.24	SRB 2nd Y-Bend (0.60), Z-Bend (0.19)	6
31	13.89		Vert Tail Torsion (0.68)	61	16.22	Vert Tail Torsion (0.39), Outb'd Elev. Twist (0.15)	17
17	14.56	0.010	Gear Train W/SRB Torsion ET Roll (0.53), SRB Torsion (0.36)	47	14.20	Gear Train W/SRB Torsion ET Roll (0.53), SRB Torsion (0.15)	3
12	14.72	0.028	Gear Train W/ET Torsion (0.12), and SRB Torsion (0.59)	47	14.20		4
3	16.85	0.037	SRB 3rd Z-Bend (0.61), ET Shell (0.24)	64	16.69	SRB 3rd Z-Bend (0.55), ET Shell (0.19)	1
29	17.61		Crew MOD Y (0.06), Out-of-Phase FWD FUS Side Bend (0.29)	72	18.30	Crew MOD Y (0.06), Out-of-Phase FWD FUS Side Bend (0.21)	4
14	18.90	0.030	SRB Axial (0.78)	87	20.75	SRB Axial (0.59), Y-Bend (0.28)	10
26	21.54	0.02	Fuselage Torsion, Side Bend, Yaw (0.25), OMS POD (0.17)	72	18.30	Fuselage Torsion, Side Bend, Yaw (19), OMS POD (0.15)	18

TABLE 8. (Concluded)

Test Mode				Analysis Mode			Percent Error
Mode No.	Freq.	Damp	Description	Mode No.	Freq.	Description	
7	23.84	0.022	SRB 4th Z-Bend (0.65)	112	24.89	SRB Z-Bending (0.41)	4
30	24.81	0.012	SRB 4th Y-Bending (0.63)	123	26.35	SRB Y-Bending (0.47)	6

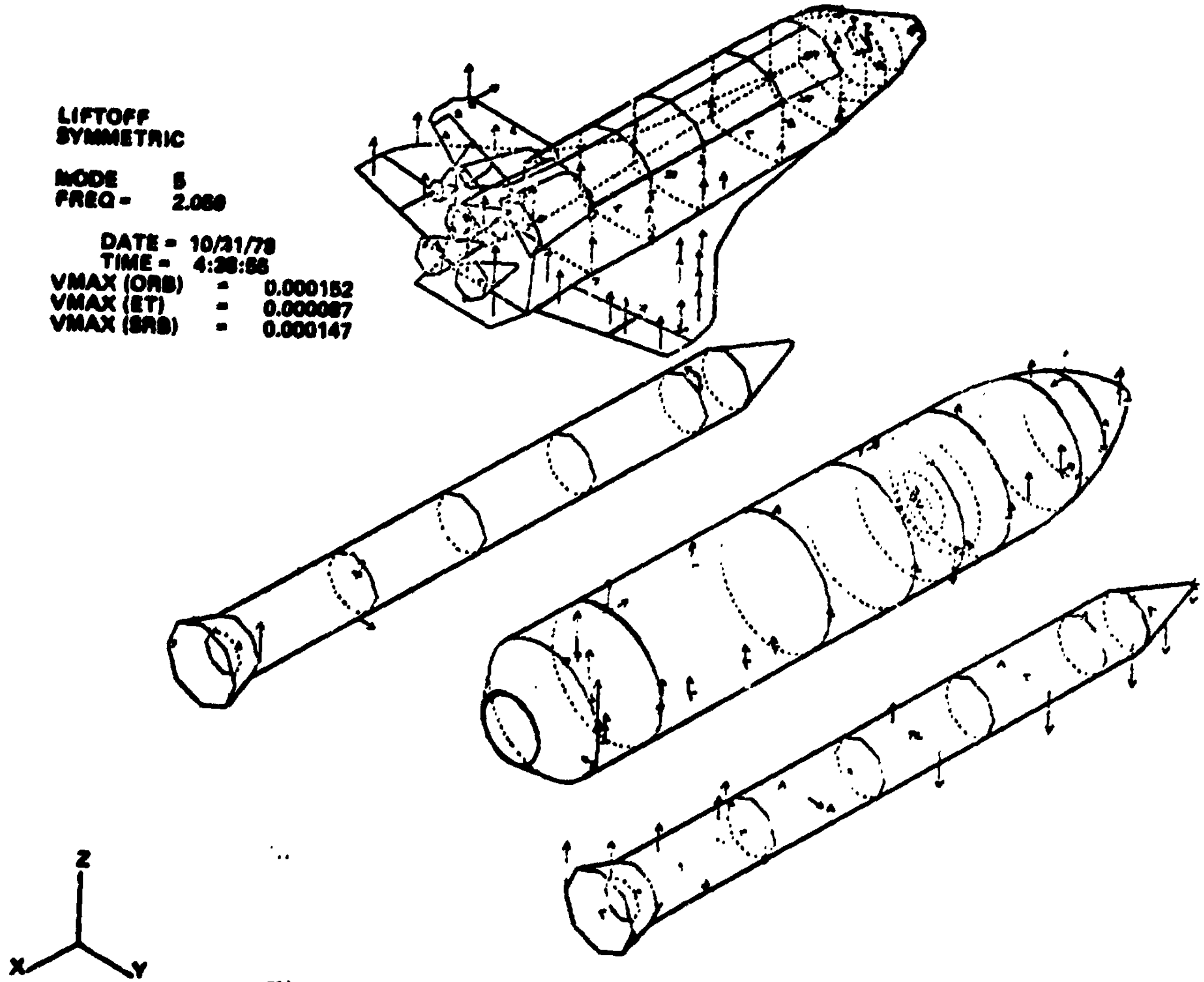

Figure 4. Space Shuttle MVGVT Orbiter/ET/SRB.

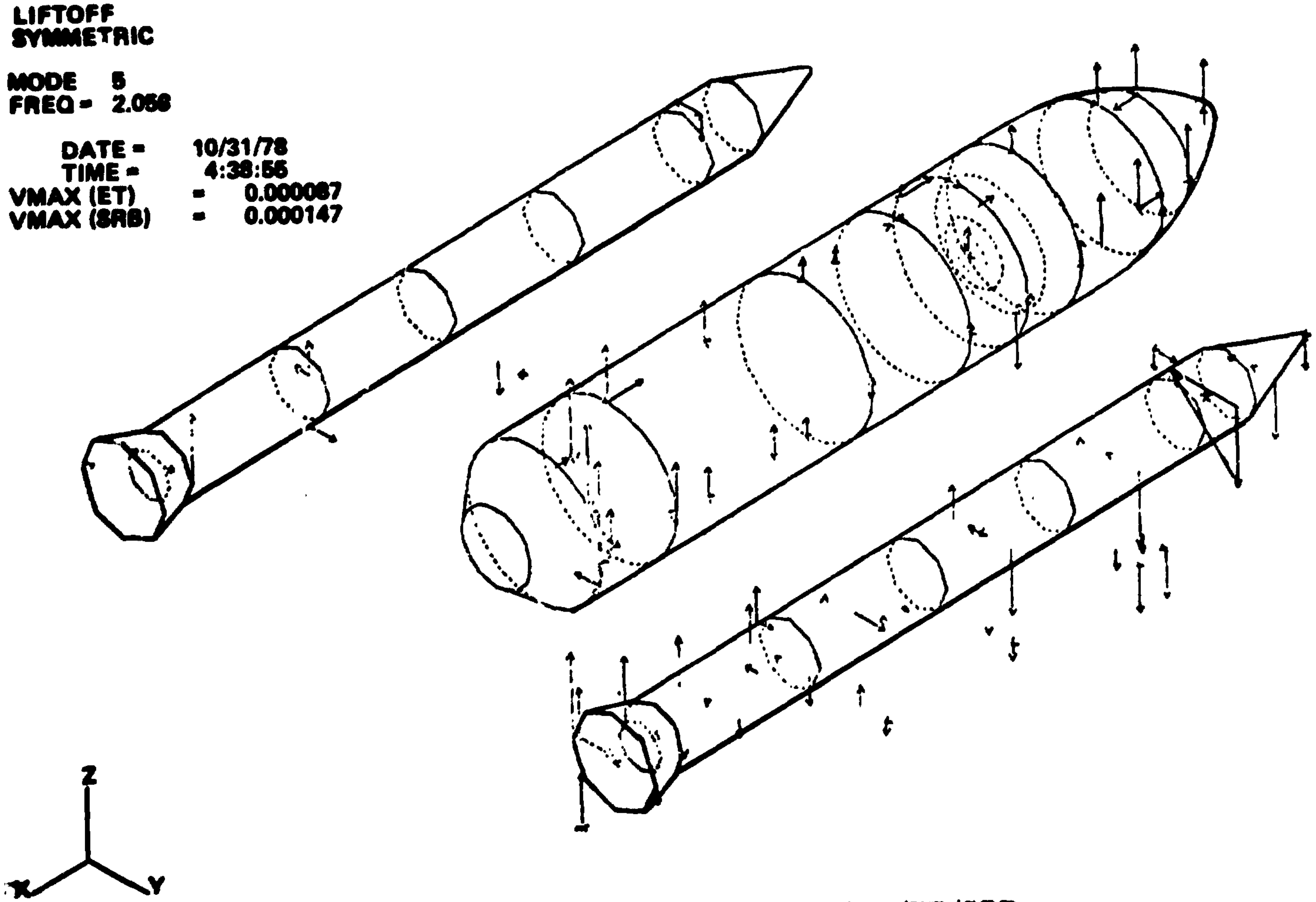

Figure 5. Space Shuttle MVGVT Orbiter/ET/SRB.

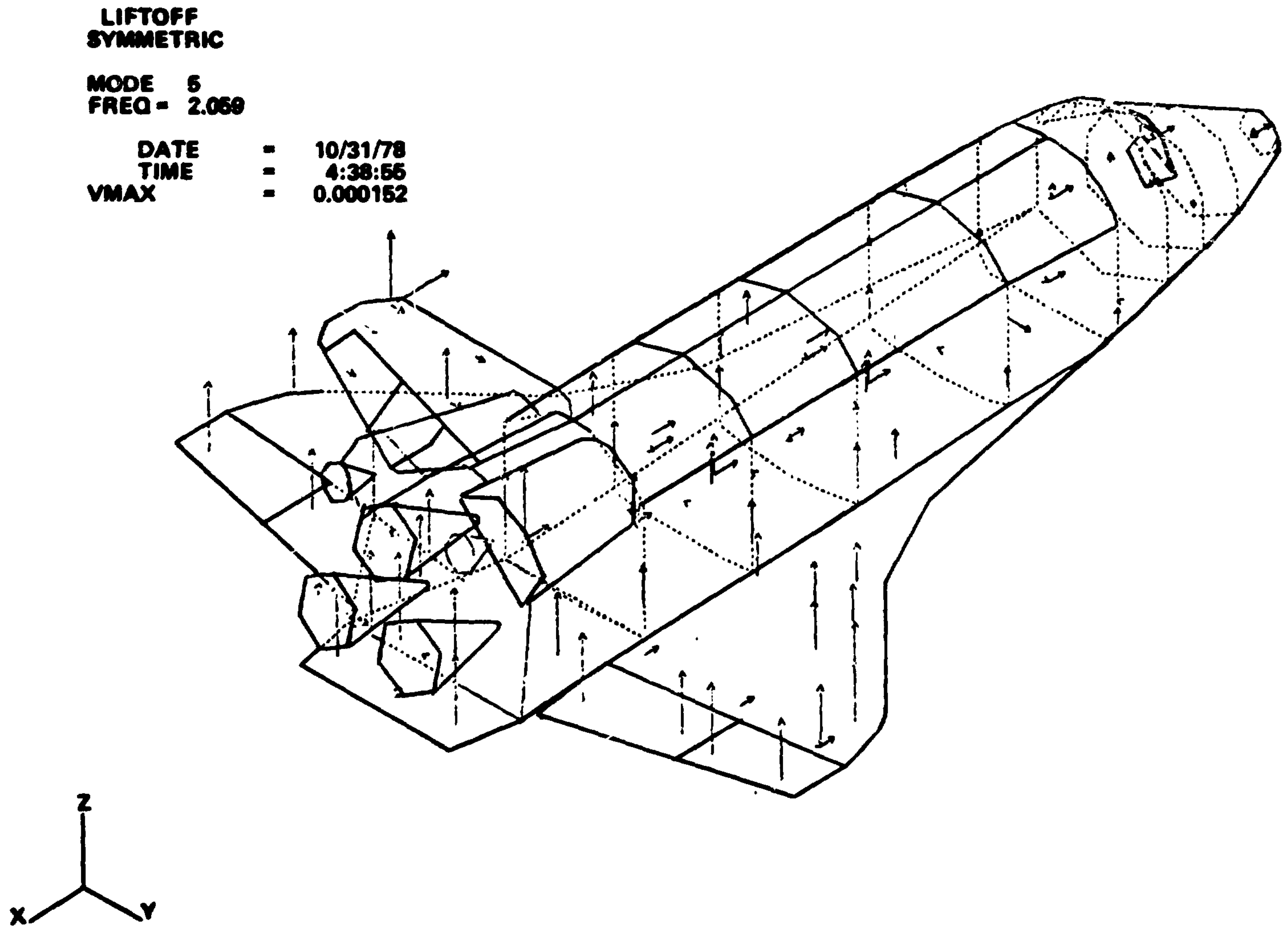

Figure 6. Space Shuttle MVGVT Orbiter/ET/SRB.

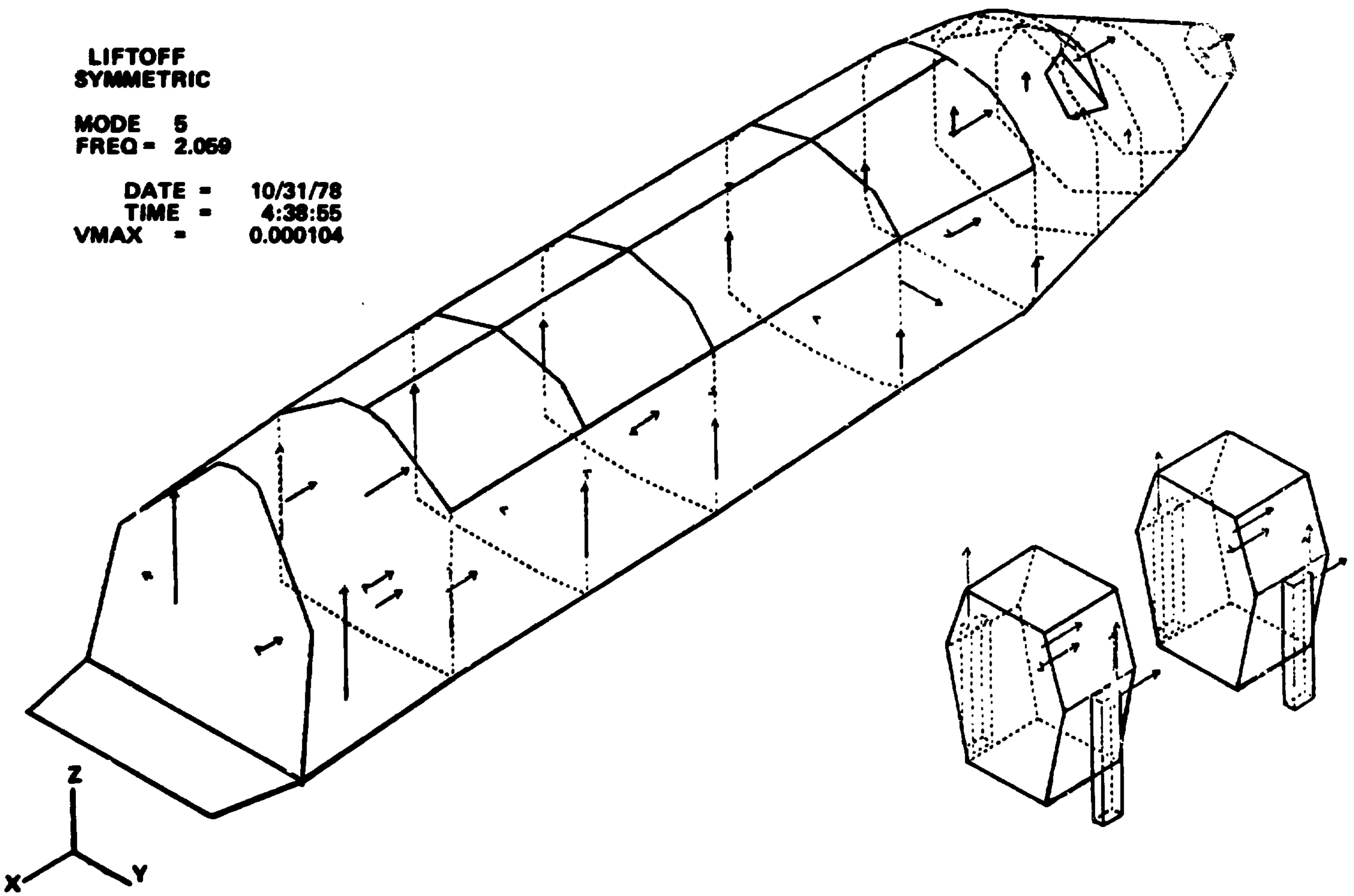

Figure 7. Space Shuttle MVGVT Orbiter/ET/SRB.

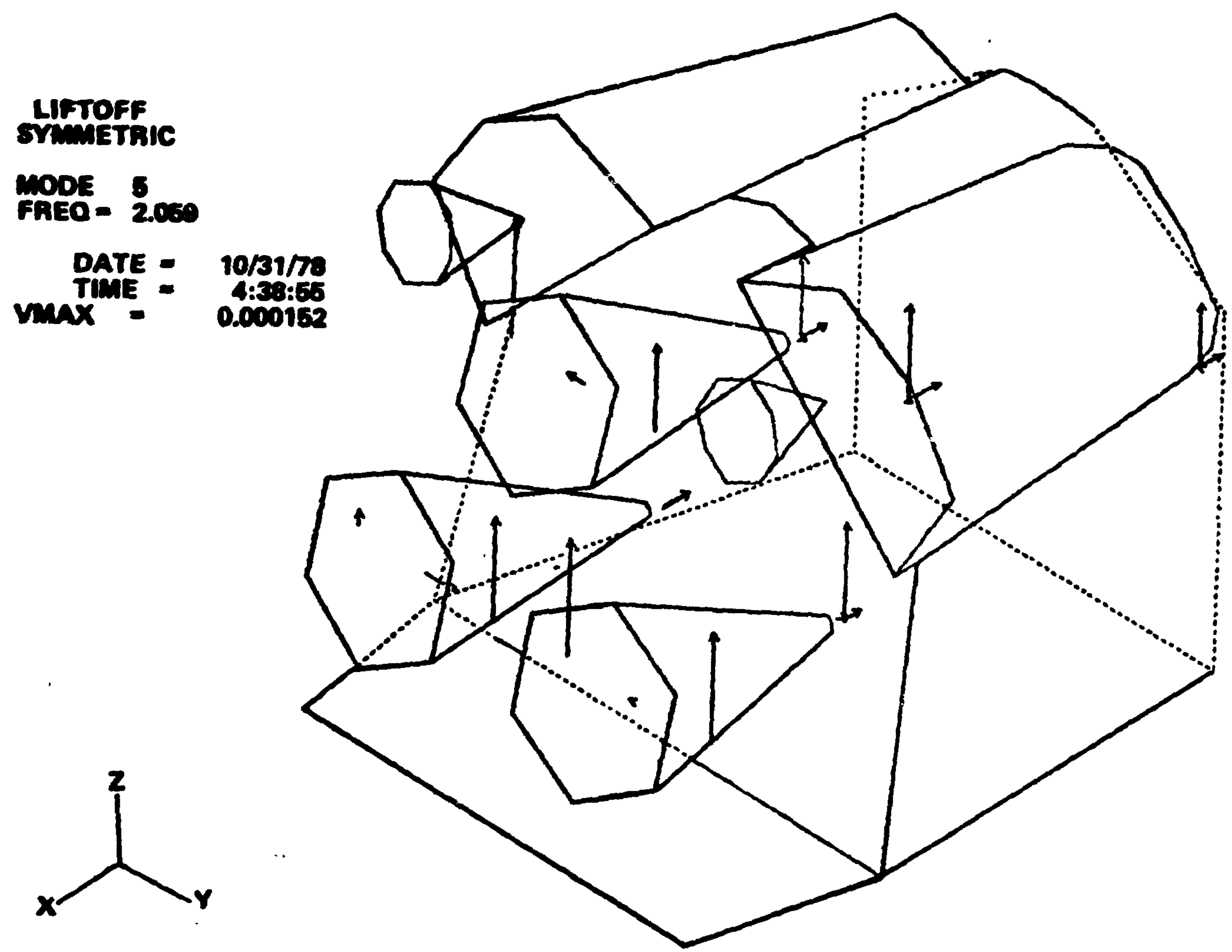

Figure 8. Space Shuttle MVGVT Orbiter/ET/SRB.

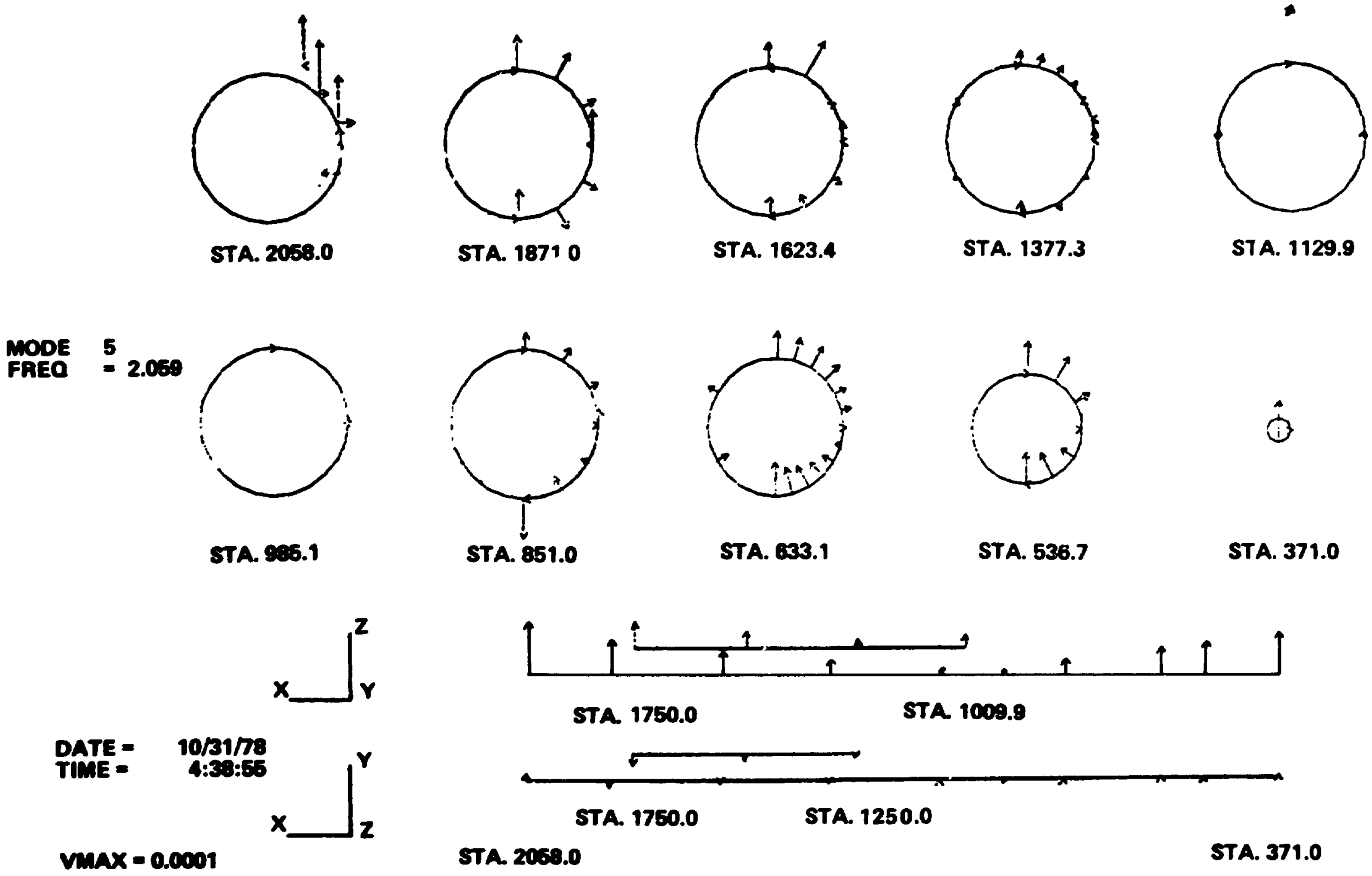

Figure 9. Space Shuttle MVGVT Orbiter/ET/SRB External Tank Lift-Off Symmetric.

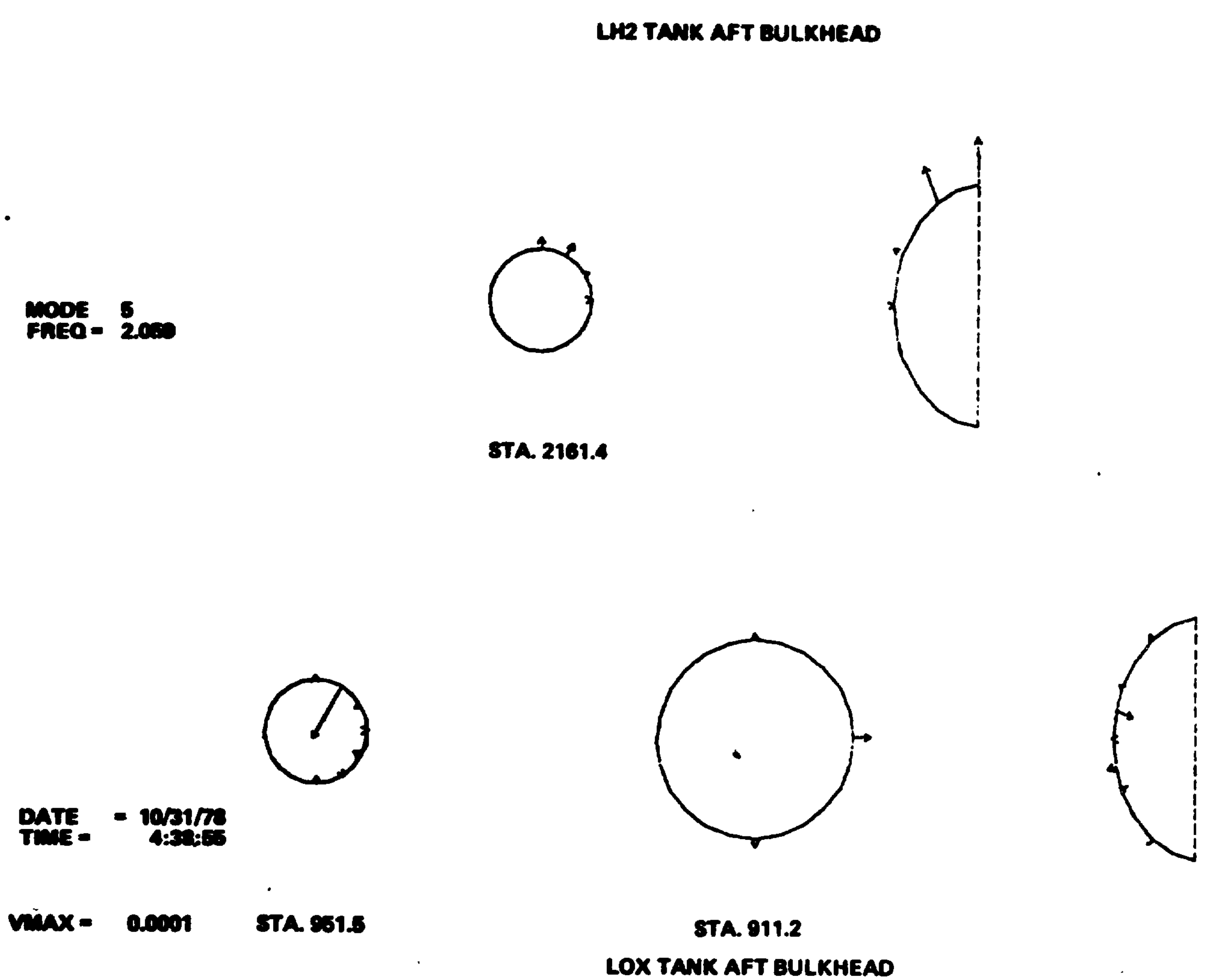

Figure 10. Space Shuttle MVGVT Orbiter/ET/SRB External Tank Lift-Off Symmetric.

L I F T O F F

SYMMETRIC
MODE 3
FREQ 2.0588

DATE 10/31/78
TIME 4:33:33

REF. FORCE F310Z

	ACC LOC	CO G/LB	QUAD G/LB	ACC G	PHASE		ACC LOC	CO G/LB	QUAD G/LB	ACC G	PHASE
1	FTC01X	-0.000005	-0.000033	0.0175	-100.0	45	FT045X	-0.000007	-0.000010	0.0212	-99.3
2	FTC02Y	-0.000001	0.000008	0.0040	95.1	46	FT046Z	0.000016	0.000059	0.0064	77.2
3	FTC03Z	0.000073	0.000009	0.0070	74.8	47	FT047X	-0.000007	-0.000013	0.0226	-99.8
4	[illegible]	-0.000002	0.000002	0.0013	131.1	48	FT048X	-0.000007	-0.000013	[illegible]	-98.9
5	[illegible]	0.000004	0.000014	0.0076	72.1	49	FT049Z	0.000015	0.000072	[illegible]	78.4
6	[illegible]	0.000003	0.000015	0.0031	77.8	50	FR050X	-0.000007	-0.000013	0.0227	-98.6
7	[illegible]	-0.000007	-0.000040	0.0210	-100.0	51	FR051Z	0.000016	0.000067	[illegible]	75.3
8	[illegible]	-0.000002	0.000002	0.0014	142.9	52	FR052X	-0.000007	-0.000032	0.0171	-103.0
9	[illegible]	0.000006	0.000023	0.0125	74.8	53	FR053Y	-0.000001	0.000001	[illegible]	107.7
10	[illegible]	-0.000007	-0.000039	0.0203	-103.1	54	FL054X	-0.000008	-0.000033	[illegible]	[illegible]
11	[illegible]	-0.000002	0.000002	0.0014	142.8	55	FT055Z	0.000016	0.000077	[illegible]	78.4
12	[illegible]	0.000004	0.000015	0.0080	73.3	56	FR056Y	0.000000	[illegible]	[illegible]	67.6
13	[illegible]	-0.000008	-0.000045	0.0233	-100.3	57	FR057X	-0.000004	-0.000027	[illegible]	[illegible]
14	[illegible]	0.000006	0.000021	0.0115	73.5	58	[illegible]	-0.000004	-0.000018	[illegible]	[illegible]
15	[illegible]	[illegible]	-0.000001	0.0016	-160.5	59	[illegible]	0.000017	0.000087	[illegible]	[illegible]
16	[illegible]	-0.000005	-0.000030	0.0158	-99.9	60	[illegible]	-0.000003	-0.000017	[illegible]	-99.5
17	[illegible]	-0.000001	0.000000	0.0036	179.4	61	[illegible]	-0.000005	-0.000033	[illegible]	[illegible]
18	[illegible]	-0.000005	-0.000029	0.0159	-99.1	62	[illegible]	-0.000004	-0.000028	0.0172	[illegible]
19	[illegible]	0.000005	0.000023	0.0120	77.3	63	[illegible]	-0.000003	[illegible]	[illegible]	[illegible]
20	[illegible]	0.000007	0.000044	0.0232	81.0	64	[illegible]	[illegible]	-0.000015	[illegible]	[illegible]
21	[illegible]	0.000009	0.000033	0.0174	74.0	65	FR065Z	0.000019	0.000109	[illegible]	[illegible]
22	[illegible]	-0.000001	-0.000002	0.0012	-120.2	66	FT066X	-0.000003	-0.000015	[illegible]	[illegible]
23	[illegible]	0.000007	0.000034	0.0181	77.8	67	[illegible]	0.000018	0.000109	0.0571	[illegible]
24	[illegible]	-0.000002	-0.000001	0.0014	-147.7	68	FL068Y	-0.000001	-0.000009	0.0016	[illegible]
25	[illegible]	-0.000007	-0.000040	0.0211	-99.2	69	FL069X	-0.000007	-0.000013	[illegible]	[illegible]
26	[illegible]	0.000010	0.000051	0.0267	78.7	70	FL070Y	[illegible]	[illegible]	[illegible]	-115.5
27	[illegible]	-0.000007	-0.000043	0.0223	-99.5	71	MT071X	-0.000008	-0.000007	0.0195	[illegible]
28	[illegible]	-0.000007	-0.000041	0.0213	-99.2	72	MT072Y	-0.000000	0.000008	0.0044	91.2
29	[illegible]	0.000011	0.000054	0.0283	77.9	73	[illegible]	0.000021	[illegible]	0.0538	79.0
30	[illegible]	-0.000007	-0.000049	0.0237	-99.4	74	[illegible]	-0.000007	-0.000008	[illegible]	[illegible]
31	[illegible]	0.000013	0.000032	0.0275	76.4	75	[illegible]	-0.000005	-0.000024	[illegible]	-101.6
32	[illegible]	-0.000003	-0.000031	0.0164	-99.8	76	[illegible]	0.000000	0.000001	0.0005	89.3
33	[illegible]	-0.000001	-0.000001	0.0007	-141.7	77	[illegible]	0.000022	0.000120	[illegible]	79.5
34	[illegible]	-0.000007	-0.000039	0.0206	-99.8	78	[illegible]	0.000024	0.000104	0.0551	77.1
35	[illegible]	-0.000002	0.000001	0.0011	156.0	79	MT079Y	[illegible]	0.000001	0.0013	154.1
36	[illegible]	-0.000005	-0.000027	0.0141	-101.1	80	MT080Z	0.000027	0.000152	[illegible]	79.9
37	[illegible]	0.000012	0.000053	0.0283	77.2	81	[illegible]	0.000023	0.000129	0.0677	79.2
38	[illegible]	0.000019	0.000006	0.0039	32.6	82	[illegible]	-0.000003	-0.000011	[illegible]	[illegible]
39	[illegible]	-0.000006	-0.000027	0.0144	-102.2	83	ML083Z	0.000004	0.000020	[illegible]	78.5
40	[illegible]	0.000011	0.000056	0.0293	78.9	84	MR084Z	0.000026	[illegible]	0.0705	79.3
41	[illegible]	-0.000002	-0.000001	0.0011	-144.0	85	MR085Y	-0.000000	-0.000004	0.0022	-93.0
42	[illegible]	0.000015	0.000066	0.0349	76.9	86	MR086Z	0.000027	0.000145	0.0765	79.3
43	[illegible]	0.000001	-0.000001	0.0004	-49.7	87	WR087Z	0.000013	0.000049	0.0263	75.0
44	ID044Z	0.000014	0.000068	0.0339	78.2	88	WR088Z	0.000017	0.000065	0,0347	75.6

Figure 11. Space Shuttle MVGVT Dwell Data Orbiter *** External Tank *** Solid Rocket Boosters.

ORIGINAL PAGE IS
OF POOR QUALITY

[illegible]

	ACC LOC	CO G/LB	QUAD G/LB	ACC G	PHASE		ACC LOC	CO G/LB	QUAD G/LB	ACC G	PHASE
89	VR089Z	0.000013	0.000070	0.0367	79.5	133	EF133N	0.000006	0.000028	0.0150	78.4
90	VR090Z	0.000016	-0.000067	0.0387	76.2	134	EF134X	-0.000002	-0.000002	0.0011	-133.2
91	VR091Z	0.000019	0.000074	0.0395	75.8	135	EF135N	0.000002	0.000001	0.0011	27.0
92	VR092Z	0.000019	0.000078	0.0417	76.4	136	EF136Z	-0.000012	-0.000059	0.0312	-101.0
93	VR093Z	0.000022	0.000087	0.0464	75.5	137	EF137N	-0.000004	-0.000026	0.0137	-98.4
94	VR094X	-0.000005	-0.000025	0.0133	-100.6	138	EF138N	-0.000008	-0.000044	0.0233	-99.8
95	VR095X	-0.000004	-0.000025	0.0130	-99.0	139	EF139X	0.000005	0.000030	0.0156	80.7
96	VR096X	-0.000006	-0.000027	0.0146	-102.4	140	EF140N	-0.000009	-0.000051	0.0268	-99.7
97	VR097Y	-0.000000	0.000001	0.0004	99.2	141	EF141Y	-0.000001	0.000001	0.0010	139.5
98	VR098Z	0.000024	0.000100	0.0532	76.7	142	EF142N	0.000009	0.000044	0.0232	79.0
99	VR099Z	0.000025	0.000098	0.0522	75.9	143	EF143N	0.000008	0.000038	0.0202	78.9
100	VR100Z	0.000022	0.000112	0.0590	78.8	144	EF144N	0.000008	0.000039	0.0207	78.2
101	VR101Z	0.000028	0.000100	0.0544	77.4	145	EF145N	0.000007	0.000032	0.0171	77.8
102	VR102Z	0.000024	0.000115	0.0608	78.0	146	EF146N	0.000003	0.000020	0.0105	89.3
103	VR103Z	0.000023	0.000101	0.0538	77.0	147	EF147N	0.000004	0.000015	0.0079	75.6
104	VL104Z	0.000011	0.000036	0.0265	77.7	148	EF148N	0.000001	0.000004	0.0020	69.7
105	VL105Z	0.000014	0.000081	0.0427	80.4	149	EF149N	-0.000001	-0.000010	0.0052	-93.8
106	VL106Z	0.000016	0.000099	0.0520	81.0	150	EF150N	-0.000003	-0.000021	0.0111	-98.0
107	VL107Z	0.000018	0.000104	0.0545	80.2	151	EF151N	-0.000005	-0.000031	0.0162	-99.8
108	VL108Z	0.000019	0.000117	0.0613	80.6	152	EF152N	-0.000006	-0.000039	0.0205	-98.1
109	VR109Z	0.000021	0.000115	0.0606	79.8	153	EF153N	-0.000008	-0.000043	0.0227	-100.4
110	DL110Y	-0.000000	-0.000004	0.0022	-93.3	154	EF154N	-0.000009	-0.000055	0.028[illegible]	-99.8
111	DL111Z	0.000020	0.000119	0.0625	80.4	155	EF155N	-0.000006	-0.000021	0.0114	-105.6
112	VR112Y	-0.000000	0.000017	0.0090	90.8	156	EF156N	0.000003	0.000019	0.0097	82.0
113	VR113Y	-0.000000	0.000023	0.0120	90.9	157	EF157R	0.000005	0.000028	0.0146	79.3
114	VR114X	-0.000016	-0.000110	0.0571	-98.2	158	EF158Y	0.000000	0.000002	0.0013	82.4
115	VR115Y	-0.000002	0.000024	0.0127	95.5	159	EF159R	0.000005	0.000023	0.0120	78.4
116	VR116Z	0.000019	0.000122	0.0638	81.3	160	EF160R	0.000003	0.000015	0.0081	77.6
117	VR117Y	-0.000002	0.000026	0.0135	95.5	161	EF161R	0.000000	0.000001	0.0006	71.3
118	VR118Y	-0.000005	-0.000009	0.0052	-120.4	162	EF162Z	-0.000006	-0.000026	0.0137	-102.6
119	VR119Y	0.000004	0.000017	0.0090	77.8	163	EF163R	-0.000002	-0.000012	0.0065	-100.5
120	CR120Y	-0.000002	-0.000003	0.0015	-130.6	164	EF164R	-0.000005	-0.000023	0.0120	-101.9
121	CR121Z	0.000017	0.000089	0.0422	78.3	165	EF165R	-0.000025	0.000065	0.0354	109.4
122	CR122Y	-0.000000	0.000038	0.0643	90.8	166	EF166X	0.000001	0.000002	0.0011	76.1
123	CR123Z	0.000019	0.000101	0.0529	79.5	167	EF167Y	-0.000000	0.000001	0.0004	100.2
124	CR124Y	-0.000002	-0.000006	0.0034	-109.7	168	EF168Z	0.000005	0.000022	0.0118	78.1
125	CR125X	[illegible]	-0.000046	0.0236	-98.4	169	EH169X	0.000001	-0.000005	0.0028	-78.9
126	EF126X	[illegible]	-0.000002	0.0014	-128.6	170	EH170Y	-0.000000	0.000002	0.0012	101.9
127	EF127Y	0.000000	[illegible]	0.0026	[illegible]	171	EH171X	-0.000001	-0.000001	[illegible]	[illegible]
128	EF128Z	-0.000010	[illegible]	0.0341	[illegible]	172	[illegible]	[illegible]	-0.000007	0.0038	-110.4
129	EF129X	-0.000006	-0.000028	0.0147	[illegible]	173	[illegible]	[illegible]	-0.000016	0.0051	[illegible]
130	[illegible]	0.000010	0.000052	[illegible]	[illegible]	174	EH174X	0.000001	[illegible]	0.0011	[illegible]
131	[illegible]	[illegible]	0.000004	[illegible]	[illegible]	175	[illegible]	[illegible]	[illegible]	[illegible]	80.1
[illegible]	[illegible]	[illegible]	[illegible]	[illegible]	[illegible]	[illegible]	[illegible]	[illegible]	[illegible]	[illegible]	[illegible]

Figure 11. (Continued).

ORIGINAL PAGE IS
OF POOR QUALITY

LIFTOFF

SYMMETRIC
MODE 8
FREQ 2.[illegible]

DATE 10/31/78
TIME 4:38:58

REF. FORCE FB10Z

	ACC LOC	CO G/LB	QUAD G/LB	ACC G	PHASE
177	EM177Y	-0.000001	0.000001	0.0008	141.1
178	EM178X	-0.000000	-0.000082	0.0910	-92.0
179	EM179Y	-0.000001	0.000001	0.0007	132.2
180	EM180X	-0.000000	-0.000001	0.0007	-103.7
181	EM181Z	-0.000003	-0.000012	0.0361	-103.1
182	EA378T	-0.000002	-0.000005	0.0026	-111.6
183	EM183Z	0.000002	0.000014	0.0072	79.9
184	EA184R	0.000006	0.000023	0.0122	77.9
185	EA185Y	-0.000031	0.000000	0.0004	153.4
186	EA186R	0.000004	0.000022	0.0116	78.5
187	EA187R	0.000004	0.000018	0.0094	76.1
188	EA188R	0.000002	0.000011	0.0960	80.0
189	EA189R	-0.000001	-0.000005	0.0026	-99.5
190	EA190R	-0.000000	-0.000000	0.0003	-126.9
191	EA191R	-0.000001	-0.000005	0.0026	-103.2
192	EA192Z	-0.000004	-0.000017	0.0091	-104.0
193	EA193R	0.000002	0.000008	0.0042	74.4
194	EA194R	0.000003	0.000014	0.0075	77.9
195	EA195R	-0.000005	-0.000019	0.0103	-104.0
196	EA196Y	0.000000	0.000002	0.0039	76.5
197	EA197R	0.000002	0.000006	0.0032	74.1
198	EA198R	-0.000002	-0.000007	0.0036	-109.4
199	EA199R	0.000009	0.000040	0.0215	76.9
200	EA200Y	-0.000001	-0.000001	0.0006	-121.9
201	EA201R	0.000016	0.000065	0.0346	76.2
202	EA202R	0.000001	0.000004	0.0021	79.0
203	EA203R	-0.000001	-0.000004	0.0023	-106.1
204	EA204Z	-0.000008	-0.000031	0.0167	-104.1
205	EA205R	0.000004	0.000015	0.0083	74.1
206	EA206R	-0.000005	-0.000021	0.0111	-104.7
207	EA207R	-0.000007	-0.000032	0.0168	-102.7
208	EA208Y	-0.000003	0.000001	0.0013	147.1
209	EA209X	0.000006	0.000042	0.0222	81.6
210	EA210R	0.000013	0.000057	0.0301	77.4
211	EA211Y	0.000000	0.000001	0.0004	77.8
212	EA212R	0.000011	0.000049	0.0261	77.6
213	EA213R	0.000005	0.000023	0.0122	76.6
214	EA214X	-0.000000	0.000001	0.0006	105.1
215	EA215R	-0.000002	-0.000010	0.0053	-100.7
216	EA216Z	-0.000012	-0.000034	0.0208	-102.2
217	EA217R	0.000006	0.000027	0.0142	76.8
218	EA218R	0.000008	0.000037	0.0197	77.3
219	EA219X	-0.000002	-0.000012	0.0061	-100.8
220	EA220R	-0.000009	-0.000045	0.0081	-100.7

	ACC LOC	CO G/LB	QUAD G/LB	ACC G	PHASE
221	EA221Y	-0.000000	-0.000000	0.0002	-127.4
222	EA222X	-0.000032	0.000009	0.0049	102.2
223	EA223Y	-0.000001	-0.000002	0.0011	-103.2
224	EA224Z	-0.000018	-0.000082	0.0432	-102.3
225	EA225X	0.000002	0.000007	0.0038	76.2
226	EA226Y	0.000003	0.000013	0.0069	77.3
227	EA227Z	-0.000016	-0.000087	0.0460	-100.6
228	EA228X	0.000011	0.000006	0.0064	28.1
229	EA229Z	-0.000017	-0.000074	0.0394	-102.8
230	EF230Y	-0.000000	0.000000	0.0002	170.0
231	EA231Y	0.000005	0.000024	0.0128	79.0
232	EA232Z	-0.000017	-0.000076	0.0433	-102.4
233	EA233Y	-0.000005	-0.000030	0.0156	-98.8
234	EA234X	-0.000002	-0.000010	0.0054	-99.0
235	EA235X	0.000004	0.000019	0.0101	77.2
236	EA236R	0.000005	0.000021	0.0110	77.4
237	EA237R	0.000004	0.000015	0.0079	74.3
238	EA238T	-0.000004	-0.000007	0.0043	-118.6
239	EA239R	0.000006	0.000027	0.0143	76.9
240	EA240T	-0.000003	-0.000019	0.0034	-104.3
241	EA241R	0.000010	0.000043	0.0223	76.5
242	EA242T	-0.000006	-0.000018	0.0099	-108.3
243	EA243X	0.000003	0.000016	0.0083	77.5
244	RF244X	0.000001	0.000002	0.0012	67.4
245	RF245Y	-0.000001	-0.000001	0.0008	-143.3
246	RF246Z	-0.000012	-0.000062	0.0326	-101.2
247	RT247Y	0.000009	0.000046	0.0242	79.5
248	RR248Z	-0.000021	-0.000106	0.0560	-101.4
249	RR249Y	-0.000011	-0.000049	0.0261	-102.7
250	RL250X	0.000001	0.000002	0.0011	69.8
251	RL251Y	-0.000000	0.000003	0.0018	93.1
252	RL252Z	0.000002	0.000009	0.0019	73.8
253	RT253X	0.000001	0.000003	0.0017	67.9
254	RT254Y	0.000008	0.000044	0.0230	79.5
255	RT255Z	-0.000007	-0.000036	0.0190	-101.5
256	RT256X	0.000000	0.000003	0.0016	54.9
257	RT257Y	0.000012	0.000068	0.0358	79.8
258	RR258X	0.000002	0.000009	0.0048	74.6
259	RR259Z	-0.000027	-0.000134	0.0708	-101.5
260	RL260X	-0.000001	-0.000034	0.0019	-106.8
261	RL261Y	-0.000017	-0.000076	0.0405	-102.4
262	RT262Y	0.000009	0.000061	0.0330	81.5
263	RR263X	-0.000028	-0.000[illegible]	[illegible]	-102.0
264	RR264Y	-0.000018	-0.000075	0.0398	-103.3

Figure 11. (Continued).

	ACC LOC	CO G/LB	QUAD G/LB	ACC G	PHASE		ACC LOC	CO G/LB	QUAD G/LB	ACC G	PHASE
265	RT265X	-0.000001	0.000001	0.0007	120.2	309	LT313Y	-0.000005	-0.000046	0.0239	-96.8
266	RT266Y	0.000011	0.000059	0.0041	79.4	310	LR315Z	0.000024	0.000120	0.0633	78.0
267	RR267X	0.000000	0.000001	0.0304	[illegible]	311	LL317Z	0.000000	-0.000013	0.0069	-39.8
268	RR268Z	-0.000022	-0.000114	0.0602	[illegible]	312	LR401Y	-0.000003	-0.000030	0.0157	-96.4
269	RR269X	0.000092	0.000007	0.0038	78.4	313	LR402Z	0.000012	0.000058	0.0306	78.4
270	RR270Y	-0.000030	-0.000112	0.0602	-103.2	314	LR403X	0.000008	0.000049	0.0256	80.2
271	RT271Y	0.000010	0.000052	0.0278	79.2	315	LT404X	-0.000003	-0.000009	0.0048	-108.4
272	RR272Z	0.000004	0.000022	0.0113	80.3	316	RR297X	0.000003	0.000012	0.0065	77.0
273	RR273Y	0.000013	0.000071	0.0377	78.4	317	RR298Z	-0.000018	-0.000009	0.0471	-101.4
274	RT274Y	0.000010	0.000051	0.0267	78.4	318	RL299Z	-0.000007	-0.000033	0.0172	-101.4
275	RR275Z	-0.000007	-0.000058	0.0279	-97.7	319	RR300X	0.000002	0.000007	0.0038	75.5
276	RL276Y	0.000090	-0.000027	0.0141	-99.6	320	RR301Z	-0.000017	-0.000086	0.0433	-101.4
277	RL277Y	0.000006	0.000032	0.0166	79.2	321	RR302Z	-0.000007	-0.000033	0.0176	-101.5
278	RL278Z	0.000012	0.000059	0.0310	78.8	322	RR303X	0.000001	0.000003	0.0017	73.2
279	RT279Y	0.000011	0.000048	0.0254	77.1	323	RR389Z	-0.000006	-0.000030	0.0139	-102.1
280	RR280Z	-0.000005	-0.000032	0.0169	-99.5	324	RL305Z	-0.000002	-0.000009	0.0047	-103.6
281	RR281Y	-0.000014	-0.000070	0.0367	-101.2	325	RR306X	0.000000	0.000001	0.0007	72.9
282	RT282X	-0.000001	-0.000039	0.0046	-99.6	326	RR307Z	-0.000005	-0.000029	0.0117	-102.3
283	RT283Y	0.000018	0.000053	0.0284	76.6	327	RL308Z	0.000009	0.000038	0.0203	76.4
284	RR284X	0.000001	0.000004	0.0020	75.1	328	LR398X	-0.000001	0.000002	0.0011	103.9
285	RR285Z	-0.000001	-0.000008	0.0042	-93.6	329	LR399Z	-0.000002	-0.000008	0.0042	-100.9
286	RL286X	0.000001	0.000001	0.0007	56.2	330	LL400Z	-0.000011	-0.000057	0.0303	-101.2
287	RL287Z	0.000024	0.000112	0.0592	78.1	331	EF601N	0.000002	0.000007	0.0038	73.4
288	RR288Z	0.000000	0.000000	0.0001	10.8	332	EF602N	0.000004	0.000020	0.0105	78.4
289	RL289Y	-0.000007	-0.000031	0.0422	-98.0	333	EF603N	0.000002	0.000010	0.0052	77.4
290	RL290Y	0.000018	0.000080	0.0426	77.3	334	EF604N	0.000001	0.000005	0.0028	73.9
291	RD291X	0.000008	0.000015	0.0079	79.1	335	EF605N	-0.000017	-0.000067	0.0359	-103.8
292	LD292Y	0.000000	-0.000000	0.0004	-0.6	336	EF606N	-0.000002	-0.000007	0.0040	-104.4
293	RR293Z	0.000019	0.000090	0.0476	78.4	337	EF607N	0.000000	0.000001	0.0034	65.1
294	RT294X	-0.000008	-0.000003	0.0023	-133.0	338	EF608N	-0.000002	-0.000009	0.0048	-100.3
295	RT295Y	0.000012	0.000066	0.0345	79.5	339	EF609N	0.000001	0.000001	0.0006	58.8
296	RT296Z	0.000016	0.000085	0.0445	79.2	340	EF610N	-0.000001	-0.000008	0.0041	-103.4
297	RL381Y	-0.000018	-0.000070	0.0369	-100.7	341	EF611N	-0.000003	-0.000021	0.0110	-102.2
298	RL330Y	-0.000003	-0.000013	0.0067	-103.0	342	EF612N	0.000001	0.000010	0.0052	81.8
299	RL331Z	0.000014	0.000098	0.0312	81.7	343	EA701N	0.000012	0.000054	0.0209	77.1
300	AJ337Y	-0.000002	0.000003	0.0018	[illegible]	344	EA702N	0.000010	0.000045	0.0230	76.4
301	AJ339Y	-0.000000	-0.000030	0.0015	-109.7	345	EA703N	0.000006	0.000013	0.0075	63.9
302	AJ340Z	0.000038	0.000010	0.0054	72.5	346	EA704N	0.000004	0.000016	0.0035	75.9
303	AJ347Z	0.000004	0.000011	0.0060	72.0	347	EA705N	0.000002	0.000005	0.0028	70.1
304	PT355Y	-0.000002	-0.000000	0.0010	-168.3	348	EA706N	0.000000	0.000000	0.0007	7.8
305	PT356Y	-0.000002	-0.000008	0.0019	[illegible]	349	EA707N	-0.000000	-0.000000	0.0002	170.8
306	LT309X	-0.000001	-0.000000	0.0004	[illegible]	350	[illegible]	-0.000038	0.000527	0.2732	94.1
307	LT310Y	-0.000013	[illegible]	[illegible]	[illegible]	351	[illegible]	[illegible]	[illegible]	0.4971	[illegible]
308	LT301Z	[illegible]	[illegible]	[illegible]	[illegible]	352	[illegible]	[illegible]	[illegible]	[illegible]	[illegible]

Figure 11. (Continued).

LIFTOFF

SYMMETRIC
MODE 5
FREQ 2.0503

DATE 10/31/76
TIME 4:39:33

REF. FORCE FB10Z

	ACC LOC	CO G/LB	QUAD G/LB	ACC G	PHASE
353	[illegible]	0.000013	0.000837	0.4441	87.0
354	[illegible]	-0.000159	0.000349	0.3327	97.8
355	[illegible]	-0.000316	-0.000066	0.0037	-153.8
356	[illegible]	-0.000067	0.000049	0.0429	143.6
357	AC33Z	-0.000073	-0.000000	0.0015	-174.7
358	AC61X	0.000029	0.000094	0.0031	21.3
359	[illegible]	-0.000143	0.000000	0.0737	164.9
360	[illegible]	-0.000274	0.000019	0.0097	165.5
361	[illegible]	-0.000028	-0.000029	0.0452	-161.3
362	[illegible]	-0.000113	0.000036	0.0663	163.7
363	[illegible]	0.000000	-0.000010	0.0070	-39.9
364	[illegible]	-0.000016	-0.000001	0.0083	-177.9
365	[illegible]	0.000074	-0.000035	0.0702	-23.7
366	AG12Z	[illegible]	0.000019	0.0099	77.9
367	[illegible]	-0.000019	[illegible]	0.0028	170.2
368	[illegible]	[illegible]	[illegible]	0.0333	-16.0
369	[illegible]	[illegible]	[illegible]	0.0043	112.0
370	[illegible]	[illegible]	0.000010	0.0129	22.3
371	[illegible]	-0.000193	0.000083	0.1109	153.7
372	[illegible]	-0.000001	0.000029	0.0447	160.5
373	[illegible]	[illegible]	0.000002	0.0013	57.5
374	AJ13Z	0.000011	0.000000	0.0058	0.2
375	[illegible]	[illegible]	[illegible]	0.0015	50.2
376	[illegible]	0.000010	-0.000000	0.0053	-1.0
377	[illegible]	[illegible]	0.000002	0.0014	62.1
378	[illegible]	0.000010	-0.000000	0.0034	-2.2
379	AJ43Z	0.000011	-0.000000	0.0059	-1.4
380	AC41X	0.000023	0.000003	0.0147	6.1
381	AC42Y	-0.000162	0.000035	0.0837	161.2
382	AC43Z	0.000108	-0.000043	0.0605	-22.7
383	LG12Y	-0.000036	-0.000010	0.0194	-163.0
384	[illegible]	0.000023	-0.000056	0.0354	-70.2
385	[illegible]	[illegible]	[illegible]	0.0290	152.2
386	[illegible]	0.000037	-0.000040	0.0203	-47.1
387	LG32Y	-0.000033	0.000012	0.0239	167.0
388	LG33Z	0.000046	-0.000036	0.0376	-30.4
389	RG12Y	-0.000017	0.000030	0.0176	119.4
390	RG13Z	-0.000001	0.000003	0.0171	91.9
391	[illegible]	-0.000010	0.000063	0.0328	99.5
392	[illegible]	-0.000013	0.000037	0.0285	109.7
393	[illegible]	-0.000028	0.000032	0.0451	108.9
394	RG33Z	-0.000030	0.000045	0.0277	123.7
395	AJ43Y	0.000001	0.000002	0.0019	37.2
396	RL407X	0.000000	0.000006	0.0031	88.2

	ACC LOC	CO G/LB	QUAD G/LB	ACC G	PHASE
397	[illegible]	0.000001	0.000010	0.0030	82.4
398	AJ335Y	0.000005	0.000021	0.0112	77.5
399	AJ341Y	-0.000002	[illegible]	0.0020	[illegible]
400	AJ348Z	0.000009	0.000005	0.0073	32.6
401	AJ349Z	0.000003	0.000010	0.0036	73.3

Figure 11. (Concluded).

ORIGINAL PAGE IS OF POOR QUALITY

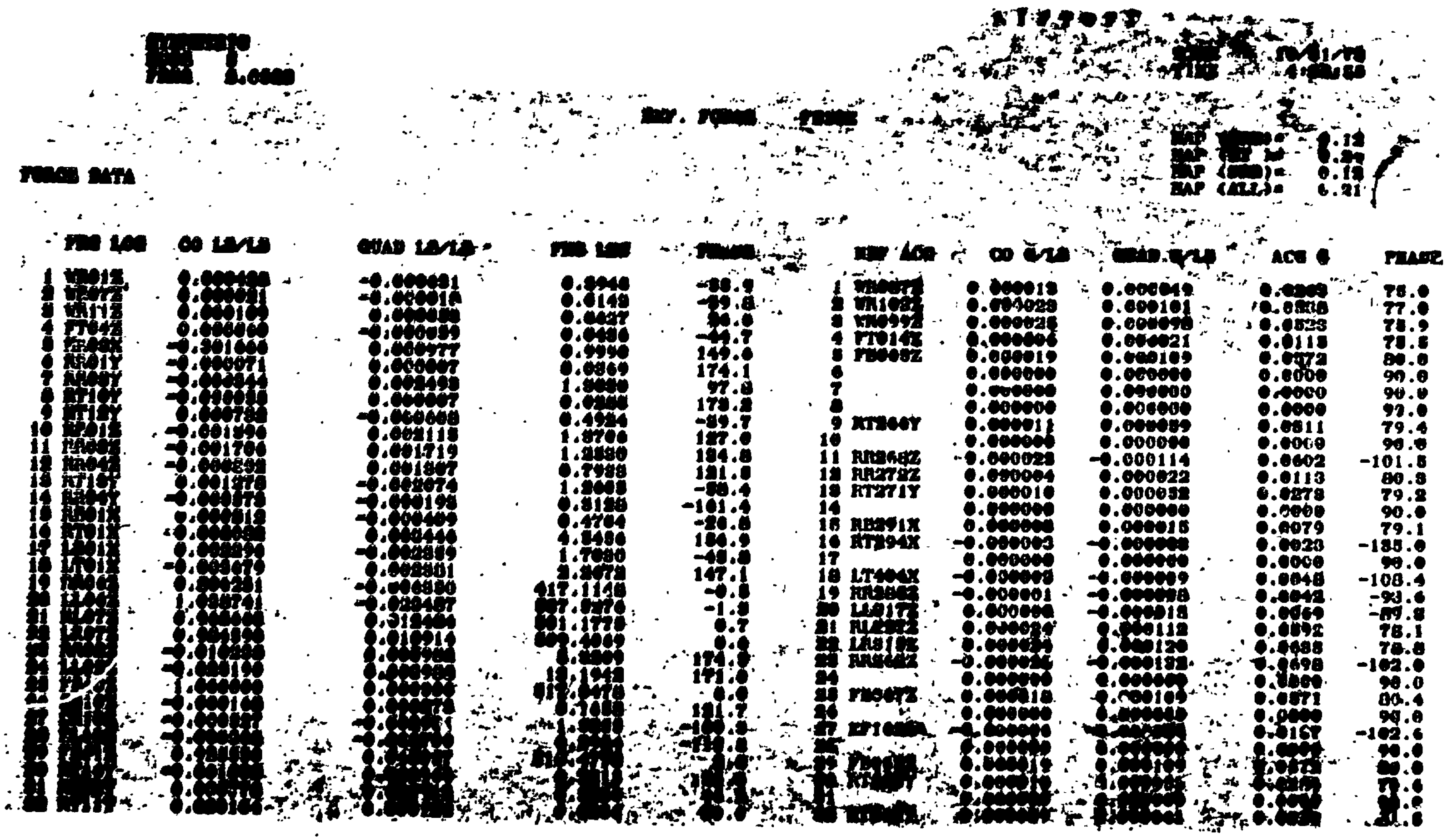

Figure 12. Space Shuttle MVGVT Dwell Data Orbiter *** External Tank *** Solid Rocket Boosters.

L I F T O F F

GENL NORMLZD MASS MATRIX

MODE	FREQ	0.6667	0.3303	0.1961	0.3137	2.0723
1	0.6667	1.0000				
2	0.3353	-0.0491	1.0000			
3	0.1961	[illegible]	-0.4[illegible]	1.0000		
4	0.3137	0.0014	-0.3319	0.0035	1.0000	
5	2.0723	0.0914	0.3870	0.1820	-0.0929	1.0000

Figure 13. Space Shuttle MVGVT Symmetric Orthog Orbiter *** External Tank ** Solid Rocket Boosters.

LIFTOFF

FREQUENCY OF DWELL = 0.0588
DAY 10/31/78 TIME 4:30:35

MODE = 8

LOCATION	X	Y	Z	THX	THY	THZ	TOTAL
ORBITER							
[illegible]	0.0041	0.0029	0.0122	[illegible]	0.0007	[illegible]	0.0171
[illegible]	[illegible]	0.0030	[illegible]	[illegible]	[illegible]	[illegible]	[illegible]
[illegible]	0.0013	[illegible]	0.0020	[illegible]	0.0030	[illegible]	[illegible]
[illegible]	0.0019	[illegible]	0.0049	[illegible]	0.0000	[illegible]	[illegible]
[illegible]	[illegible]	0.0030	[illegible]	[illegible]	[illegible]	[illegible]	[illegible]
[illegible]	0.0010	[illegible]	0.0037	[illegible]	[illegible]	[illegible]	[illegible]
[illegible]	[illegible]	[illegible]	0.0147	[illegible]	[illegible]	[illegible]	[illegible]
[illegible]	[illegible]	[illegible]	0.0038	[illegible]	[illegible]	[illegible]	[illegible]
[illegible]	[illegible]	[illegible]	0.0029	[illegible]	[illegible]	[illegible]	[illegible]
[illegible]	[illegible]	0.0000	[illegible]	[illegible]	[illegible]	[illegible]	[illegible]
[illegible]	0.0014	[illegible]	[illegible]	[illegible]	0.0030	[illegible]	[illegible]
[illegible]	[illegible]	[illegible]	[illegible]	[illegible]	[illegible]	[illegible]	[illegible]
[illegible]	[illegible]	[illegible]	[illegible]	0.0011	0.0014	[illegible]	[illegible]
[illegible]	[illegible]	[illegible]	[illegible]	[illegible]	[illegible]	[illegible]	[illegible]
[illegible]	0.0000	[illegible]	[illegible]	0.0000	[illegible]	[illegible]	[illegible]
TOTAL ORB	0.0160	0.0004	0.0811	0.0011	0.0021	[illegible]	0.1013
EXTERNAL TANK							
[illegible]							[illegible]
[illegible]							[illegible]
[illegible]							[illegible]
[illegible]							[illegible]
INTERTANK							[illegible]
[illegible]							[illegible]
[illegible]							[illegible]
[illegible]							[illegible]
TOTAL ET							0.1334
SLD RKT BSTRS							
[illegible]	[illegible]	0.0000	0.0160	[illegible]	[illegible]	[illegible]	[illegible]
[illegible]	0.0027	0.1323	0.2106	[illegible]	[illegible]	[illegible]	[illegible]
[illegible]	0.0065	[illegible]	0.0221	0.0000	0.0000	0.0000	0.0491
PROP 1	[illegible]	[illegible]	[illegible]	[illegible]	[illegible]	[illegible]	[illegible]
PROP 2	[illegible]	0.0000	0.0000	0.0000	0.0000	0.0000	[illegible]
PROP 3	0.0012	[illegible]	0.0000	0.0000	0.0000	0.0000	0.0012
PROP 4	0.0031	[illegible]	0.0000	0.0000	0.0000	0.0000	0.0031
TOTAL SRB	0.0088	[illegible]	0.2495	0.3439	0.0024	0.0032	0.7632

TOTAL:ORB/ET/SRB. 1.0000

Figure 14. MVGVT Kinetic Energy Distribution Symmetric Motion Orbiter *** External Tank *** Solid Rocket Boosters.

ORIGINAL PAGE IS
OF POOR QUALITY

LIFTOFF

MODE	FREQ	CMC
1	0.0667	0.0001178277
2	0.0833	0.0000013298
3	0.1661	0.0000004487
4	0.3167	0.0000026606
5	2.0333	0.0000293971

Figure 15. Space Shuttle MVGVT Symmetric Orthog Orbiter *** External Tank *** Solid Rocket Boosters.

L I F T O F F

-0.0330	-0.0014	0.0660	2.1079	2.4728	2.9277	3.1429	3.1833	3.8720	4.7514	5.1589	5.3031	5.6950
5.7742	6.3969	6.5798	6.9179	7.6[illegible]	7.9203	8.0747	8.0988	8.[illegible]551	8.8134	9.0763	9.21[illegible]	9.2918
9.6029	9.6994	9.8176	10.3371	10.5518	10.8995	10.9110	11.0583	11.1373	11.1773	11.5431	11.9[illegible]	12.[illegible]
12.4442	12.5457	12.7330	12.9653	12.9[illegible]7	13.1457	13.6141	13.7109	13.7984	13.9032	14.1960	14.3[illegible]	14.5702
14.6101	14.7232	14.7920	15.0900	15.1567	15.1967	15.37[illegible]	15.5072	15.5829	15.7823	15.[illegible]	16.0[illegible]39	16.1726
16.0383	16.4452	16.9336	17.0031	17.[illegible]18	17.5847	17.8347	18.1931	18.2803	18.8137	1[illegible].4741	18.5743	18.8719
18.8799	19.0047	19.0220	19.6027	19.1[illegible]3	19.2042	19.2067	19.[illegible]	19.[illegible]82	19.6271	1[illegible].7473	1[illegible]	20.[illegible]21
[illegible]	2[illegible].7[illegible]	20.[illegible]50	20.[illegible]770	21.[illegible]20	21.2757	21.8185	22.0667	22.3109	22.4931	22.[illegible]79	22.831[illegible]	22.[illegible]
[illegible]	23.2651	23.3113	23.[illegible]13	23.[illegible]17	23.5[illegible]0	23.6046	23.[illegible]020	23.6918	23.9[illegible]6	23.9[illegible]13	24.[illegible]970	24.[illegible]
[illegible]	2[illegible].6051	24.7514	25.[illegible]439	25.1709	25.29[illegible]	25.2305	25.[illegible]248	25.6705	25.8[illegible]51	2[illegible]329	26.07[illegible]	26.[illegible]15
[illegible]	2[illegible].2363	26.3427	26.[illegible]252	26.7759	26.8274	2[illegible].96[illegible]	2[illegible].0913	27.1[illegible]79	27.2725	27.2791	27.[illegible]	27.[illegible]771
[illegible]7.9503	[illegible]3.0133	28.1123	28.1976	28.4210	28.6[illegible]3	29.0018	29.0546	29.6597	29.8[illegible]	[illegible].84[illegible]2	30.3796	30.[illegible]3
[illegible]0929	31.0579	31.7622	31.7[illegible]01	32.0[illegible]71	32.0599	32.17[illegible]	32.2602	32.[illegible]03	32.3149	[illegible].6898	32.8[illegible]9	32.[illegible]5
33.3219	33.8270	34.2233	34.[illegible]358	34.[illegible]72	35.0028	35.21[illegible]	35.3931	35.7014	35.8040	[illegible]261	36.0261	[illegible].2072
[illegible]	35.6353	3[illegible].9102	36.9415	36.9975	37.1603	37.2457	37.3327	38.1399	38.3478	38.6292	3[illegible].43[illegible]	39.55[illegible]6
39.7093	39.9713	40.0550	40.1803	40.2861	2.0333							

MODE	FREQ	GENL NORMLZD MASS MATRIX												
3	2.0333	-0.0296	-0.1733	-0.0207	-0.[illegible]	0.0227	0.0344	0.0573	-0.1469	0.1029	-0.0366	-0.0182	-0.4027	[illegible]
		0.[illegible]	-0.0[illegible]2	-0.[illegible]2	-0.0[illegible]44	-0.1563	0.0350	0.0383	-0.0[illegible]7	-0.0177	0.0[illegible]6	-0.0[illegible]9	-0.0[illegible]	-0.[illegible]11
		0.[illegible]	-0.0[illegible]	0.[illegible]3	-0.0174	-0.0[illegible]	-0.0914	0.0111	-0.0602	0.0103	-0.0[illegible]6	-[illegible]7	-0.0136	-0.[illegible]
		-0.01[illegible]7	0.0151	0.0[illegible]91	-0.1204	0.17[illegible]1	0.0593	-0.03[illegible]	0.0279	-0.0136	-0.0[illegible]9	-0.[illegible]3	-0.0[illegible]	0.[illegible]1
		-0.0069	0.0630	-0.0034	-0.0023	-0.0[illegible]4	0.0063	0.0403	-0.0[illegible]0	0.0156	-0.1[illegible]2	-0.[illegible]	0.03[illegible]	-0.[illegible]4
		0.0146	-0.0039	0.0[illegible]2	0.0692	0.[illegible]73	0.0074	-0.1869	0.0769	0.0[illegible]11	0.0[illegible]3	-0.0026	0.0218	-0.2019
		-0.1351	-0.2723	0.2277	-0.0[illegible]59	-0.1[illegible]8	-0.1919	0.0509	0.1118	0.1113	-0.0272	0.12[illegible]	-0.0[illegible]	-0.[illegible]6
		0.0[illegible]49	-0.04[illegible]	-0.2[illegible]	0.0333	-0.0[illegible]9	-0.0[illegible]54	-0.229[illegible]	-0.0082	0.0023	0.0916	0.0213	-0.0[illegible]	-0.[illegible]632
		-0.0[illegible]43	-0.0[illegible]7	0.0[illegible]3	0.0[illegible]68	0.0[illegible]7	0.0064	0.0214	0.0398	0.[illegible]98	-0.0218	[illegible]6	0.0136	0.1[illegible]
		0.2515	-0.0014	-0.0[illegible]7	-0.3165	0.0710	-0.0104	-0.0122	-0.0329	-0.0510	0.0012	-0.0670	0.1016	-0.0[illegible]7
		-0.0[illegible]49	0.9199	-0.1[illegible]	-0.0[illegible]3	-0.0798	0.0746	-0.0[illegible]9	-0.[illegible]9	0.0[illegible]0	-0.1142	-0.11[illegible]2	-0.0[illegible]	-0.0793
		0.0021	-0.0819	-0.0[illegible]23	-0.0176	-0.0211	0.0[illegible]31	0.13[illegible]	0.0[illegible]9	0.0973	-0.1032	-0.2031	-0.1[illegible]	0.0671
		-0.1738	0.1293	-0.0237	0.0121	0.1498	0.1287	-0.2375	-0.2230	-0.0456	-0.2505	-0.2165	-0.1445	0.0514
		-0.1363	0.0413	0.0018	-0.0126	-0.0383	-0.0136	0.0075	0.0683	0.0762	-0.0679	-0.00[illegible]4	-0.0531	0.[illegible]03
		0.0069	-0.0222	-0.0410	-0.0637	0.1733	0.0770	-0.0504	0.0695	0.0370	0.0546	-0.0517	0.0099	0.0112
		0.0286	-0.0218	-0.0100	0.0028	0.0919	1.0030							

Figure 16. Space Shuttle MVGVT Symmetric X-Orth Orbiter *** External Tank *** Solid Rocket Boosters.

```
ANAFRQ=   2.108
TSTFRQ=   2.059

ANAMOD=   4
TSTMOD=   5

F = A + B * X
A =     0.003
B =     0.679

YINTER=   0.003
XINTER=  -0.005
SLOPE =  34.177

STDDEV=   0.398

CO-DET=   0.599
CO-COR=   0.774
STDERR=   0.063

UNORMX=   0.143
UNORMY=   0.180
```

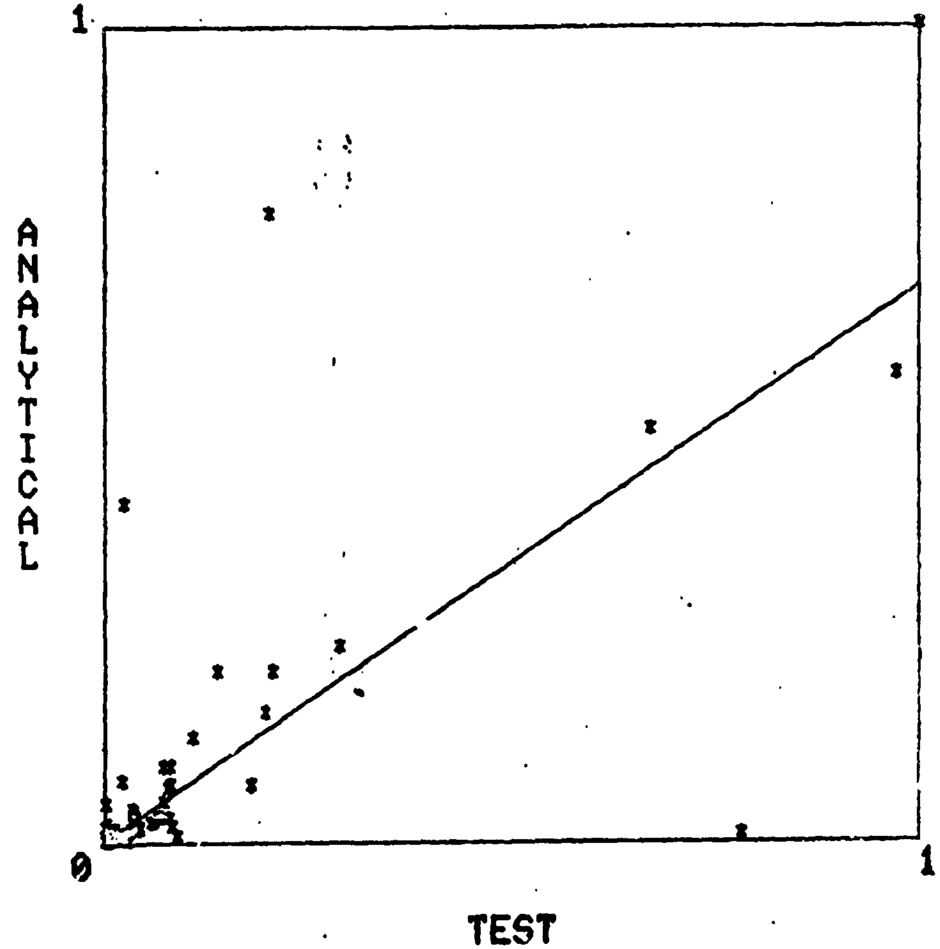

Figure 17. Linear regression analysis.

ANAFRQ= 2.454
TSTFRQ= 2.059

ANAMOD= 5
TSTMOD= 5

F = A + B * X
A = 0.010
B = 0.071

YINTER= 0.010
XINTER= -0.140
SLOPE = 4.080

STDDEV= 0.210

CO-DET= 0.010
CO-COR= 0.099
STDERR= 0.080

UNORMX= 0.143
UNORMY= 0.329

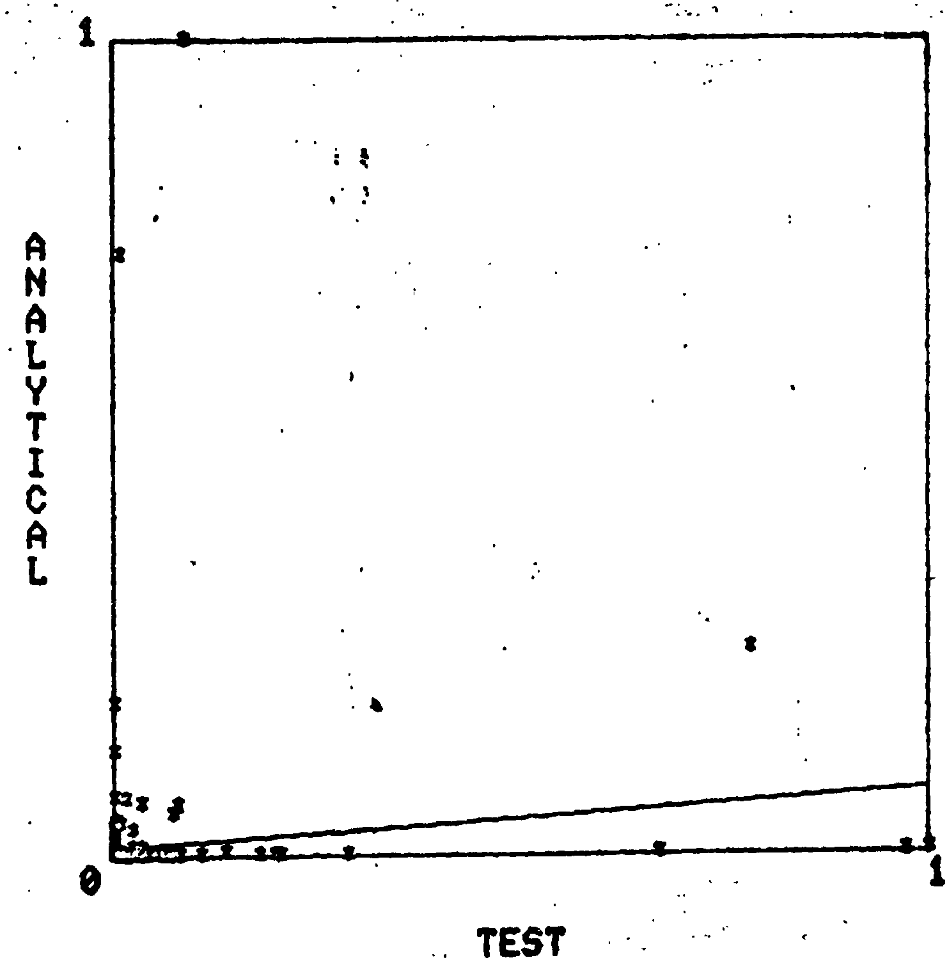

Figure 18. Linear regression analysis.

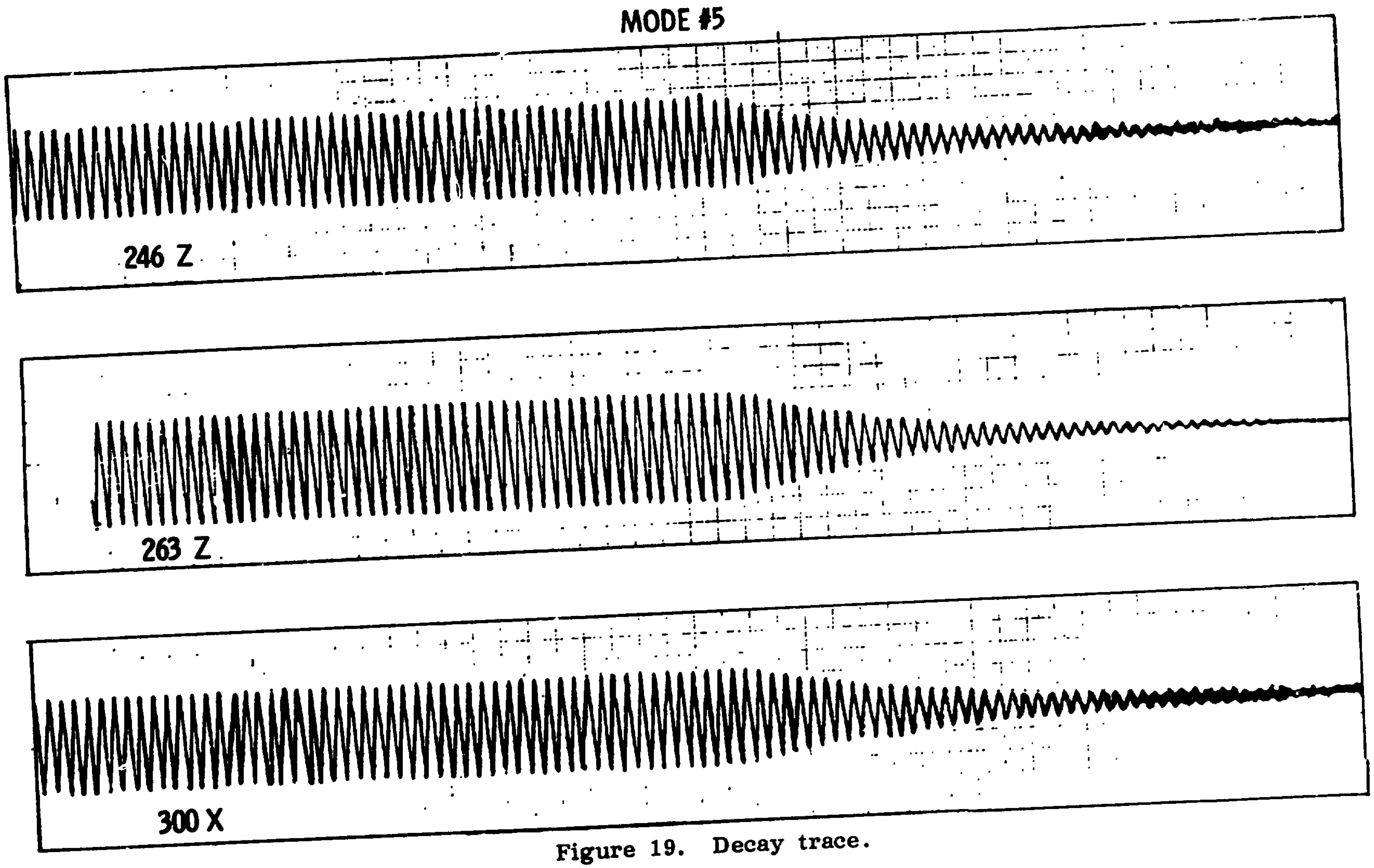

Figure 19. Decay trace.

The kinetic energy distribution for the mode is given in Figure 14. From this listing it can be seen that the principal kinetic energy is in the SRB (76 percent) and that the mode is a roll/pitch mode of the SRB. The cross orthogonality between the analytical mode and the test mode is shown in the lower matrix in Figure 16. The upper matrix in the same figure corresponds to the analytical modal frequency.

The linear regression analysis presented in (Figures 17 and 18) is another aid in matching the analytical mode to the test mode. Ideally the analytical mode matches the test mode when the plotted line is at a 45 degree angle. The decay trace is shown in Figure 19, where selected accelerometers are monitored and the input force is cutoff. Modal damping can be calculated from these decay traces.

e. Payload Bay Response Sweeps. Nine payload bay sweeps were performed during the liftoff testing. Accelerometers were special patched for those sweeps. Accelerometer readings were recorded on the two simulated payloads and on the payload bay. The shakers used, their phasing and frequency ranges for each sweep are shown in Table 9.

f. Pressure Rings Removed. The stiffening rings were attached to the SRB's at the aft ET/SRB interface. These rings were made up of three segments bolted together to simulate the stiffening effect of the SRM chamber pressure during burn. These rings were attached to the SRB's during all of the preceding test phases. These rings were later removed and narrow band sweeps from 1 to 4 Hz were run for symmetric and antisymmetric excitations. The SRB pitch-roll mode which responded more to pressure than other modes was tuned. The symmetric and antisymmetric modes were first tuned with two segments of the ring removed. There was no appreciable change in frequency. The third segment was thought to be stiffening the aft/SRB interface so it was also removed. Again there was no appreciable change in frequency. Table 10 summarizes the result of the above tests.

Altering the aft ET/SRB interface stiffness of the SRB was not effective in changing the pitch/roll modal frequency as the pretest analysis indicated. The analysis assumed that the forward ET/SRB attachment is free to roll. Instrumentation was installed to measure the relative amount of rotation for the last two modes. The test indicated that the interface was locked and was carrying some moment.

g. Special Test of the Forward ET/SRB Interface LOX Tank Empty. It was thought that the LOX tank weight was causing enough friction on the ET/SRB ball joint to prevent free rotation at that interface. To verify this and to determine that the bolt torque was not causing seizing, tests were run with the LOX tank empty and with the bolt torqued and loose (Table 11). The test results, as shown in Table 11, indicated that with the LOX tank empty the SRB/ET ball joint was free to rotate. The bolt torque was not effective.

TABLE 9. PAYLOAD BAY SWEEPS

Sweep No.	Shaker Used	Shaker Phasing (deg)	Frequency Range (Hz)	Frequency Increment (Hz)	Number of Oscillations Per Increment
1	FL10Y	0	2 - 50	0.1	10
	FL11Y	0			
2	FL10Y	0	2 - 50	0.1	10
	FL11Y	180			
3	FB10Z	0	2 - 50	0.1	10
	FB11Z	180			
4	FB10Z	0	2 - 50	0.1	10
	FB11Z	0			
5	LL06Z	0	2 - 50	0.1	10
	RR06Z	180			
	LR07Z	180			
	RL07Z	0			
6	LL06Z	0	2 - 50	0.1	10
	RR06Z	0			
	LR07Z	180			
	RL07Z	180			
7	RB14Y	0	2 - 50	0.1	10
	RT14Y	180			
	LB14Y	180			
	LT14Y	0			
8	RB14Y	180	2 - 50	0.1	10
	RT14Y	0			
	LB14Y	180			
	LT14Y	0			
9	LB01X	0	2 - 50	0.1	10
	LT01X	0			
	RB01X	0			
	RT01X	0			

TABLE 10. MVGVT LIFTOFF PITCH/ROLL MODE, LOX TANK FULL

Test Condition	Symmetric			Antisymmetric		
	Mode No.	Freq Hz	Damping C/cc	Mode No.	Freq Hz	Damping C/cc
With Rings	5	2.05	0.013	8	2.235	0.010
Two Segments Off	40	2.02	0.018	32	2.235	0.009
Three Segments Off	42	2.04	0.017	33	2.235	0.011

TABLE 11. MVGVT LIFTOFF TEST PITCH/ROLL MODE, LOX TANK EMPTY

Test Conditions	Symmetric			Antisymmetric		
	Mode No.	Freq. Hz	Damping C/cc	Mode No.	Freq. Hz	Damping C/cc
Bolt Loose	43	2.314	0.018	44	2.196	0.012
Bolt Torqued	45	2.314	0.017	--	-----	-----

h. Special Test of the Forward ET/SRB Interface — LOX Tank Refilled. It was thought that the ball joint had been worn smooth in the previous test (LOX tank empty), so the LOX tank was refilled to simulate the liftoff test condition and the pitch/roll modes were retuned. The test results showed no appreciable change in frequency and damping to the previous test condition with the LOX tank full. It also showed that the LOX tank weight was sufficient to lock the forward interface.

B. End Burn (Pre-SRB Seperation)

1. Configuration. The end burn (T + 125 sec) configuration tested consisted of the OV-101 Orbiter mated with an ET and two empty SRB. The ET and Orbiter test articles were the same as those used during the liftoff test and have been previously described. The two SRB tanks contained no inert propellant and since the test condition simulated was end burn, the pressure rings used to simulate internal pressure for liftoff were not required. The SRB nozzles were omitted as in liftoff.

2. Suspension. The end burn configuration utilized the same suspension system as was used in liftoff. However, the pressures in the HDS system and the pitch and yaw air bags were reduced to obtain a softer suspension system. This was done to maintain an adequate separation between the rigid body modes and the elastic modes.

3. Test Results and Analysis.

a. Suspension System Modes. The six rigid-body modes were obtained and are summarized in Table 12.

b. Flight Control Transfer Functions. Nine flight control transfer functions were taken for the SRB and Orbiter in roll, pitch, and yaw. These sweeps are presented in Table 13 and show the shakers and phasing used, the type motion produced, and the frequency range covered.

The last three sweeps were taken using shakers on both the Orbiter and the SRB simultaneously to excite the Shuttle pitch, roll, and yaw. Shaker force ratios were specified for these sweeps to simulate actual flight conditions. Significant response frequencies were identified for flight controls and are presented in Table 14.

c. Pogo Wide Band Sweep. Wide band frequency sweeps were run independently on all three orbiter main engines. The excitation force in each case was along the engine longitudinal axis The three pogo sweeps are listed in Table 15. Four engine axial modes were identified by the pogo group above 16 Hz and dwells were taken for each mode.

d. Modal Test Results versus Pretest Analysis. All acceptable modes tuned during the end burn symmeteric tests are shown in Table 16. The antisymmeteric modes are listed in Table 17. The correlating pretest analytical frequency and the computed modal damping from the decay traces are also shown in those tables. The last column gives the percent error between the test and the analytical mode.

TABLE 12. SRB BURNOUT SUSPENSION SYSTEM MODES

Mode No.	Test Frequency Hz	Predicted Frequency Hz	Damping C/cc	Description of Motion
3	0.255	0.302	.077	Z-Translation
53	0.275	0.258	.009	Y-Translation
51	0.549	0.528	.037	θX(Roll)
54	0.549	0.603	.034	θZ(Yaw)
1	0.647	0.59	.022	X-Translation
2	0.657	0.671	.048	∂Y(Pitch)

TABLE 13. SRB B/O FCS SWEEPS

Sweep No.	Shakers	Phase (deg)	Type Motion		SMTAS Sweep No.			Remarks
					2-7 Hz	7-17 Hz	17-30 Hz	
1	LT/RB14Y LT/LB14Y	180/0 0/180	SRB Yaw		7	8	9	
2	FL10Y FL11Y	0 0	ORB Yaw		5	10	11 & 11A	
3	RR06Z/RL07Z LL06Z/LR07Z	0/180 0/180	SRB Pitch		1	12	13	
4	FB10Z/FB11Z	0/0	ORB Pitch		3	14	15	
5	RR06Z/RL07Z LL06Z/LR07Z	180/0 0/180	SRB Roll		2	17		
6	FB10Z/FB11Z	0/180	ORB Roll		6	16		6-1 (No. 4) Rerun
7	RR06Z/RL07Z LL06Z/LR07Z FB10Z/FB11Z	0/180 0/180 180/180	SRB/ORB Pitch			2-15 Hz 18	15-30 Hz 19	Shakers SRM Shakers-1.0* ORB Shakers-3.0 *= Reference
8	RB14Y/RT14Y LB14Y/LT14Y FL10YFL11Y	0/180 180/0 0/0	SRB/ORB Yaw			22	23	SRM Shakers-1.0* FL10Y -2.0 FL11Y -4.0
9	RR06Z/RL07Z LL06Z/LR07Z FB10Z/FB11Z FL10Y	0/180 180/0 0/180 0	SRB/ORB Roll	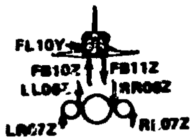		20	21	SRM Shakers-1.0* FL10Y -1.15 FB10Z -1.54 FB11Z

TABLE 14. PRIMARY FCS RESPONSE FREQUENCIES SRB BURNOUT TRANSFER FUNCTIONS

Sensor/Axis			Primary Response Frequency (2-7 Hz Freq Range)	
			SRB Shakers	ORB Shakers
ORB RGA'S	1307 Bulkhead	Roll	2.5*,3.9,5.2	2.7*,4.1,5.3*
		Pitch	2.6*,4.8,6.1	2.7,3.4*,6.1
		Yaw	2.5,4.3	4.2
	Nav Base	Roll	2.5*,4.2	2.7*,4.5,5.4,6.8
		Pitch	Low Coherence	3.4
		Yaw	2.5	Low Coherence
SRB RGA'S	LSRB	Pitch	2.6*,4.8,6.0	2.6*,6.8
		Yaw	2.5,2.6,4.4	2.6,4.0,4.4,5.3,6.7
	RSRB	Pitch	2.6,4.8,6.0	2.6*,4.9
		Yaw	2.5,2.6,4.7	2.6,4.0,4.4,5.3,6.7
ORB Accel		Normal	2.6,4.8*	3.4
		Lateral	2.5*,4.2	2.6,4.2

* Dominant Modes

** Off Axis Response to 4.8 Hz SRB Pitch Shaker Excitation

TABLE 15. SRB B/O POGO SWEEPS

Sweep No.	Shakers	SMTAS Sweep No.		
		2-12 Hz	12-30 Hz	30-50 Hz
1	MT01X Upper SSME Axial	1	2	3
2	ML02X Lower Left SSME Axial	4	5	6
3	MR03X Lower Right SSME Axial	11	10	9

TABLE 16. MVGVT MODAL CORRELATION [CONFIGURATION - BURNOUT (SYMMETRIC)]

Test Mode				Analysis Mode			
Mode No.	Freq.	Damp	Description	Mode No.	Freq.	Description	Percent Error
6	2.55	0.025	SRB Pitch (0.48), Roll (0.13), Orbiter Pitch (0.18)	4	2.50	SRB Pitch (0.22), Roll (0.56), Orbiter Pitch (0.08)	2.0
27	3.41	0.012	Orbiter Pitch (0.46), Axial (0.38), SRB Pitch (0.01), Roll (0.02)	5	3.11	Orbiter Pitch (0.37), Axial (0.32), SRB Pitch (0.19), Roll (0.06)	8.8
9	3.59	0.028	SRB Y-Bending (0.79), Z-Bending	7	3.57	SRB Y-Bending (0.51), Z-Bending	0.6
10	4.78	0.019	SRB Pitch (0.64), Orbiter Z (0.16)				
15	6.08	0.007	Orbiter Axial (0.32), Z-Bending (0.27), SRB-Z (0.17), ET Feedline (0.03)	9	6.19	Orbiter Axial (0.41), Z-Bending (0.24), SRB-Z (0.04), ET Feedline (0.14)	1.8
32	7.73	0.007	SRB Y (0.35), X (0.19), ET (0.10)	17	8.86	SRB-Y (0.57), ET (0.27)	15.0
18	8.92	0.023	Orbiter Z-Bending (0.38), SRB Pitch (0.13), Roll (0.12)	19	9.04	Orbiter Z Bending (0.48), and Axial (18), ET (0.21)	1.3
23	9.94	0.016	ET (0.51 Intertank and LWR LH_2 Tank), SRB X (0.14), Y (0.22)	22	10.64	ET (0.58 Intertank and LWR LH_2 Tank), SRB X (0.19), Y (-11)	7.0
19	11.08	0.018	ORB Z Bending (0.40), Axial (0.14), SRB Z Bending (0.22), Roll (0.09)	24	11.19	ORB Z Bending (0.29), Axial (0.13), SRB Z Bending (0.15)	1
7	12.09	0.002	LOX Dome Bulge (0.18), Feedline (0.14), SRB Axial (0.21), Y Bending (0.12)				
20	13.35	0.022	ORB Z Bending (0.50), Elevons Out-of-Phase (0.16)	28	12.31	ORB Z Bending (0.06), Elevons Out-of-Phase (0.72)	8
22	13.74	0.012	SRB 2nd Y Bending (0.20), SRB Z Bending (0.10), Elevon Rotation (0.14), LWR SSME Z (0.05)				
26	14.56	0.012	ORB 2nd Z Bending (0.40), LH_2 Tank (0.12)	36	14.3	ORB 2nd Z Bending (0.26), Wing Bending (0.21), Elevons (0.16)	2

TABLE 16. (Concluded)

Test Mode				Analysis Mode			Percent Error
Mode No.	Freq.	Damp	Description	Mode No.	Freq.	Description	
31	15.11	0.012	SRB Z Bending with Torsion (0.39), AFT Payload Axial (0.24)				
24	16.05	0.011	LH_2 Tank Shell Mode (0.20), SRB X (0.1) and Z Bending (0.1), OMS POD Axial (0.09)				
8	16.44	0.015	SRB Axial (0.27) with Y (0.15) and Z (0.09) Bending, LH_2 Tank (0.16), LOX Tank (0.16)	41	15.26	SRB Y Bending (0.23), LOX Tank (0.32), LH_2 (0.08)	7
21	17.85	0.035	SSME Z (0.45), LH_2 Tank (0.10)				
11	16.38	0.006	SRB 2nd Z Bending (0.56)	53	18.12	SRB Z Bending (0.50), Elevons (0.21)	1
30	21.78	0.014	Feedline X (0.20), LH_2 Tank (0.14), UPR SSME Z (0.07), LWR SSME X (0.06)	92	24.35	LH_2 Tank (0.31), LWR SSME X (0.08), UPR SSME Z (0.04)	12
33	28.75	0.022	UPR SSME X (0.17), LWR SSME X (0.06), LH_2 Tank (0.31)	131	32.52	UPR SSME X (0.11), Z (0.06), LWR SSME Z (0.11), X (0.06), LH_2 Tank (0.27)	13
29	30.45	0.020	UPR SSME X (0.29), LWR SSME X (0.09), Z (0.09), LOX Dome and LH_2 Tank Axial (0.21)	135	32.96	UPR SSME X (0.44), LOX Tank (0.08), LH_2 Tank (0.06)	8
25	31.62	0.018	UPR SSME Axial (0.42), LH_2 Tank (0.19)	135	32.96	UPR SSME X (0.44), LOX Tank (0.06), LH_2 Tank (0.06)	4

TABLE 17. MVGVT MODAL CORRELATION [CONFIGURATION - BURNOUT (ANTISYMMETRIC)]

Test Mode				Analysis Mode			
Mode No.	Freq (Hz)	Damp	Description	Mode No.	Freq. (Hz)	Description	Percent Error
2	2.49	0.019	SRB Z Trans (0.45), and Roll (0.08), ORB Yaw (0.14) and Roll (0.11)	4	2.53	SRB Pitch (0.54), Roll (0.04), ORB Yaw (0.23) and Roll (0.03)	1.6
18	3.98	0.015	SRB Pitch (0.60), OMS Y (0.05), V.T. and Wing Bend (0.08)			None	
20	4.19	0.015	SRB Yaw (0.36) ORB Yaw (0.17), Wing Bending (0.13)	7	4.48	SRB Yaw (0.45), ORB Yaw (0.34)	6.9
8	6.82	0.023	FWD P/L Y (0.21), FUS Y Bend (0.21), OMS POD Y (0.10)	10	6.10	FWD P/L Y (0.54), FUS Y Bend (0.14)	10.6
10	7.529	0.016	SRB X Trans (0.54) and Y Bend (0.30), ET Y Bend (0.14)	17	8.41	SRB X (0.42), Y Bend (0.23), ET Y Bend (0.21)	11.7
11	7.92	0.037	SRB Z Bend (0.24), Roll (0.23), ORB Y Bend (0.11), Torsion (0.08)	12	6.721	SRB Z Bend (0.23), Roll (0.08), Y Bend (0.08), ORB Y Bend (0.28), and Torsion (0.11)	15.1
16	8.49	0.016	Tuned on AFT Payload Y (0.04), SRB X (0.30), ORB Y (0.19)			None	
6	9.71	0.016	SRB Y Bend (0.37), ET Y Bend (0.15), AFT P/L Y (0.07), OMS POD Y (0.07)	22	10.01	SRB 1st Y Bend (0.38), Z Bend (0.20), ET Y Bend (0.24)	3.1
22	11.86	0.013	SRB Z (0.24) and Y Bend (0.22), and LH_2 Y Bend (0.32)			None	
12	12.52	0.009	ET Y Bending (0.90)	24	11.6	Elev Z (0.35), ET Y Bend (0.16)	7.4
17	13.35		LH_2 Shell (0.34), SRB Y Bend (0.18), CC Y (0.02)	36	14.83	LH_2 Shell (0.24), CC Y (0.08)	11.1

TABLE 17. (Concluded)

Test Mode				Analysis Mode			
Mode No.	Freq. (Hz)	Damp	Description	Mode No.	Freq. (Hz)	Description	Percent Error
9	14.13	0.028	ORB Y Bend (0.32) and Roll (0.07), CC Yaw (0.12)	30	13.15	CC Yaw (0.20), U-SSME Y (0.18), ORB Roll (0.08)	6.9
19	15.73	0.015	ET Y Bend (0.64), SRB Y (0.05)	41	16.25	ET Y Bend (0.53), SRB Y (0.03)	3.3
23	17.61	0.005	SRB Torsion (0.58), LH_2 Shell (0.09)			None	
14	18.67	0.013	SRB Z Bend (0.52) and Torsion (0.17)			None	

e. Special Tests.

(1) Verification of the SRB RGA Ring. As a result of the liftoff tests, an abnormally high transfer function value was observed on both the left and right forward SRB ring frames where the rate gyros are mounted. These local resonances occurred at 23 and 25 Hz respectively. These rings frames were stiffened subsequent to the liftoff test. An end burn test was used to verify that the "fix" was acceptable for flight control. A comparison of the pre-fix and post-fix test results are shown in Table 18. As can be seen from the table, a response magnitude reduction of 40 on the left SRB rate gyros and 7 on the right SRB rate gyros was obtained as a result of the structural fix.

(2) Investigation of the 1307 Bulkhead Deformation. A special test was conducted to assess the credibility of the yaw rate gyros mounted on the 1307 Orbiter bulkhead. Unexpected yaw rates were read during a symmeteric flight control sweep. Twelve additional accelerometers were mounted and read during a special 1307 bulkhead survey sweep. The bulkhead deformation in the symmetric 4.78 Hz mode is shown in Figure 20. The yaw rates computed from accelerometers are compared with rates measured by the yaw rate gyros and are shown in Table 19. This comparison indicated that the readings are credible; however, the readings reflect local deformations only. The flight control transfer functions indicated that the yaw rates were about three times the pitch rate for the 4.78 Hz symmetric mode, which was verified by the accelerometers.

(3) LOX Dome Transfer Functions. LOX dome acceleration and dynamic pressure transfer functions were obtained for the Pre-SRB separation test condition. In addition, the ET liquid level was adjusted to 100 and 80 sec burn times and the transfer functions were repeated. Since the liquid level tests were performed with the SRB's empty (not a flight condition), care must be exercised applying the data directly to the flight vehicle. In all cases the excitation was applied to the SRB bottom.

Acceleration and pressure transfer functions for the pre-SRB separation, 100 and 80 sec tests are shown in Figures 21 through 26. Acceleration and pressure frequency response amplitudes shown are per pound of the reference shaker force used in each sweep. Since two shakers were used on each SRB, the value of the indicated transfer function must be divided by two.

Modal frequencies of the two LOX tank bulge modes in the SRB thrust oscillation frequency regime were plotted as a function of burn time. These data are shown in Figure 27. The damping for each mode is plotted in Figure 28 for the burn times tested. The damping was calculated from the decay traces.

TABLE 18. SRB RGA MOUNTING RING FIX FCS EVALUATION

	Sensor	Frequency (Hz)	Transfer Function Magnitude (deg/sec) lbf
L.O. Data	LSRB RGA	23	80×10^{-5}
	RSRB RGA	25	14×10^{-5}
B.O. Data	LSRB RGA	23	2×10^{-5}
	RSRB RGA	25	2×10^{-5}
	LSRB RGA	* 37	9.6×10^{-5}
	RSRB RGA	* 30-50	Peak Not Discernable Over 30-50 Hz Range

* Based on 30-50 Hz Minisweep

Conclusion: Fix is Adequate

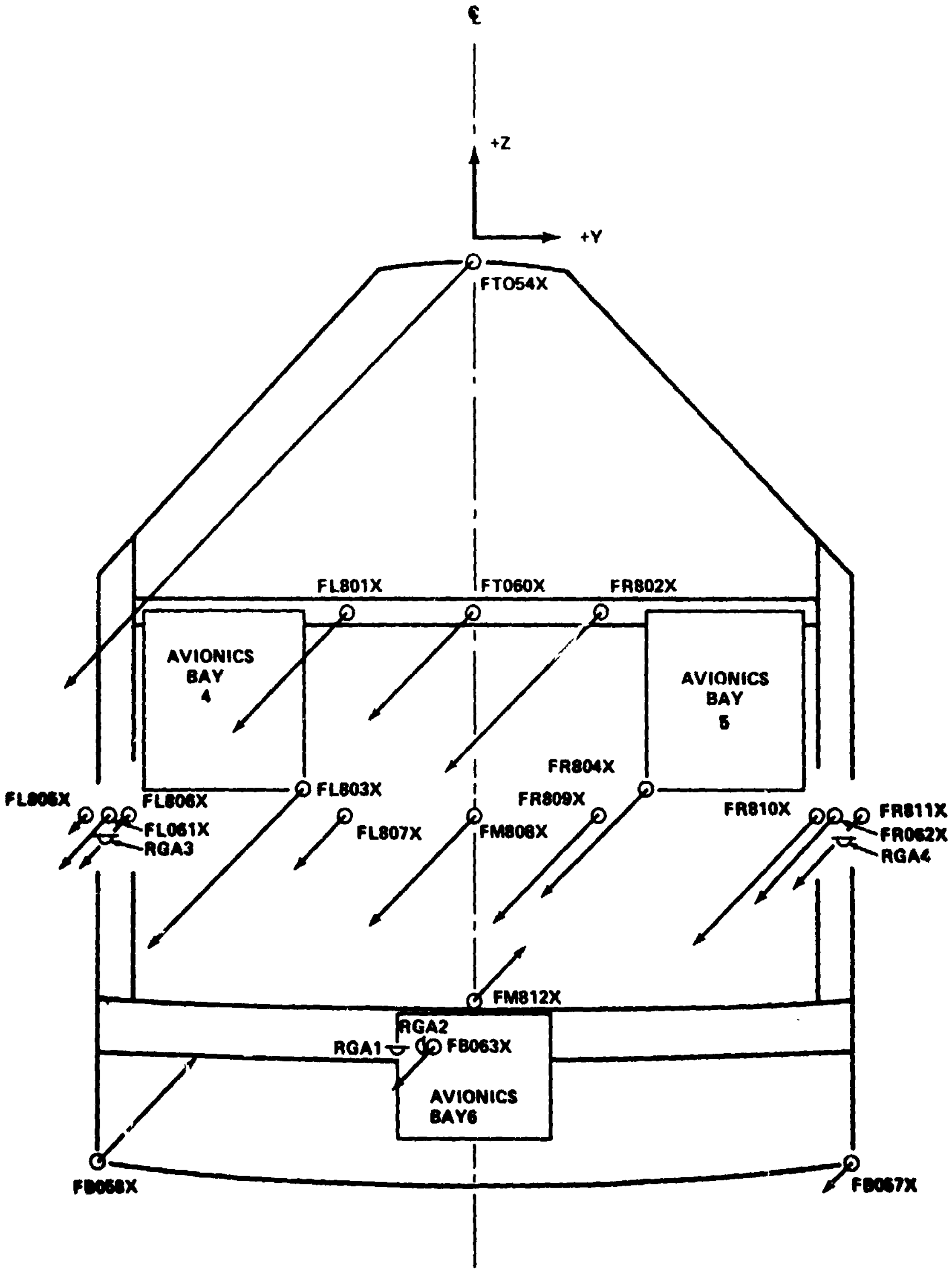

Figure 20. 1307 Bulkhead accelerations at 4.7 Hz in g's/lb.

TABLE 19. 1307 BULKHEAD COMPUTED AND MEASURED YAW RATES (DEG/SEC)

	Measured from RGA	Computed from Accel.	Ratio
Left Hand Side	1.16×10^{-4}	1.2×10^{-4}	.97
Right Hand Side	1.05×10^{-4}	1.8×10^{-4}	.58

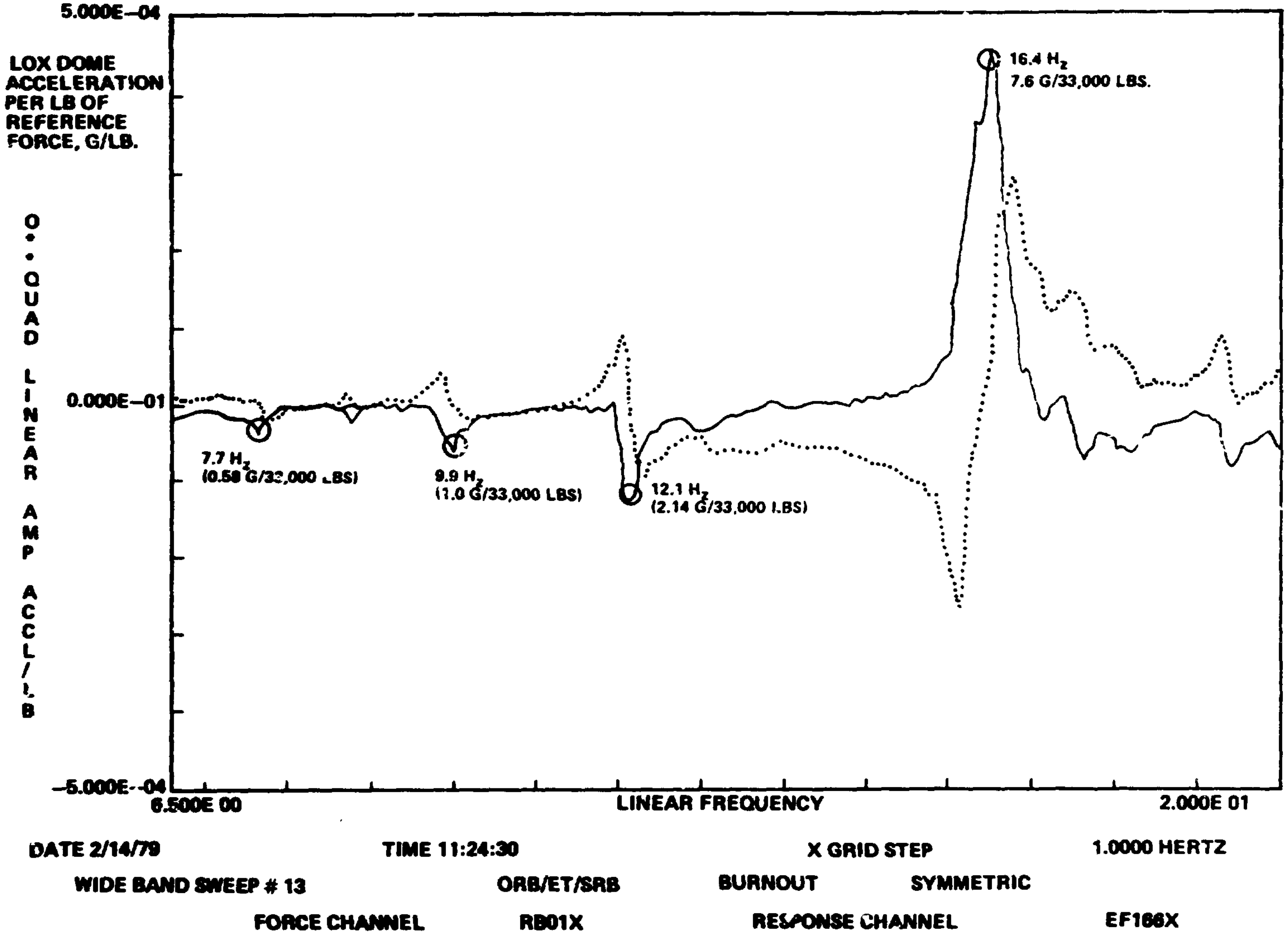

Figure 21. Lox dome acceleration transfer function, pre SRB separation.

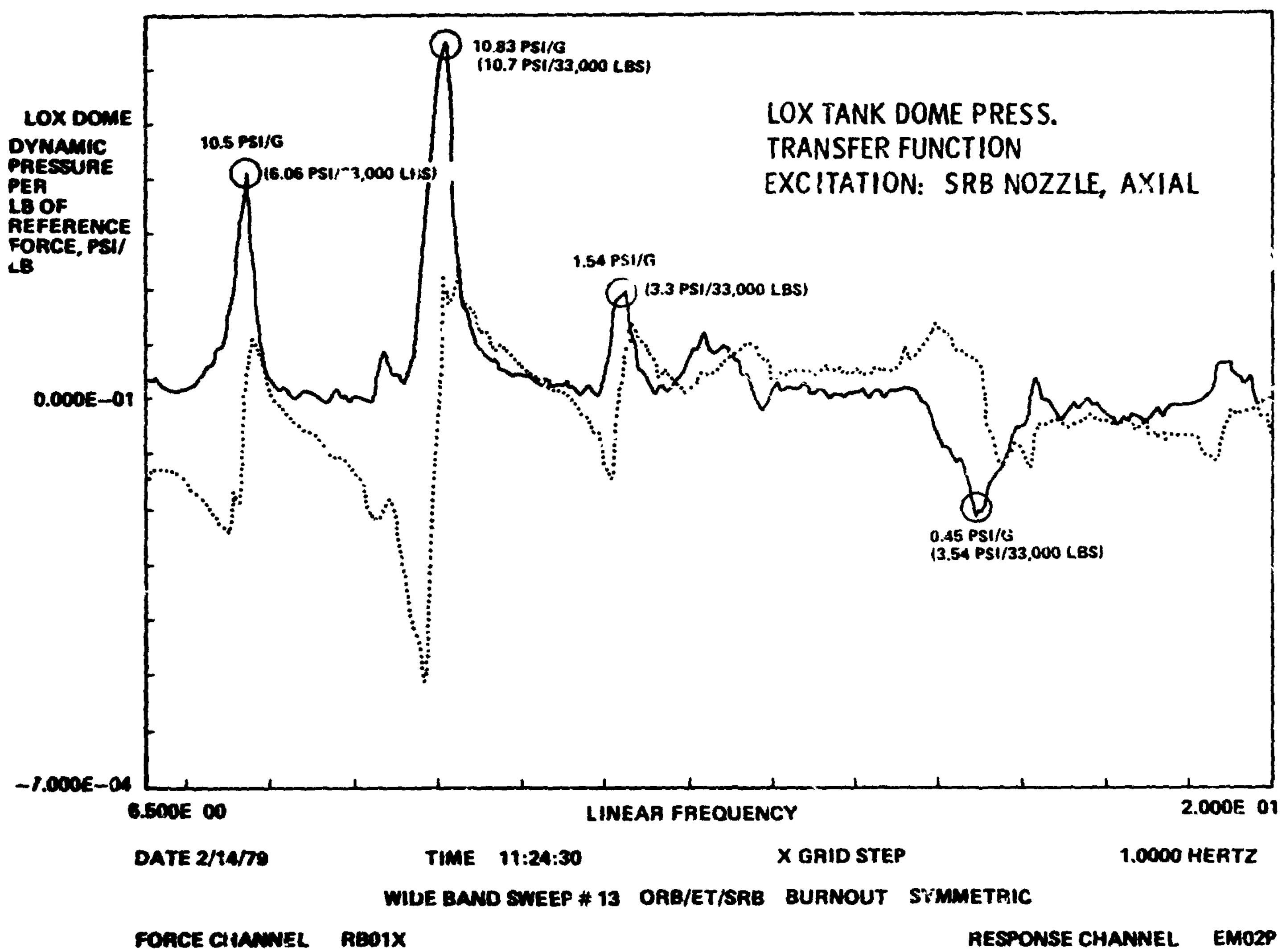

Figure 22. Lox dome pressure transfer function, pre SRB separation.

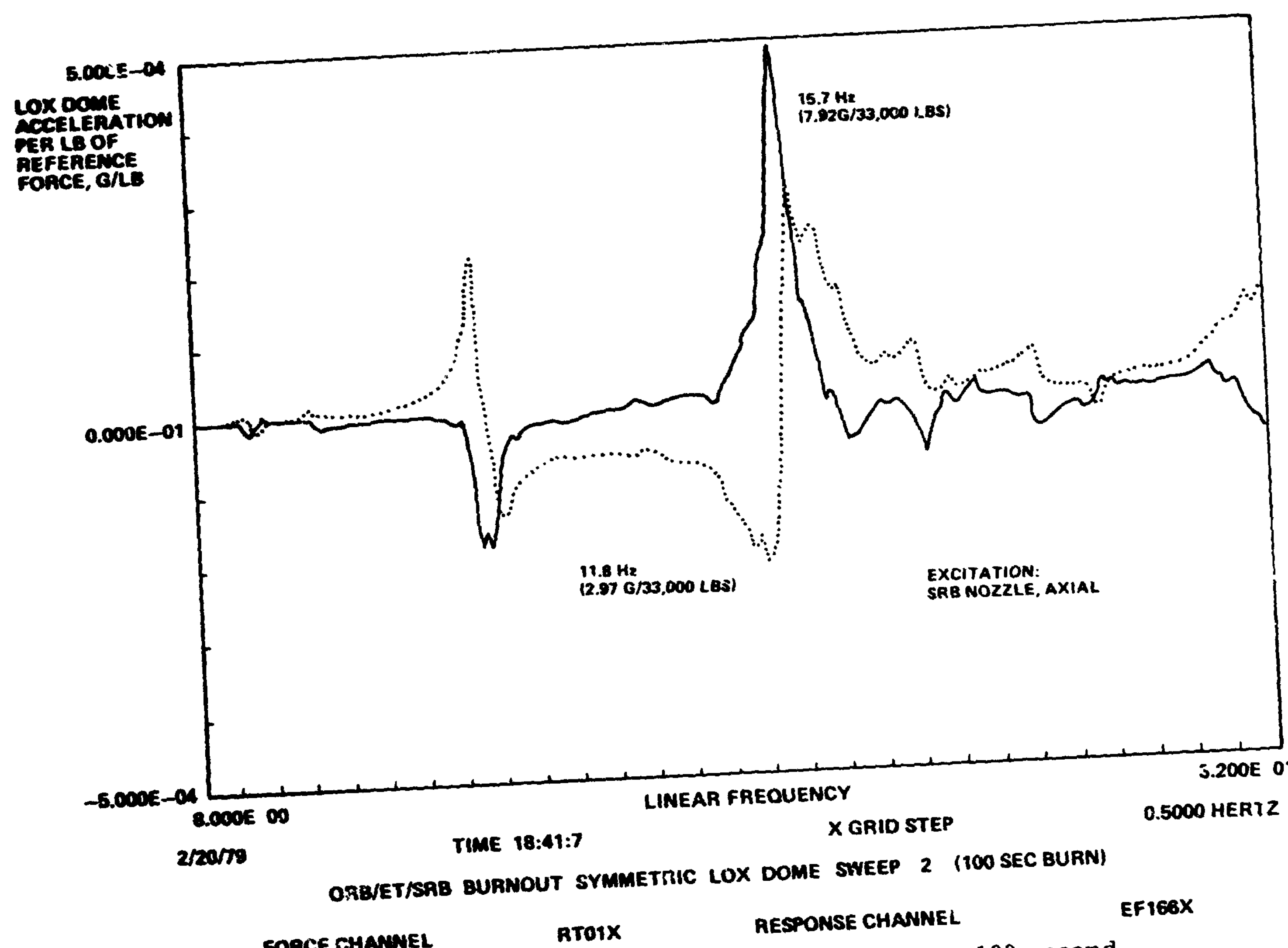

Figure 23. Lox dome acceleration transfer funct[illegible], 100 second.

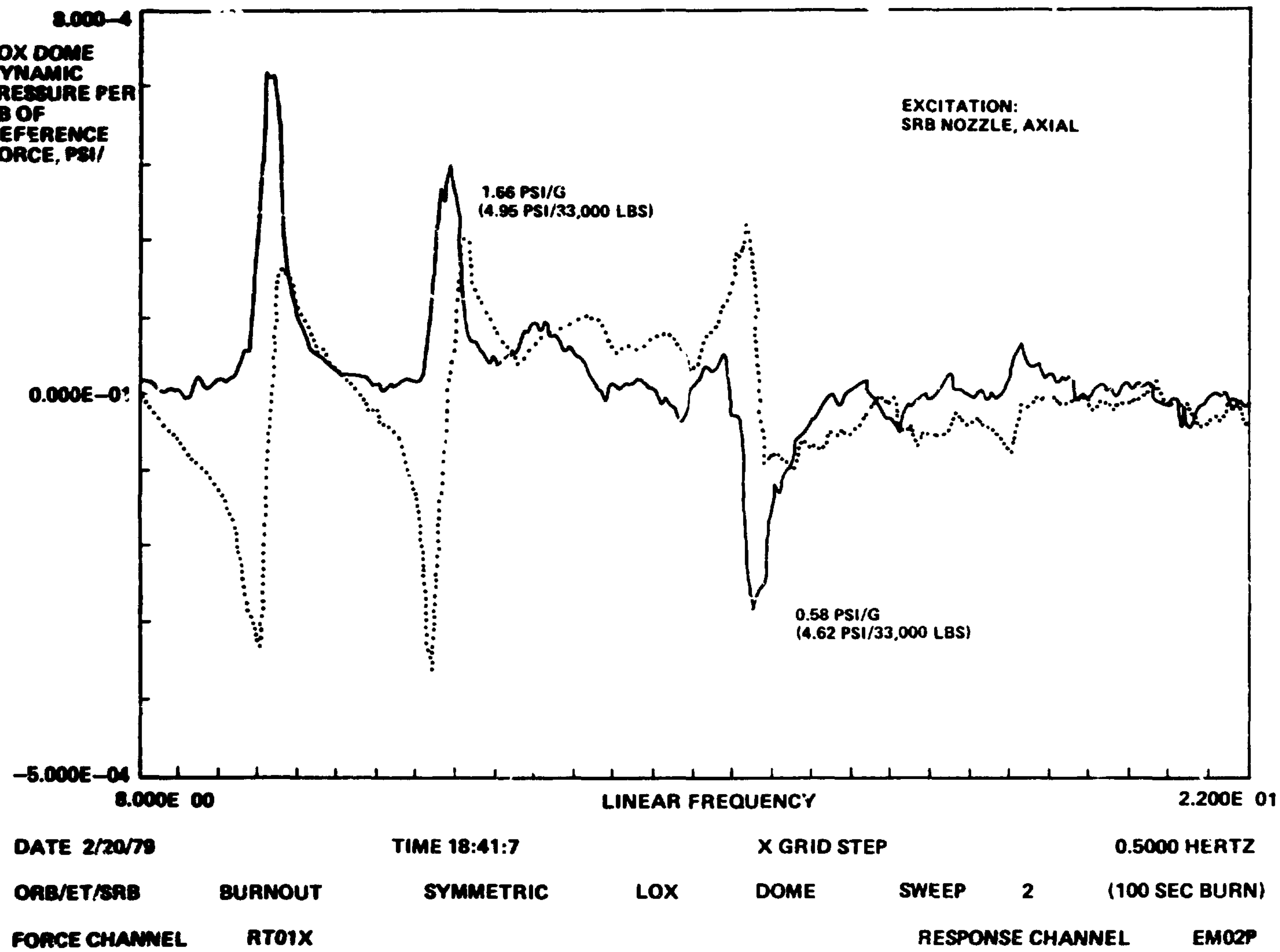

Figure 24. Lox dome pressure transfer function, 100 second.

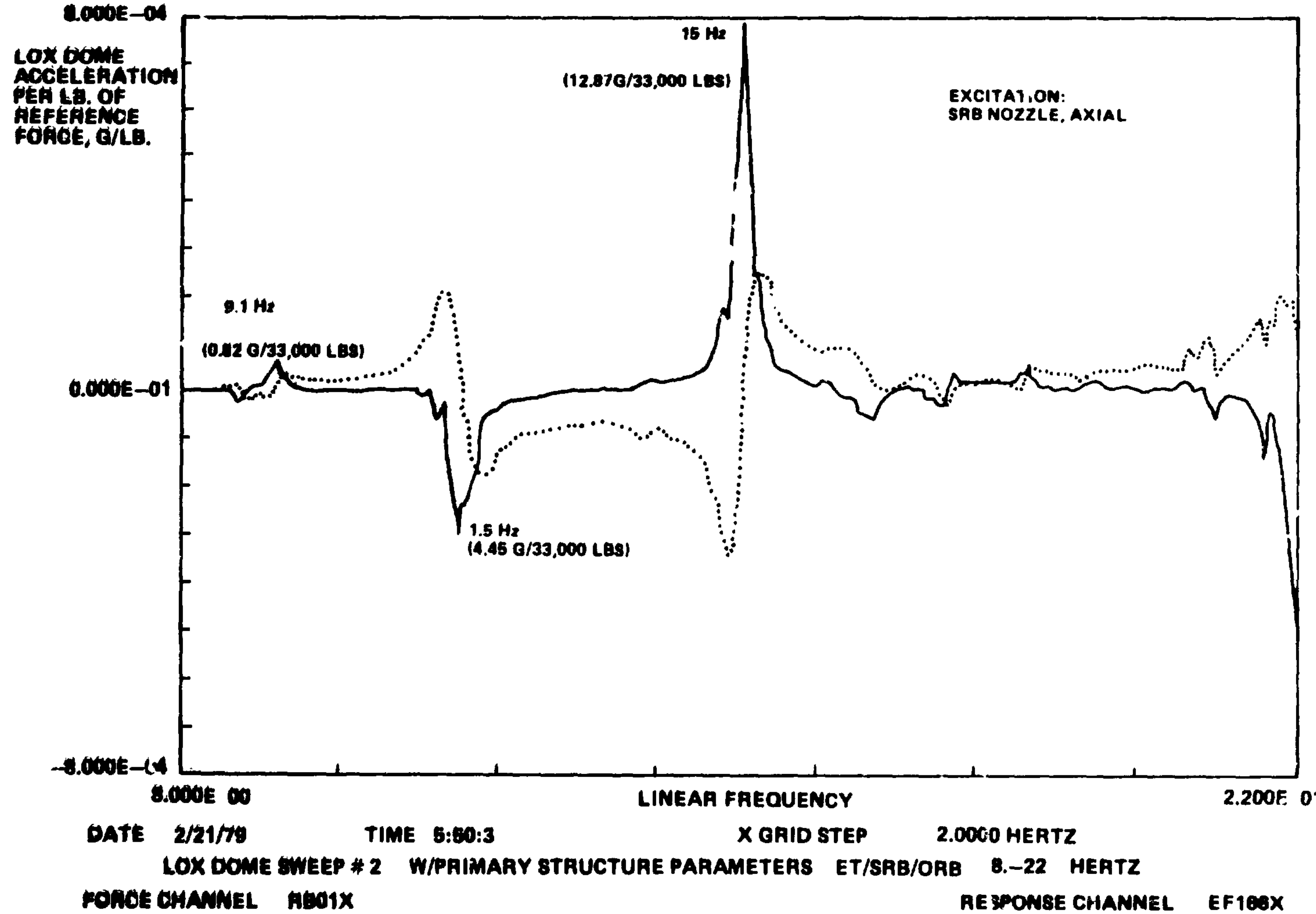

Figure 25. Lox dome acceleration transfer function, 30 second.

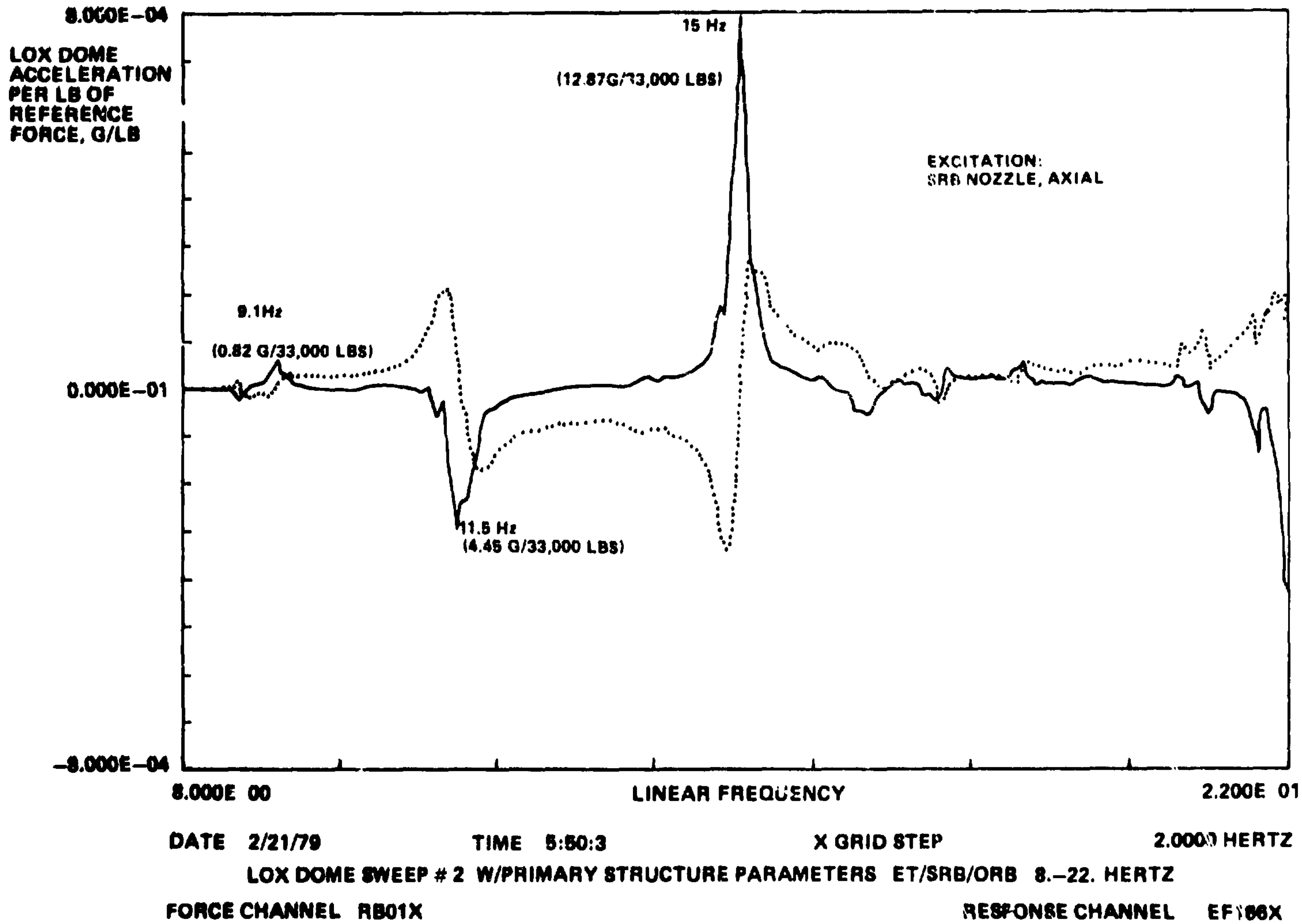

Figure 26. Lox dome acceleration transfer function, 80 second.

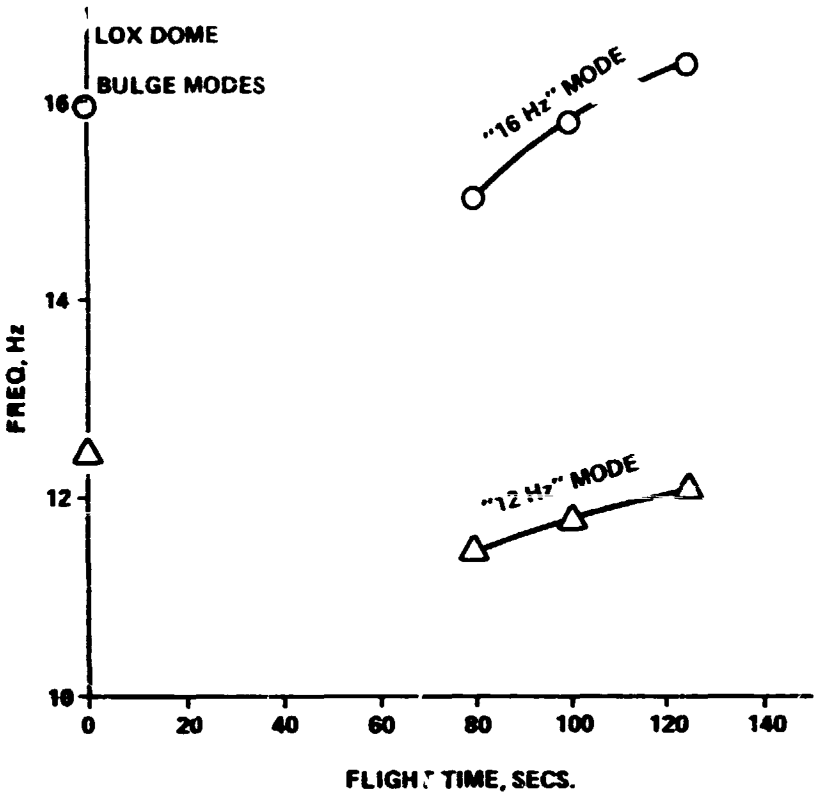

NOTE: EXCITATION APPLIED TO SRB BOTTOM ONLY; SRB'S ARE EMPTY AT 80 AND 100 SECS. LH_2 TANK EMPTY FOR ALL CASES

Figure 27. Bulge mode frequency change with flight time.

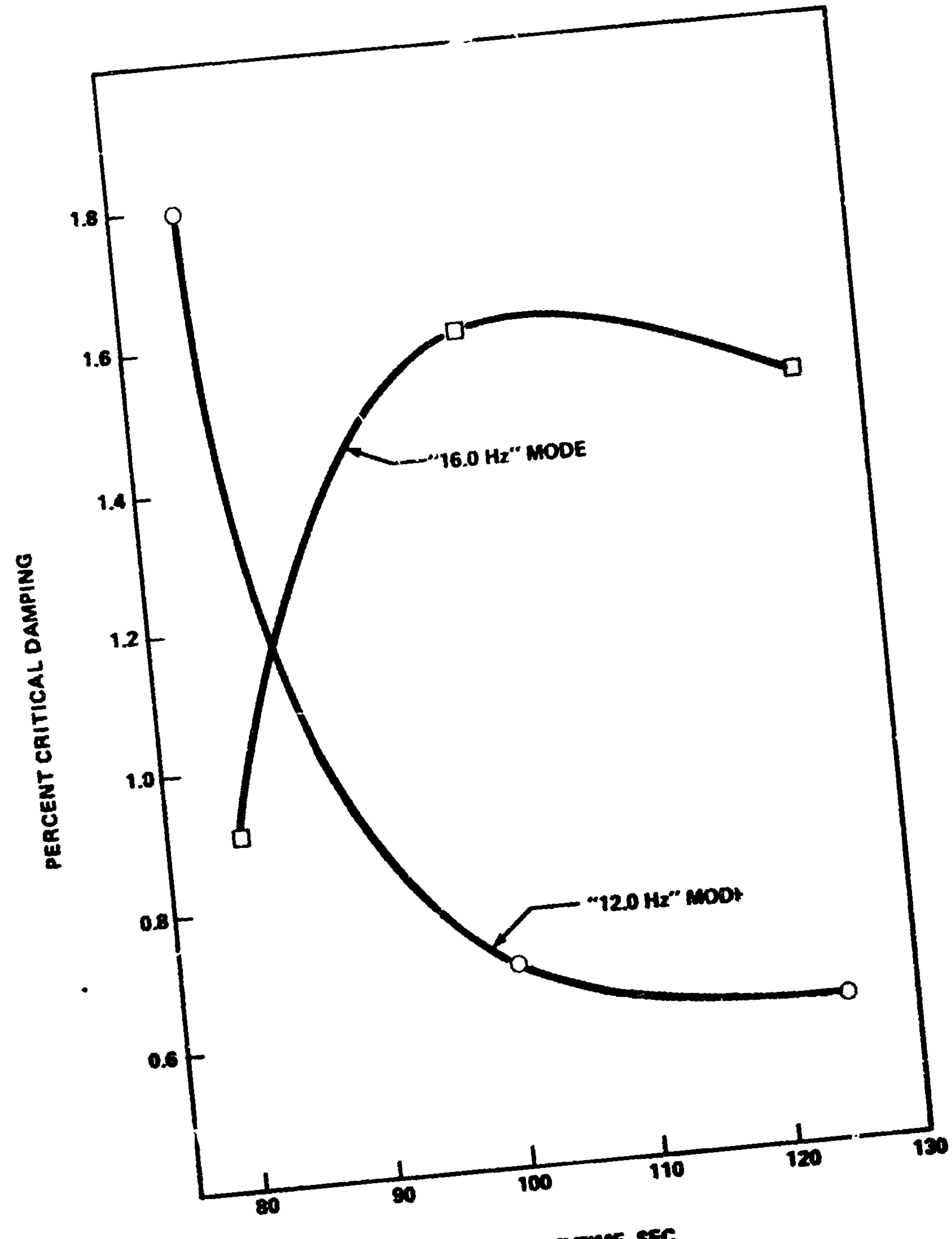

Figure 28. Critical damping curve for the lox dome bulge mode.

X. BOOST

A. Start Boost

1. Configuration. The start boost (T + 125 sec) configuration consisted of the OV-101 Orbiter mated to the ET. The Orbiter contained a 32,000 lb simulated payload. The Orbiter and ET are the same as used in the liftoff tests and have been previously described. The start boost configuration tested was canted 9 degrees. The ET LOX tank was filled with 859,800 lb to a level of 320.3 in. (X_T = 642.3 in.) of deionized sodium-chromate-inhibited water. The LH_2 tank was empty. The boost configuration was tested in Building 4550 and is depicted in Figure 29.

2. Suspension System. The overhead suspension system for the start boost configuration consisted of two pyramid shaped truss air bag assemblies. Each assembly was composed of 12 #470 Firestone air bags with reservoirs, a rod tension member, spreader beam, cable assembly, and an ET spreader beam, which connected to the test article at the forward ET/SRB attachment. For pitch and yaw stability, upper and lower Firestone air bags #319 and #312, respectively, were used. The upper air bags were attached to the forward ET attach/spreader beam, and the lower air bags were attached in the vicinity of the ET to Orbiter attachment. This suspension system is depicted in Figure 30. Early tests indicated higher lateral restraint damping than anticipated. To reduce friction, steel guides were replaced with roller bearings, and teflon sheets on steel surfaces were installed on each of the lateral restraints. In addition, the yaw or y lateral air bag pressures were reduced to zero and the cables were made slack.

3. Test Results and Analysis.

a. Suspension System Modes. Obtaining rigid body modes for the end burn configuration was found to be very difficult. This was due to the fact that the shakers used were pendulum mounted. The pendulum frequency of the shakers were close to the rigid body frequencies; hence, the excitation force was insufficient to drive the vehicle with sufficient amplitude. This problem was overcome for the start boost and mid boost suspension system test by rigidizing eight shakers. The start boost suspension system frequencies and associated damping are shown in Table 20.

b. Flight Control Transfer Functions. A set of flight control transfer functions were obtained for the start boost condition. The shakers used and the sweep frequency bands are shown in Table 21.

c. Modal Test Results versus Pretest Analysis. All acceptable modes tuned during the start boost symmetric tests are shown in Table 22. The antisymmetric modes are shown in Table 23. The correlating pretest

MATED VERTICAL GROUND VIBRATION TEST (MVGVT)

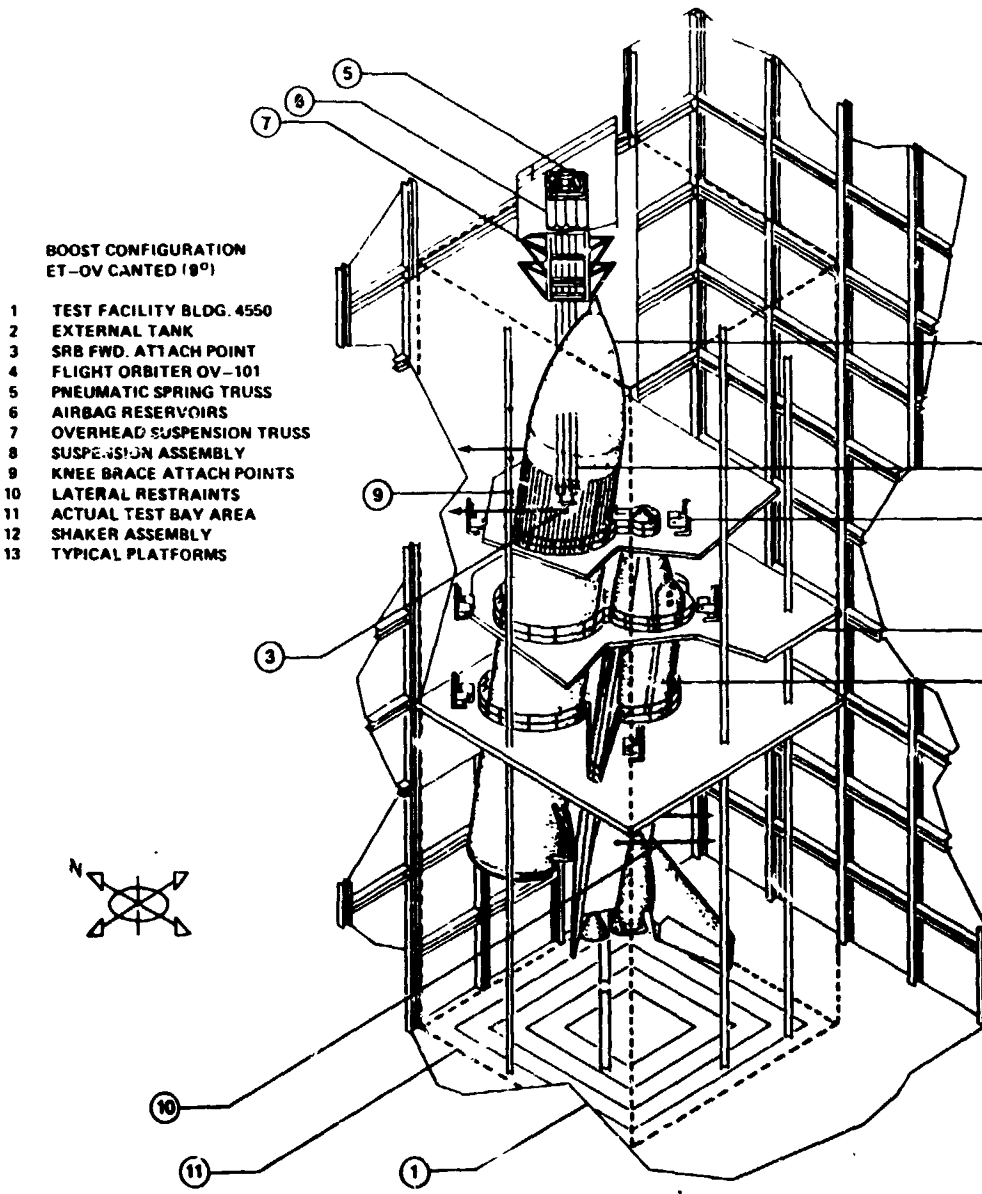

Figure 29. MVGVT boost configuration.

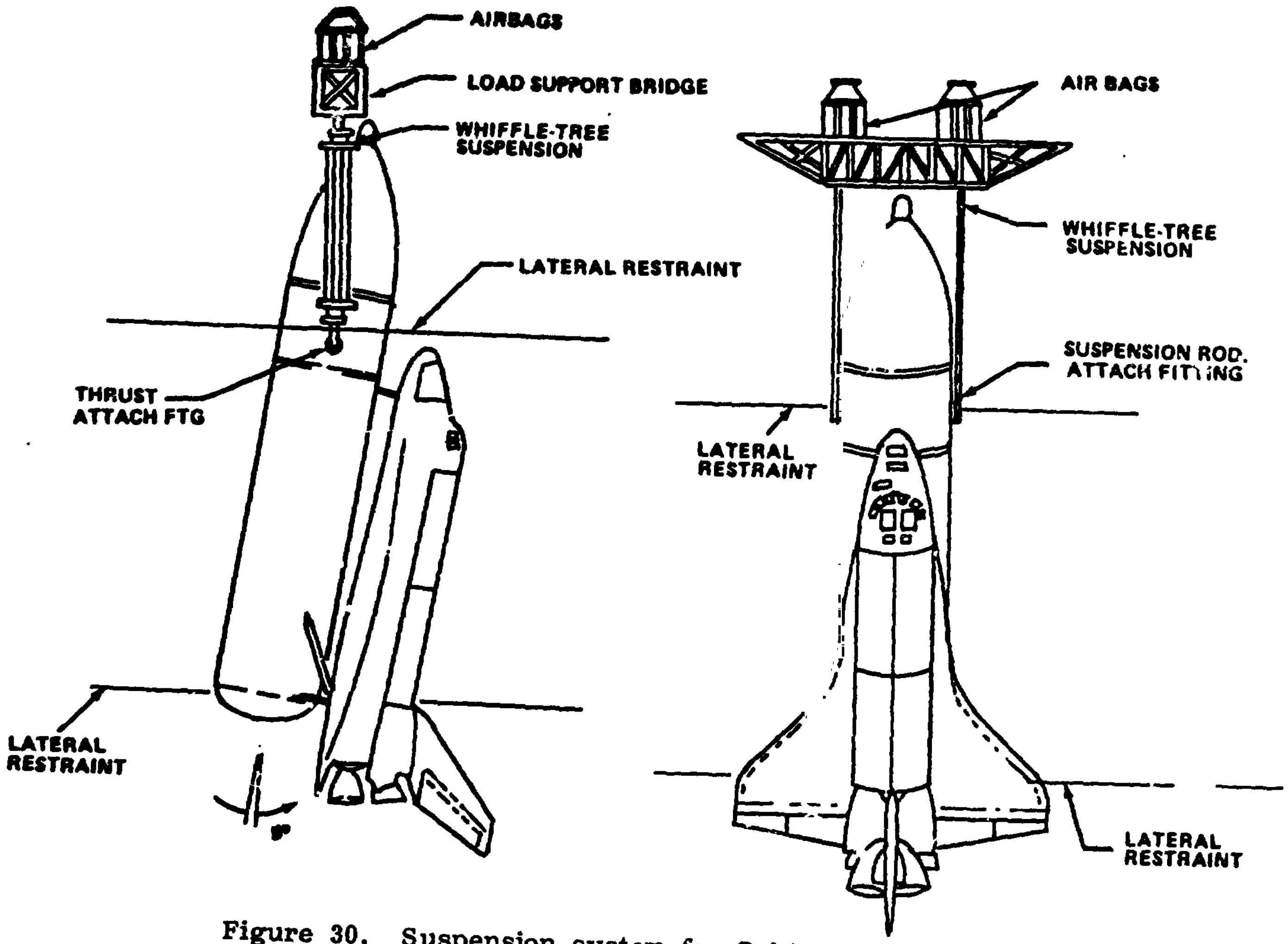

Figure 30. Suspension system for Orbiter/ET boost configuration.

TABLE 20. SUSPENSION SYSTEM MODES

Modal Description	Start-Boost		Mid-Boost		End-Boost	
	Frequency (Hz)	Damping (C/cc)	Frequency Hz	Damping C/cc	Frequency Hz	Damping C/cc
X-Translation	.647	.022	.647	.022	.804	.040
Y-Translation	.373	.04-.055	--	--	--	--
Roll	.804	>.10	.647	.075	.706	--
Pitch	.529	<.10 <.04*	.575	.032	1.077	.08-.12
Yaw	.235	.055	.471	--	.431	.018

* With rollers installed on the Z restraints

NOTE: 1. Start and Mid Boost had Y restraints with zero air bag pressure and slack in cable.

2. End Boost had Y restraints with air bag pressure and friction surface coated with teflon.

TABLE 21. FLIGHT CONTROL SWEEPS

			Sweep Frequency, Hz		
Shaker	Phase (deg)	Force (lb)	Start Boost	Mid Boost	End Boost
FL11Y	-	500	1-26	1-26	2.5-26
FB10Z	-	550	1-26	1-26	2.5-26
FB10Z FB11Z	0	550 550	1-26	1-26	2.5-26
FB10Z FB11Z	180	550 550	1-26	1-26	2.5-26
FL10Y	-	500	1-26	1-26	2.5-26
FB11Z	-	500	1-26	1-26	2.5-26

TABLE 22. START BOOST SYMMETRIC

Test			Analytical Mode	Percent Δ Frequency	Test Mode Description Dominant Motion (Kinetic Energy)
Mode No.	Freq. (Hz)	Damp (C/CC)	Freq. Hz		
6	3.431	0.014	3.27	-4.6	ORB Z Bend (0.47) and OMS X (0.15)
14	6.157	0.022	6.245	1.4	ORB X and Z Bending, Feedline X
7	6.471	0.03	6.70	3.5	1st Wing Bend (.78)
17	7.608	0.017	7.808	2.6	V.T. Pitch (0.26) O/P W/Fuse Pitch
8	8.767	0.008	8.78	0.1	Feedline X (0.57), FWD Fuse Z (0.14)
12	9.08	0.010	9.174	1	ORB Z Bend (0.47) V.T. X-Z (0.14), UPR LH_2 Tank (0.19)
10	11.43	0.031	-	-	Body Flap Rotation
11	12.64	0.016	8.779	30	Feedline Bend (0.44) and Intertank
15	13.386	0.012	12.459	-6.9	LH_2 Tank Mode (0.68) N = 2
18	16.008	0.01	19.05	19	Crew CAB X (0.05), P/L (0.08) OMS, LOX Tank
22	18.141	0.01	21.263	17.2	LOX Dome-Feedline Bend Y (0.29), Wing X (0.7)
19	19.256	0.005	19.05	-1	Feedline O/P W/LOX Dome (0.13)
16	19.55	0.03	20.29	3.7	Wing 2nd Bend (0.26), Elev (0.10)
23	24.814	-	24.2	-2.5	LOX Tank (0.35), LH_2 (0.14), Feedline (0.18)
24	27.867	-	-	-	1307 Bulkhead
21	33.366	0.014	33.24	-0.4	Feedline X (Ends O/P (0.29), LH_2 (0.39)

TABLE 23. START BOOST ANTISYMMETRIC

Test			Analytical Mode	Percent	
Mode No.	Freq. (Hz)	Damp (C/CC)	Freq. Hz	Δ Frequency	Test Mode Description Dominant Motion (Kinetic Energy)
8	3.412	0.015/ 0.22	3.76	10	FIN 1st Lat (0.80), Bend/FWD FUS LAT (0.11)
4	4.47	0.018	4.58	2	FUS Yaw Out-of-Phase (0.60)/ET Yaw (0.16), Wing Z Bending (0.13)
1	5.57	0.027	5.88	6	1st Wing Z Bending (0.31), ET Yaw and Roll (0.52)
14	6.51	0.016/ 0.091	6.33	-3	ORB/ET (0.44/0.50), F Payload Y (0.30)
21	6.902	0.004	6.60	-4	Wing Bending (0.22), In-Phase W.O.B. Elevon O_Y (0.20)
15	7.608	0.022	7.91	4	ET Roll (0.32), Out-of-Phase with ORB Roll (0.22)
9	12.720	0.016	13.61	7	Vert Tail 2nd Bend (0.51), ET (0.04)
10	13.620	0.013	16.18	19	Vert Tail Torsion (0.8), ET Shell Mode (0.06)
7	14.364	0.016	14.783	3	FUS Bending (0.14), ET Shell Mode (0.6)
5	14.677	0.017	14.563	-1	Elevons (0.38), Out-of-Phase with Wing (0.17)
16	15.264	0.044	16.184	6	Orbiter Roll, LH_2 Bending
20	16.7				Feedline Mode (0.68), ET Y Bending (0.27)
13	19.56	0.027	22.67	16	LH_2 Intertank Y Bend (0.73)
12	21.19	0.027	22.31	5	LWR Eng θ_Z (0.51), Wing X (0.15)
11	23.84	0.037	27.86	17	ET Torsion (0.25), LWR Eng Y (0.13)

analytical frequency and the computed modal damping from the decay traces are also shown in those tables. The test mode description and the percent frequency difference between test and analysis are also given.

B. Mid Boost

1. Configuration. The mid boost (T + 301 sec) configuration consisted of the OV-101 Orbiter mated to the ET. The Orbiter contained a 32,000 lb simulated payload. The mid boost configuration tested was canted 9 degrees and is depicted in Figure 29. The ET LOX tank was filled with 385,300 lb to 162 in. (X_T = 801 in.) of deionized sodium-chromate-inhibited water. The LH_2 tank was empty.

2. Suspension System. The suspension system for mid boost was the same as that described under the start boost. Again, the lateral yaw air bag pressures were reduced to zero and the cable was made slack.

3. Test Results and Analysis.

a. Suspension System Modes. The suspension system modes for mid boost were obtained with slack in the y restraints with zero air bag pressures. Excitation force was increased for this condition by rigidizing eight of the pendulum shakers. The suspension system frequencies and associated dampings are shown in Table 20.

b. Flight Control Transfer Functions. A set of flight control transfer functions were obtained for the mid boost configuration. The shakers used and the sweep frequency bands are shown in Table 21.

c. Modal Test Results versus Pretest Analysis. All acceptable modes tuned during the mid boost symmetric test are shown in Table 24. The antisymmetric modes are shown in Table 25. The correlating pretest analytical frequencies and the computed damping from the decay traces are also shown in those tables. This test mode description and the percent frequency difference between test and analysis are also given.

C. End Boost

1. Configuration. The end boost (T + 477 sec) configuration consisted of the OV-101 Orbiter mated to the ET. The Orbiter contained a 32,000 lb simulated payload. The end boost configuration tested was canted 9 degrees and is depicted in Figure 29. The ET LOX tank was filled with 88,140 lb to a liquid level of 59.5 in. (X_T = 903.5 in.) of deionized sodium-chromate-inhibited water. The LH_2 tank was empty.

2. Suspension System. The suspension system for the end boost was the same as that described under start boost except both the y and z lateral airbags were effective. The suspension system is shown in Figure 30.

TABLE 24. MID BOOST SYMMETRIC

Test			Analytical Mode	Percent	
Mode No.	Freq. (Hz)	Damp (C/CC)	Freq. Hz	Δ Frequency	Test Mode Description Dominant Motion (Kinetic Energy)
6	3.70	0.012	3.37	-9	Fuselage 1st Z-Bending
12	6.43	-	6.50	1	Feedline Axial
11	6.47	0.037	6.56	1	Wing 1st Z-Bending
13	7.59	0.017	7.81	3	V.T. Pitch (0.29), Fuselage Pitch (0.28)
15	8.65	0.006	8.85	2	Feedline 1st Z-Bending (0.73)
16	10.53	0.058	12.30 10.41	16 -1	Elevon Rotation Outboard/ Inboard Out-of-Phase
8	11.82	0.037 -0.055	11.24	-5	Body Flap Z (0.24), LH_2 (0.16), Feedline (0.08), P/L (0.07)
7	12.92	0.022	12.98	0	FUS Z-Bending (0.13), Upper LH_2 (0.13)
19	14.80	0.010	12.50	-16	LH_2 Tank (N = 2) LOX Dome, PL Axial
5	16.01	0.030			SSME Pitch (0.50), Fuselage Z (0.11), PL Axial (0.02)
17	16.44	0.008			Feedline X (0.67), Upper LH_2 N = 3 (0.24)
14	17.28	0.028	14.24/17.47	-18/1	Fuselage Z-Bending (0.40), LH_2 N = 3 (0.25)
18	19.67	0.031			Wing 2nd Z-Bending
22	20.20	0.018			Crew Cabin Axial Out-of-Phase with Orbiter
20	20.67	0.005			Tank Dome and Feedline
21	23.43	0.005			Tank Dome and Feedline
23	28.02	0.008			1307 Bulkhead Axial

TABLE 25. MID BOOST ANTISYMMETRIC

Test			Analytical Mode	Percent Δ Frequency	Test Mode Description Dominant Motion (Kinetic Energy)
Mode No.	Freq. (Hz)	Damp (C/CC)	Freq. Hz		
1	3.471	0.022	3.78	9	V.T. 1st Lat Bend (0.84), FUS -Y (0.10), ET-Y and Roll (0.04)
2	4.627	0.028	4.689	1	FUS Yaw (0.61), O/P ET Bend and Yaw (0.14), Wing Roll (0.16)
3	5.725	0.0157	5.812	1.5	Wing Bend (0.18), W/ET Yaw and Roll (0.23)
10	6.392	-	6.358	-0.5	FWD Payload (0.32) + FWD FUS Y (0.26), Wing and Elev Z (0.02)
6	7.609	0.15/0.016	8.50	11.7	ORB Roll (0.62), O/P W/ET Roll (0.35)
17	8.023	0.02	8.50	6	FUS Torsion (0.19), Y B (0.25), Wing Z (0.15)
18	11.624	0.016	11.67	0.4	IB and OB Elev ROT (0.51), O/P Wing Z (0.11)
20	11.742	0.013	12.17	3.6	LWR SSME Y (0.15), I/PW Eng I Y (0.02), Susp Sys (0.23)
4	12.681	0.011	13.662	[illegible]	V.T. 2nd Bend (0.62)
5	13.62	0.02/0.026	16.2	18.9	V.T. Torsion (0.81)
13	14.29	0.014/0.02	12.17	-14.8	FUS Y Bend (0.16), ET Shell (0.48)
15	14.48	0.028	12.38	-14.8	Elev (0.37), O/P W Wing (0.16)
11	18.08	0.022	17.811	-1.5	ET 1st Bend (0.85)
12	23.84	0.031/0.037	27.387	14.8	Wing Torsion (0.215), Elev (0.426)
8	24.012	0.01	27.85	15.9	Fuse (0.13), ET Torsion (0.22), Feedline (0.21)
14	28.96	0.01/0.02	22.08	-23.8	ET Bend and Shell (0.90)

3. <u>Test Results and Analysis.</u>

a. Suspension System Modes. The suspension system modes for end boost were obtained with air bag pressure in the y and z lateral bags. The restraint lateral friction surfaces were coated with teflon and had not been converted to roller bearings for this test condition. The suspension system frequency and associated damping are also shown in Table 20.

b. Flight Control Transfer Functions. A set of flight control transfer functions were obtained for the mid boost configuration. The shakers used and the sweep frequency bands are shown in Table 21.

c. Modal Test Results versus Pretest Analysis. All acceptable modes tuned during the end boost symmetric test are shown in Table 26. The symmetric modes were obtained with the y and z air bag restraints effective. The antisymmetric test modes are shown in Table 27. For these modes the z air bag restraint was effective; however, the y air bag had zero pressure and the cables were slack. The correlating pretest analytical frequencies and the computed modal damping from the decay traces are also shown in those tables. The test mode description and the percent frequency difference between test and analysis are also given.

D. Contingency Tests

1. <u>LOX Tank Low Level.</u> A LOX tank low level test was conducted to obtain selected pogo oriented modes. The LOX tank contained 27,600 lb of water and filled to a level of 25 in. (X_T = 938.0 in.) The y restraint air bag pressure was set at zero with slack cables. Seven symmetric modes and two antisymmetric modes were obtained. These test frequencies, corresponding analytical frequency and test mode descriptions are shown in Table 28.

2. <u>Fuselage Symmeteric Bending Mode Linearity Check.</u> The results of the horizontal ground vibration test (HGVT) indicated the fuselage first symmeteric bending mode is affected by a non-linearity associated with the cargo bay doors. It was felt that the cargo bay doors take axial loads at low force levels and stiffen the fuselage. To assess this non-linearity, plots of the frequency versus excitation force are shown in Figure 31. The frequency curves do indicate that the frequency decreases with increasing excitation force.

3. <u>SAMSO Sweeps.</u> Four payload bay wide band sweeps were run at the request of The Space and Missile System Office. These sweeps, with the shakers used, are presented in Table 29.

TABLE 26. END BOOST — SYMMETRIC

Test			Analytical Mode	Percent	Test Mode Description
Mode No.	Freq. (Hz)	Damp (C/CC)	Freq. Hz	Frequency	Dominant Motion (Kinetic Energy)
8	4.16	0.016	3.70	12	Fuse 1st Z Bend (0.12), Feedline X (0.12)
17	4.24	0.01	3.70	13	Fuse Z Bend (0.13), Payload FWD Z (0.11)
18	4.5[illegible]	0.009	3.70	18	Fuse 1 ZB (0.34), Feedline (0.17), LOX Tank (0.15), SSME Rocking (0.10), Vert Tail Pitch (0.04)
5	6.55	0.014, 0.022	6.70	6	1st Wind Bend (0.87)
9	7.25	0.006, 0.011	7.55	4	Feedline X (0.21), Out P/W LOX Dome [illegible] (0.16), Vert Tail Pitch (0.14)
20	7.26	0.006	7.55	4	ET Z Bend (0.35), Feedline X (0.22) and Orb Axial Out P/W ET
17A*	7.92	0.015, 0.009			V.T. Pitch (Without Water)
10	8.53	0.007	8.97	5	Feedline X (0.89)
11	9.32	0.020	9.7[illegible]	4	1st Fuse Z Bend (0.50), ET Z Bend
16	13.19	0.012	11.8	1.	Fuse 2nd Z Bend (0.57)
19	14.44	0.013	14.6	1	Fuse Z Bend (0.30), Feedline (0.12), LH_2 (0.11)
13	14.99	0.009			ET Z Bend, LH_2 Tank Shell (0.30), ORB ZB (0.27), FWD PL X (0.10) Out P/W AFT PL X (0.06)
21A*	15.93	0.044			SSME's Pitching (0.65), OMS POD S X (0.24)
14	17.26	0.01	17.3	0	LOX Dome Bulge
22	18.20	0.025			SSME Pitch (0.23), OMS X (0.15), Feedline (0.22)
15	18.26	0.01			Feedline X (0.44), LOX Dome Bend
18A*	18.85				LWR SSME's X
27	29.35	0.018			OMS POD X and θ_X Out P/W SSME X
21	34.83	0.011	32.95	-5	UPR SSME X (0.24), LWR SSME Torsion (0.09), OMS POD X (0.11), Fus. X (0.18), Feedline X (0.15)

TABLE 27. END BOOST ANTISYMMETRIC

Test			Analytical Mode	Percent Δ Frequency	Test Mode Description Dominant Motion (Kinetic Energy)
Mode No.	Freq. (Hz)	Damp (C/CC)	Freq. Hz		
1	3.47	0.016	3.83	10.4	V.T. 1st Lat Bend (0.87)
3	5.06	0.02[illegible]	4.83	-4.5	ORB Yaw (0.35), O/P ET Yaw (0.19), Wing B[illegible]d O/P V.T. Bend (0.32)
4	5.65	0.016/0.025	5.89	4.2	Wing Bend (0.19), O/P ET Roll, LWR SSME Y (0.08) O/P V.T.
19	6.47	0.016	8.23	27.2	LWR Engine O/P (0.90)
7	6.98	0.018	6.40	-8.3	FWD PL Y (0.26), FWD FUS Y (0.26), ET Yaw (0.26)
13	7.73	0.018	6.40	-17.2	FUS Roll (0.29), O/P ET Roll (0.29), O.B Elev ROT (0.29)
5	8.04	0.011	8.02	-0.2	FWD PL Y (0.24), ET Roll (0.20), FUS Torsion (0.15)
9	9.27	0.016	8.02	-13.4	AFT PL Y (0.32), Elev ROT (0.10)
8	10.80	0.032	10.88	0.7	ET Y Bend (0.21), V.T. Y Bend (0.04)
10	11.62	0.021	12.39	6.6	Elev ROT (0.20) I/P Wing Bend (0.05)
2	12.72	0.018/0.017	13.64	7.2	V.T. 2nd Y Bend (0.64)
14	13.62	0.028	14.63	7.4	V.T. Torsion (0.16)
16	14.48	-	-	-	Wing Bend O/P Elev ROT
11	20.67	0.025	-	-	ET Y Bending, LH_2 (0.42) - Ogive (0.3[illegible])
15	21.31	0.037	19.47	-8.6	Wing Torsion
20	22.13	0.044/0.027	22.31	-0.8	LWR Engs. Z O/P (0.43), FUS Roll (0.[illegible])
12	24.19	0.007	-	-	Feedline X and Bend (0.47), LWR SSME Z and Y (0.15)

TABLE 28. LOX TANK LOW LEVEL BOOST

Test			Analytical Mode*	Percent Δ Frequency	Test Mode Description Dominant Motion (Kinetic Energy)
Mode No.	Freq. (Hz)	Damp (C/CC)	Freq. Hz		
SYMMETRIC MODES					
2	4.20	0.013	3.66	-12.8	FUS 1st Z Bend (0.45), ET Pitch (0.37), V.T. Pitch (0.05)
1	4.55	0.018	3.66	-19.6	FUS 1st Z Bend (0.46), LOX Tank ZB (0.15)
3	15.85	0.018	15.03	-5.2	Feedline X (0.32), Susp. System (0.28)
7	17.26	0.01	19.57	13.4	LOX Tank Bulge (Possible)
6	18.26	0.055			LWR SSME X and Z (0.26), Feedline X (0.19), OMS (0.19)
4	20.25	0.01	19.90	-1.7	Feedline X and Z (0.68), LOX Bulge (Possible)
5	34.64	0.01	32.75	-5.4	Eng. 1 X (0.23) O/P LWR SSME
ANTISYMMETRIC MODES					
23	5.10	0.018	4.88	-4.3	Wing Z B (0.33), FUS (0.13) and ET (0.21) Yaw
24	15.19	-	-		Wing Z B (0.39) O/P FUS Roll (0.14), FL (0.13)

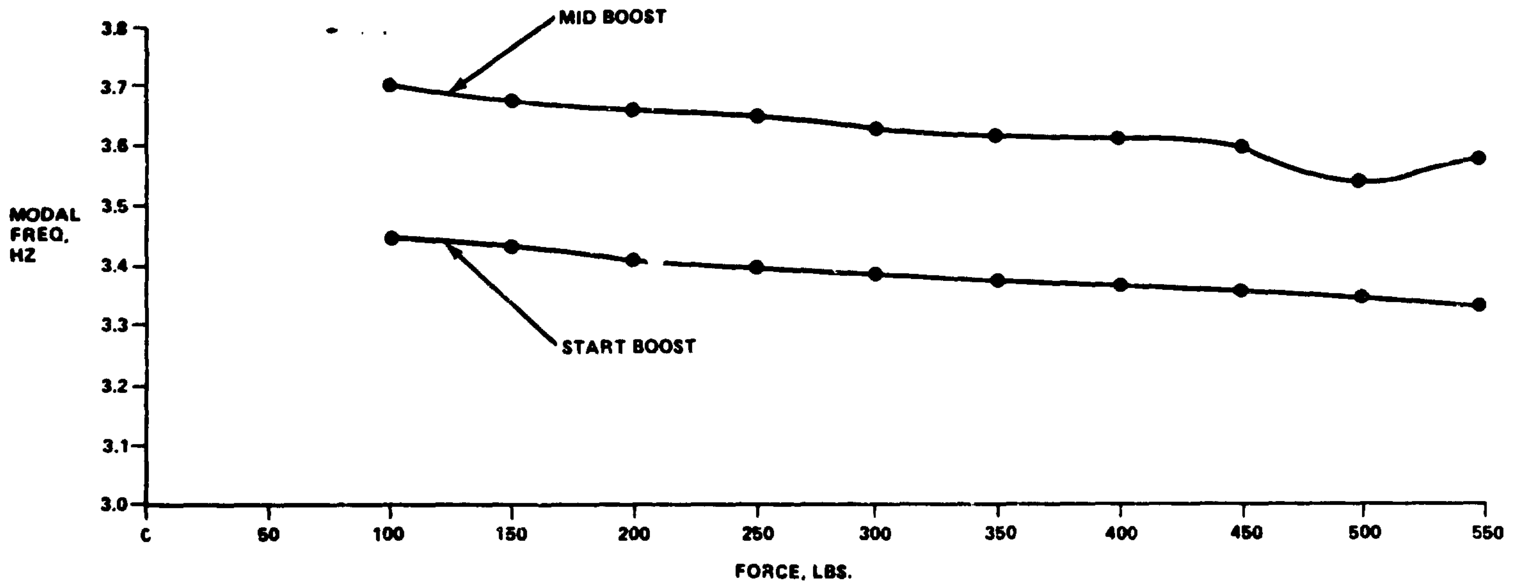

Figure 31. First fuselage symmetric bending linearity check.

TABLE 29. SAMSO SWEEPS

Shaker	Phase (deg)	Frequency Range (Hz)
FL10Y-FL11Y	0	2.5-50
	180	2.5-50
FB10Z-FB11Z	0	2.5-50
	180	2.5-50

XI. CONCLUSION

The following is a summary of the most significant results derived from the MVGVT Shuttle Test Program:

1) The left and right SRB forward mounted rate gyros exhibited abnormally high transfer functions which required a structural redesign.

2) The effect on the frequencies and mode shapes with the SRB stiffening ring on and off was neglible. This lack of difference may have been due to the additional flexibility of the ET at the aft ET/SRB interface.

3) The SSME axial modes did not correlate well with pre-test analysis. The pre-test math model used was a symmetric halfshell. A three-dimensional antisymmetric math model of the SSME engine and thrust structure was determined to be required.

4) The forward ET/SRB interface, which is a ball and socket design, was found to be fixed in the liftoff test. This interface is intended to transmit only shear forces between the ET and SRB. The ET/SRB interface was fixed due to the frictional forces created by the weight of the loaded ET and Orbiter.

5) Pre-test SRB Y bending modes for SRB end burn did not correlate well with test. This required additional shell modeling of the aft SRB/ET interface.

6) Unexpected large rate gyro yaw rates were observed on the Orbiter 1307 Orbiter bulkhead during symmetric (pitch) flight control sweeps. This was found to be due to local deformation which the flight controls group assessed as acceptable. The math model of the 1307 bulkhead was remodeled, however.

7) Test rate gyro values showed greater response variations than those used in the analytical studies in determining the Redundancy Management (RM) Trip Levels. For STS-1 flight, RM software trip levels and cycle counter levels were increased. The Fault Isolation Routine was modified to inhibit kicking out RGA's and accelerometers after first sensor failure. Changes to the control system for the other flights will be evaluated after STS-1 flight.

With the advent of structural complexity of space vehicles with increasing unsymmeterical jointed structures, the difficulty of dynamist modeling is becoming increasingly greater; therefore, modal survey testing will always be a necessary tool to aid the dynamist in the area of math modeling, and loads, controls, pogo and flutter design. Table 30 lists the various past full scale test programs with the major problems uncovered in each.

TABLE 30. FULL SCALE DYNAMIC TESTING EXPERIENCE IN PAST PROGRAMS

Test Program	Problems Discovered	Hardware Impacted	Consequences if Not Discovered
MVGVT	SRB mounted rate gyros exhibited abnormally high transfer functions. The rate gyros mounted on the forward SRB ring frames resonated at local frequencies and high gains, which were critical to flight controls.	Structural redesign was required to stiffen SRB ring frame which raised the local resonant frequencies and reduced the gain.	Flight control instability and possible loss of vehicle.
MVGVT	Axial SSME frequencies and mode shapes did not correlate with pretest analysis. A half shell dynamic math model using symmetry was used in the pretest analysis.	A new three dimensional asymmetric math model of the SSME engines and thrust structure was required. No hardware changes were necessary.	Pogo stability analyses would have been suspect.
MVGVT	Test rate gyro values showed greater response variations than analysis. Response variations between RGA's were much larger than those used in the analytical studies in determining the Redundancy Management (RM) trip levels.	*RM software trip levels and cycle counter levels were increased. The fault isolation routine was modified to inhibit kicking out RGA's and ACC's after first sensor failure.	Flight control instability and possible loss of vehicle.

*Above for STS-1 flight only, other flights will be evaluated.

TABLE 30. (Continued)

Test Program	Problems Discovered	Hardware Impacted	Consequences if Not Discovered
DTV	Design deficiency in the SPS tank supports. Unexpectedly high local resonant coupling was detected between SPS tank and bulkhead support.	The upper support bracket for the SPS tanks was redesigned to eliminate a strong tank cantilever mode.	Hardware failure resulting in loss of mission and possible crew loss.
DTV	High LOX and fuel dynamic tank bottom pressures. These pressures were under predicted by a factor of 2. The significance of these pressures was not understood until after Pogo occurred on AS-502.	The higher tank pressures contributed to the S-IC Pogo accumulator hardware design.	Potential loss of vehicle and crew due to Pogo.
DTV	High 18 Hz S-IC Crossbeam mode gains. DTV data showed that an accumulator should not be used on the inboard engine.	Elimination of a planned inboard engine accumulator.	Potential loss of vehicle and crew due to Pogo between an 18 Hz accumulator mode and the 18 Hz crossbeam mode.
DTV	Local rotation of the flight gyro support plate. Vehicle dynamic shears and moments deformed support plate. The math model under predicted this deformation by 135%.	The gyros were relocated to the bottom of the support plate where the local rotation was much less. This required wire harnesses of new length. The flight control filter network was redesigned.	Flight control instability resulting in loss of vehicle.

TABLE 30. (Continued)

Test Program	Problems Discovered	Hardware Impacted	Consequences if Not Discovered
MARL	Design deficiency in the IU stable platform. Coupling between the stable platform and the ring modes of the IU provided a mechanism for acoustically driving the platform accelerometer against the stops.	Short channel stiffeners were added to AS-501 on the pad. Damping material and a software "reasonableness" test were added later in the program.	Large guidance errors that could cause loss of lunar mission.
DTV	Design deficiency in the CSM interface. The single torsional sway brace produced unpredicted high coupling between command module torsional motion and S-IC engine deflection.	Additional torsional sway braces were installed on AS-501 on the pad. Subsequently, the F-1 engines were reorificed to reduce loads at engine cutoff. An engine precant program was implemented to maintain structural integrity in case of engine out.	structural failure of the CSM interface with loss of vehicle and possible crew loss.
Skylab ATM Test	Strong cross coupling between longitudinal and lateral motions indicated a possible structural failure at S-IC cutoff.	A 1-2-2 engine cutoff hardware and software mod was developed to reduce the longitudinal input to the ATM. Hardware redesigns were laid out in case they were proven necessary by further study.	Hardware failure with potential loss of mission.

TABLE 30. (Concluded)

Test Program	Problems Discovered	Hardware Impacted	Consequences if Not Discovered
Skylab Modal Survey Test	The strong cross coupling in the ATM proved to be attenuated rather than amplified by the way ATM cross coupling reacted through vehicle interface.	Test of the total Skylab launch configuration proved the 1-2-2 fix was adequate and that no hardware changes were required.	This test saved a possible redesign of the ATM by verifying structural integrity under the 1-2-2 cutoff.
Short-stack	Strong pitch/longitudinal coupling caused by the lunar module increased the S-IC Pogo gain factor by 30%. This effect coupled with the tank pressure underprediction was the reason AS-502 Pogo was not predicted.	Development and installation of the outboard LOX accumulators.	Pogo instability with potential loss of vehicle and crew.
Mini A/C	The mechanism triggering S-II Pogo was defined. Coupling between the first four LOX tank hydroelastic modes when they coalesced with the 16 Hz center engine crossbeam mode produced the Pogo instabilities.	An accumulator was developed for the center engine. A backup cutoff system was also developed. The accurate math model developed during this test supported extensive thrust structure design mods on subsequenc vehicles without further testing.	Pogo instability with potential loss of vehicle and crew.

BIBLIOGRAPHY

STS 79-0006, Mated Vertical Ground Vibration Test Liftoff Configuration on-site Data Evaluation Report, Space Division, Rockwell International, January 1979.

STS 79-0032, Mated Vertical Ground Vibration Test Pre-SRB Separation Configuration on-site Data Evaluation Report, Space Division, Rockwell International, March 1979.

SD-78-SH-0170, Mated Vertical Ground Vibration Test Boost Configuration on-site Data Evaluation Report, Space Division, Rockwell International, July 28, 1978.

ED23-77-205, Finite Element Model of the MVGVT Overhead Suspension System for Boost, MSFC, October 7, 1977.

ED23-78-30, MVGVT Suspension System Rigid Body Modes, MSFC, March 8, 1978.

Technical Letter ASD-ED23-21632, Vibration Analysis of the Coupled Building-Vehicle System for the Mated Vertical Ground Vibration Test, Teledyne Brown Engineering, May 21, 1975.

JSC 08201, Mated Vertical Ground Vibration Test, Test Requirements and Specifications Document, JSC, February 6, 1978.

MVGVT-FTOR-002 Volume 1, Mated Vertical Ground Vibration Test Liftoff Configuration Test Operations Report, MSFC, Feb[illegible]y 1979.

MVGVT-FTOR-003 Volume 1, Mated Vertical Ground Vi[illegible] Test Burnout Configuration Test Operations Report, MSFC, [illegible]979.

MVGVT-FTOR-001 Volume 1, Mated Vertical Ground Vibratio[illegible] Boost Configuration Test Operations Report, MSFC, October 1978.

APPROVAL

MATED VERTICAL GROUND VIBRATION TEST

By W. Ivey

The information in this report has been reviewed for security classification. Review of any information concerning Department of Defense or nuclear energy activities or program has been made by the MSFC Security Classification Officer. This report, in its entirety, has been determined to be unclassified.

ROBERT S. RYAN
Chief, Structural Dynamics Division

GEORGE D. HOPSON
Director, Systems Dynamics Division

☆ U.S. GOVERNMENT PRINTING OFFICE: 1980—640-247/114 REGION NO.4